

https://dspace.org/

Performance Modeling of Cognitive NOMA-aided IoT Networks with Energy Harvesting

Selematsela, Neo Edwin

2024
University of the Witwatersrand, Johannesburg
https://hdl.handle.net/10539/45443
Selematsela, Neo Edwin . (2024). Performance Modeling of Cognitive NOMA-aided IoT Networks with Energy Harvesting [Masters dissertation, University of the Witwatersrand, Johannesburg]. WIReDSpace. https://hdl.handle.net/10539/45443

Downloaded from a DSpace repository. https://dspace.org/

UNIVERSITY OF THE WITWATERSRAND

School of Electrical and Information Engineering



MSc Research Dissertation
August-2024

Performance Modeling of Cognitive NOMA-aided IoT Networks with Energy Harvesting

N.E Selematsela (Student No. 1262347)

Supervisors:
Prof. Fambirai Takawira
Dr. Chabalala Chabalala

Declaration

I declare that this dissertation is my own work and that the resources I have used are recognized by means of complete references. I pledge that it has not been submitted before for any degree or examination to any other University.



(Candidate Signature)

01/08/2024

Date

Abstract

In an attempt to address rocketed connectivity and bandwidth demands in 5G wireless networks, Non-Orthogonal Multiple Access (NOMA) and Cognitive Radio (CR) concepts have been proposed. The former addresses increased connectivity requirements by allowing multiple users in the same NOMA group to utilise the same channel resources. The latter enhances spectrum efficiency by intelligently allowing spectrum sharing between primary and secondary networks, if secondary to primary network interference is properly managed. To prolong connectivity/service life-time of battery capacity constrained Internet of Things (IoT) devices, Energy Harvesting (EH) technique has been identified as the technology that can enable such devices to harvest energy from ambient sources present in the environment. This research work is motivated by the observed surge in adoption of IoT devices around the globe. The resulting adoption has brought about the need to investigate performance of different IoT system models and hence, understand potential applicability and optimization options for different services.

The focus of this dissertation is to model and analyse the performance of an EH Cognitive Radio Non-Orthogonal Multiple Access (CR-NOMA) IoT network. To accomplish this, a simplified energy harvesting CR-NOMA IoT network is considered. The considered network consists of primary and secondary network components. The primary network contains Macro Base-Station (MBS) and Primary Network users (PUs), while the secondary network is made up of Secondary Base-Station (SBS) and multiple CR-NOMA groups containing two Secondary Users (SUs) each. To analytically capture the stochastic nature of energy harvesting process and cater for residual energy from one transmission frame to the next, each SU's energy level in the battery is discretized to represent the state of each SU during each transmission frame; with this, we derive a complete Markovian model for the considered system model using queueing theory and Markovian analysis. Two Markovian models are developed for the considered system model, with one assuming that the SUs are harvesting energy from the SBS (one energy source) and the other, adopting an assumption that energy is harvested from both the SBS and MBS (two energy sources).

The considered system performance is analysed in terms of up-link system outage probability and mean capacity. To provide detailed insights, closed-form analytical expressions for up-link outage probability and mean capacity for each user in the CR-NOMA group are derived using the Markovian models as the basis. Produced analytical results are confirmed through simulations using Matlab. Simulation results matched the analytical results, this confirmed the validity of the derived analytical expressions for SUs outage probability and mean capacity.

Both performance metrics are studied and the impact of varying different network parameters on outage probability and mean capacity is investigated. For outage probability, results are generated which demonstrate SUs outage performance as we vary Signal-to-Interference-plus-Noise Ratio (SINR), interference threshold, and battery power level. Similarly, mean capacity results are generated to illustrate each SU mean capacity performance while varying their battery levels, this is done for different values of primary transmit power and interference threshold. Performance results observed as different parameters are varied for outage probability and mean capacity align with the theoretical performance expected when those parameters are changed. The significance of this work lies in providing analytical tools to assess the performance of the CR-NOMA IoT system with energy harvesting (EH). These tools enable easy computation of system performance indicators such as outage performance and mean capacity. Attempting the same assessment through simulation would be a cumbersome process.

Acknowledgements

I would like to pass my gratitude to my supervisor, Prof. Fambirai Takawira. For the opportunity you offered to work with me, and an unwavering support you gave during this difficult but fulfilling learning journey. I thank you.

I would like to further express my heartfelt appreciation to my co-supervisor, Dr. Chabalala Chabalala. Thank you, for your technical support and motivation throughout this journey. Your mentor-ship kept me going in the worst phases of this work. You kept believing in me, and for that, i am deeply indebted to you.

For financial support, I would like to thank CeTAS program through Prof. Takawira.

Finally, my appreciation goes to my family and inner circle of friends, for their understanding and moral support throughout this journey.

Acronyms

AWGN	Additive White Gaussian Noise
CR	Cognitive Radio
CSI	Channel Sate Information
CR-NOMA	Cognitive Radio NOMA
EH	Energy Harvesting
IoT	Internet of Things
MBS	Macro Base Station
NOMA	Non-Orthogonal Multiple Access
OFDMA	Orthogonal Frequency Division Multiple Access
OMA	Orthogonal Multiple Access
PU	Primary User
QoS	Quality of Service
RF	Radio Frequency
SBS	Secondary Base Station
SIC	Successive Interference Cancellation
SINR	Signal-to-Interference-Noise-Ratio
SU	Secondary User
TDMA	Time Division Multiple Access

Contents

Declaration i
Abstract ii
Acknowledgements iv
Acronyms v
List of Figures vii
List of Tables ix

1 Background **1**
1.1 Introduction 1
1.2 Problem Statement 1
1.3 Research Question 4
1.4 Research Methodology 5
1.5 Research Contributions 5
1.6 Dissertation Structure 6

2 Literature Review **7**
2.1 Background Concepts 7
2.1.1 Cognitive Radio (CR) 7
2.1.2 Non-Orthogonal Multiple Access Technique (NOMA) 7
2.1.3 Energy Harvesting (EH) 9
2.1.4 Queueing Statistical Modeling 10
2.2 Relevant Research Work 10
2.2.1 Cognitive Radio NOMA-aided (CR-NOMA) Networks . . . 10
2.2.1.1 Performance Analysis 10
2.2.1.2 Resource Allocation (RA) and Optimization 12
2.2.2 Queuing Analysis of Coupled Data-Energy Queues 14
2.3 Summary 15

3 Energy-Harvesting Cognitive Radio NOMA IoT Network **16**
3.1 Introduction 16
3.2 System Description 18
3.2.1 Computing SU_1 Outage Probability and Mean Capacity: . . 23

3.2.2 Computing SU_2 Outage Probability and Mean Capacity: . . 26
3.2.3 Assumptions Made in Literature 28
3.2.4 This Dissertation Approach 29
3.3 System Markov Analysis 30
3.3.1 System Markov Analysis With Respect to SU_1 31
3.3.1.1 SU_1 Energy Harvesting from SBS 32
3.3.1.2 SU_1 Energy Harvesting from SBS and MBS 35
3.3.2 System Markov Analysis with respect to SU_2 40
3.3.2.1 SU_1 and SU_2 Energy Harvesting from SBS 42
3.3.2.2 SU_1 and SU_2 Energy Harvesting from SBS and MBS 44
3.4 Simulation Results and Discussion 49
3.4.1 Distributions Confirmations 50
3.4.2 Markovian Analysis 54
3.5 Summary 56

4 Outage Probability Analysis **57**
4.1 Introduction 57
4.2 Outage Probability Experienced by SU_1 57
4.2.1 Case 1 58
4.2.1.1 Imperfect SIC Scenario: 59
4.2.1.2 Perfect SIC Scenario: 59
4.2.2 Case 2 60
4.2.2.1 Imperfect SIC Scenario: 61
4.2.2.2 Perfect SIC Scenario: 62
4.3 Outage Probability Experienced by User 2 62
4.4 Simulation Results and Discussion 67
4.5 Summary 77

5 Mean Capacity Analysis **78**
5.1 Introduction 78
5.2 Mean Capacity SU_1 79
5.3 Mean Capacity SU_2 81
5.4 Simulation Results and Discussion 92
5.5 Summary 97

6 Conclusion **98**
6.1 Introduction 98
6.2 Summary and Conclusions 98
6.3 Future Work 99

References **100**

List of Figures

2.1 Cognitive Radio Network 8
2.2 Basic Downlink NOMA Illustration with SIC at UE Receivers . . . 9

3.1 CR-NOMA IoT System 17
3.2 CR-NOMA IoT Frame Structure 18
3.3 Energy Harvesting CR-NOMA IoT Network 20
3.4 n_i Distribution: Battery Power Conditioned on I_{it} 51
3.5 SBS: Energy Harvesting CDF Distribution 52
3.6 SBS and MBS: Energy Harvesting CDF Distribution 53
3.7 SBS: State Probability vs Battery States for Different Values of Primary Transmit Power P_p 54
3.8 SBS and MBS: State Probability vs Battery States for Different Values of Primary Transmit Power P_p 55

4.1 Outage Probability vs SINR Threshold for Different Values of Primary Transmit Power P_p (Watts) 69
4.2 Outage Probability vs SINR Threshold for Different Values of Primary Transmit Power P_p (Watts) 70
4.3 Outage Probability vs SINR for Different Values of eta 71
4.4 Outage Probability vs SINR for Different Values of eta 72
4.5 Outage Probability vs Interference Threshold for Different Values of Primary Transmit Power P_p (Watts) 73
4.6 Outage Probability vs Interference Threshold for Different Values of Primary Transmit Power P_p (Watts) 74
4.7 Outage Probability vs Battery Level for Different Values of Primary Transmit Power P_p (Watts) 75
4.8 Outage Probability vs Battery Level for Different Values of Primary Transmit Power P_p (Watts) 76

5.1 Mean Capacity vs Battery Level for Different Values of Primary Transmit Power P_p (Watts) 93

5.2 Mean Capacity vs Battery Level for Different Values of Primary Transmit Power P_p (Watts) 94
5.3 Mean Capacity vs Battery Level for Different Values of Interference Threshold I_{it} 95
5.4 Mean Capacity vs Battery Level for Different Values of Interference Threshold I_{it} 96

List of Tables

3.1 Table of Symbols 19
3.2 Table of Simulation Parameters 49

Chapter 1

Background

1.1 Introduction

Multitudes of Internet of Things (IoT) devices around the globe are connected via mobile networks. This connectivity enables development of new innovative services and applications with extreme capacity and performance demands. Wireless networks need to evolve to accommodate the surging number of connectivity requirements. IoT devices are energy constrained and to compensate for their limited energy storage capabilities, researchers have developed Energy Harvesting (EH) [1] technique. This technique allows IoT devices to harvest energy from multiple different ambient sources. EH is envisioned to prolong the battery life of wireless IoT devices. To cater for recent network deployments with high bandwidth and connectivity demands, technologies like Cognitive Radio (CR) [2] and Non-Orthogonal Multiple Access (NOMA) [3] techniques have been developed. The former is designed to achieve efficient spectrum utilization while the latter addresses high connectivity requirements. To ensure that network deployments accommodate services with increased connectivity and bandwidth demands, the network models proposed should facilitate how the above mentioned technologies (CR, NOMA, and EH) can be effectively integrated within a single system model to leverage the benefits all these technologies at the go.

1.2 Problem Statement

Different system models designed using a combination of CR, NOMA and EH techniques have been studied in literature, these includes the following:

- CR-NOMA networks without EH aspect.

- EH CR networks without NOMA element.
- Simple EH systems without the incorporation of CR and NOMA.
- System models that incorporated CR, NOMA and EH concepts.

Though, the above system models have been extensively studied in literature, performance analysis of a CR-NOMA IoT system with EH that captures the stochastic nature of energy harvesting process, while also catering for residual energy between subsequent transmission frames has not been covered.

Referencing the above listed system models that have already been studied, the following research works investigate system models where CR-NOMA networks are modelled without EH component. Authors in [4–10], analysed the performance of CR-NOMA systems using metrics such as error rate, transmission rate, and outage probability. Optimal performance of CR-NOMA systems have been studied in [11–14], where different optimization techniques were used to analyse optimal performance of CR-NOMA systems. These studies did not incorporate EH in their system models, this is what separates their work to the one carried out in this dissertation.

Studies in [15–18], worked on performance analysis and optimization of CR networks with EH. Studies in [15, 16] focused on investigating optimal power allocation in CR networks. Authors in [17] worked on optimal channel access policy to maximize secondary user throughput. The study in [18], investigated optimal charging policies and then, analysed end-to-end outage probability of the proposed system model. All these studies did not incorporate NOMA in their system models. The first two papers [15, 16] focused mainly on optimization issues, which is a different focus area to the research work in this submission. The last paper [18] referenced, does analyse outage probability as we do in this research work, but their approach is completely different because their system model does not incorporated NOMA.

Authors in [19–21] investigated performance of system models with data-energy queues, but their system designs did not incorporate neither CR nor NOMA concepts. The study in [19], worked on a simple assumption that an energy packet routes one workload or data packet. In this dissertation, mean system capacity is statistically derived showing its dependence on channel conditions and available battery energy from which user transmit power is computed. Thus, our approach closely resembles the real-world scenario as we also cater for residual energy from one transmission frame to the next. Authors in [20] studied an optimal power control policy and proposed an online power control algorithm for their system

model. Though, their analysis used queueing theory as in this dissertation, power control is not the area of our focus and their system model is missing CR and NOMA components. The study in [21] made an assumption that either one chunk of energy is harvested or none is, in the considered energy harvesting time interval. This assumption does not closely represent an actual practical energy harvesting process in which one or more energy chunks can be harvested during the considered energy harvesting duration. In our study, we approach energy harvesting as an exponentially distributed random process which closely represents practical energy harvesting process and caters for energy residuals from one transmission frame to the next.

Authors in [22–28] proposed system models similar to the one proposed in this study, their models include combination of the three technologies: CR, NOMA, and EH. Though, there are similarities in the system models they proposed with regard to the involved technologies, the focus of their research work is different from what is in scope for this dissertation. Articles [22, 23] focused on optimal resource allocation in EH cognitive NOMA networks, which has a different focus area from the work done in this dissertation. Authors in [25, 27] investigated throughput maximization analysis which is not our focus area. Authors in [28] focused only on outage probability analysis and their system model simulated Device-to-Device (D2D) network communication. The study in [26] performs analysis of bit error rate which is not in scope for this research work. Though, article [28] does analyse outage probability, which is within the scope of work in this dissertation, their system model considers D2D communication and is not part of our focus. The work in [28] also does not include mean capacity analysis. The works in [23, 24] have system models that incorporated both CR, NOMA, and EH technologies. The research work they looked at focuses on security analysis, which is out of scope for the work in this dissertation, though it can be a potential extension.

The studies in [29–31] carried out performance analysis for system models with CR, NOMA, and EH. Though, their analysis carry out outage probability analysis, they considered downlink NOMA as opposed to uplink NOMA analysis considered in this dissertation. They included EH component when performing their analysis, but different from the work carried out in this dissertation, the downlink power selection in their works is based on energy-harvested power (P_{EH}), and the interference threshold power ($\frac{I_{it}}{H}$), where I_{it} is the interference threshold power and H is the channel gain (scalar), $P_t = min\left(P_{EH}, \frac{I_{it}}{H}\right)$. There has been no consideration for residual energy from one transmission frame to the next in their analysis as is done in this dissertation. At each transmission frame, they only considered energy harvested in that frame to be used during the transmission. This assumption does

not consider the residual energy that might have been left unused from the previous transmission frame. Residual energy comes in to play based on the practical consideration that it is not in every case that harvested energy will be used up within that transmission frame. The residual energy occurs when the transmit power selection is constrained on the interference constraint, where the battery power equivalent to interference threshold is less than the available battery energy power.

Though, multiple works have been done covering system models deploying CR, NOMA, and EH as discussed in the previous paragraphs in this section, there is currently no work that closely resemble the work done in this dissertation. Specifically, with regards to how the analysis of outage probability and mean capacity are carried out. We first develop Markovian model which realistically caters for the stochastic nature of energy harvesting and the residual energy from one transmission frame to the next. Then, use the derived Markovian model to develop closed-form expressions for SUs outage probability and mean capacity. These performance metrics are verified using simulations in matlab. This dissertation will aid in understanding the performance of CR-NOMA IoT systems with Energy Harvesting (EH), including aspects such as IoT battery energy evolution, outage probability, and achievable transmission rates. This will in-turn allow other researchers, vendors, and operators to have some basis for optimization considerations. The results of this study can also be used in deciding viable use cases for CR-NOMA IoT systems with EH.

1.3 Research Question

The main research question for this study is:

- How does battery energy and channel dynamics affect performance of an EH CR-NOMA IoT system?

In order to tackle the above main question, the following sub-questions need to be addressed:

1. How can system states of an EH CR-NOMA IoT system be modelled using queueing theory and Markovian analysis?
2. How can outage probability of an EH CR-NOMA IoT system be statistically modeled using queueing theory and Markovian analysis?
3. How can mean capacity of an EH CR-NOMA IoT system be derived using Markovian analysis and queueing theory?

1.4 Research Methodology

The methodology below has been adopted in addressing the research questions above:

- Perform a thorough literature review around performance modeling of network designs that deploy any combination of NOMA, CR and EH technologies.
- Consider a system model where CR-NOMA and EH technologies coexists in the same network design.
- Derive Markovian model of the considered system model.
- Use Markovian analysis and queueing theory to determine outage probability for the considered EH CR-NOMA IoT system.
- Use Markovian analysis and queueing theory to derive a closed-form expression for mean capacity for the considered EH CR-NOMA IoT system.
- Verify the derived analytical expressions using Matlab simulations.

1.5 Research Contributions

The main contributions of this research work can be summarized as follows:

- A system model for EH CR-NOMA enabled IoT network is considered.
- Markovian model for the considered EH CR-NOMA IoT system is accurately derived.
- Analytical outage probability for the considered EH CR-NOMA IoT system is accurately determined.
- The considered EH CR-NOMA IoT system mean capacity is accurately derived.
- System behaviour of the considered EH CR-NOMA IoT system is analysed by varying different network parameters and observing its outage and mean capacity performance.

1.6 Dissertation Structure

This dissertation is structured as follows; literature review covering background concepts and relevant research work is covered in Chapter 2. Chapter 3 covers description of the considered EH CR-NOMA IoT network and its Markovian analysis. Chapter 4 outlines EH CR-NOMA IoT network outage probability analysis. The considered EH CR-NOMA IoT system mean capacity analysis is covered in Chapter 5. The conclusion of the work done in this dissertation is covered in Chapter 6, this chapter also covers potential future research directions to improve this body of work.

Chapter 2

Literature Review

2.1 Background Concepts

2.1.1 Cognitive Radio (CR)

The surge in bandwidth hungry wireless applications have led to an increased demand for the scarce wireless radio spectrum resource [32]. In order to address this problem, the Federal Communications Commission (FCC) approved that unlicensed devices can utilize licensed spectrum in a way that the licensed user (primary user) would not be affected [33]. This approval inspired the development of hierarchical spectrum sharing systems in which the secondary users are allowed to access and use the underutilized spectrum of the primary users without harmfully degrading their QoS, one of these spectrum sharing systems is CR networks.

In CR Networks, there exists two types of users, these are; the Primary Radio (PR) user and the secondary user. The PR user operates in the primary network and has the licensed spectrum, while the CR user has no licensed spectrum and operates on unlicensed or re-uses the PR user licensed spectrum [33]. The PR user preempt the CR user if the PR becomes active while the CR user is using the spectrum, the CR user would then switch to another available idle spectrum from the spectrum pool [34]. There are other multiple works in literature that touch on the concept of CR networks, these include but not limited to [35–37]. High-level overview of CR network is presented in Fig. 2.1.

2.1.2 Non-Orthogonal Multiple Access Technique (NOMA)

NOMA is the radio access technology designed with the principal aim of improving system capacity in a cost-effective manner for cellular networks [38]. NOMA is considered as a promising multiple access technique for 5G and beyond 5G sys-

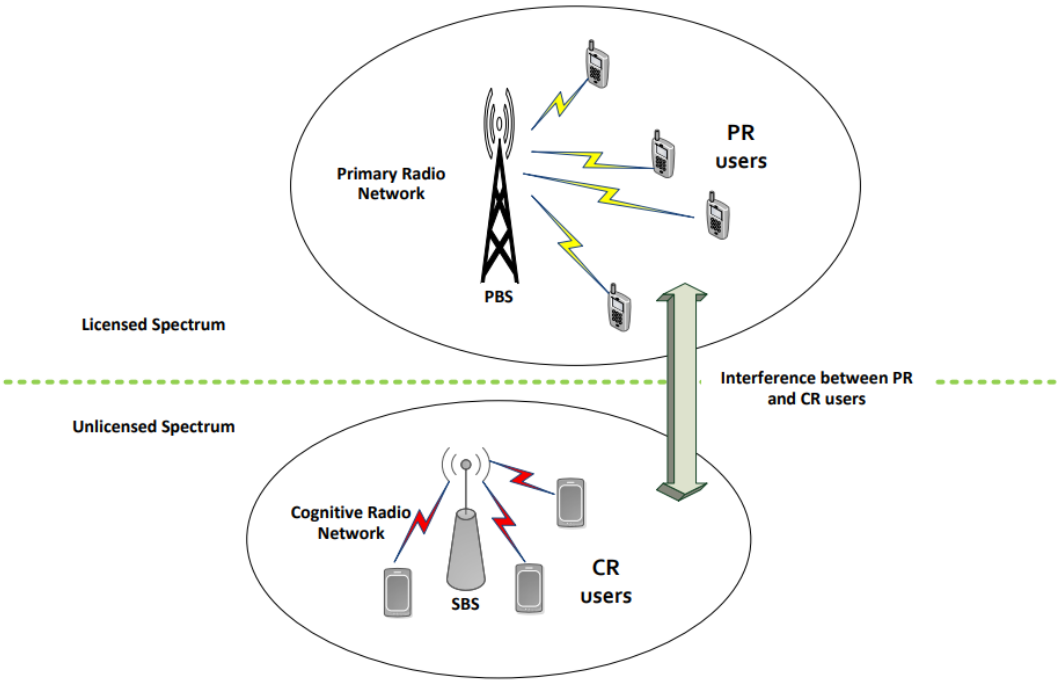


Figure 2.1: Cognitive Radio Network

tems. With NOMA, multiple User Equipments (UEs) can be co-scheduled to share the same radio resources in time, frequency or code [39]. Multiple schemes have been proposed for NOMA including, power domain NOMA [40, 41], Sparse Code Multiple Access (SCMA) [42], Pattern Division Multiple Access (PDMA) [43], Resource Spread Multiple Access (RSMA) [44], Multi-User Shared Multiple Access (MUSA) [45], Interleave-Grid Multiple Access (IGMA) [46], Welch-bound Equality Spread Multiple Access (WSMA) [47], Interleave-Division Multiple Access (IDMA) [48], Non-orthogonal Coded Multiple Access (NCMA) [49], Asynchronous Coded Multiple Access (ACMA) , Low Code Rate Spreading (LCRS) , Non-Orthogonal Coded Access (NOCA) , Low Code Rate and Signature based Shared Access (LSSA), as well as User Grouped Multiple Access (UGMA) [50]. All these techniques follow the superposition principle, the main difference among them is the signature design of the UEs which is based on spreading, coding, scrambling, or interleaving distinctness [39]. More work around NOMA can also be referenced in other research works such as in [51, 52]. In its simplest form, NOMA can be illustrated as shown in Fig. 2.2 for downlink.

The scheme assumes two UEs case with a single transmitter, and a single receiver antenna, served by a single antenna base-station. The base-station always

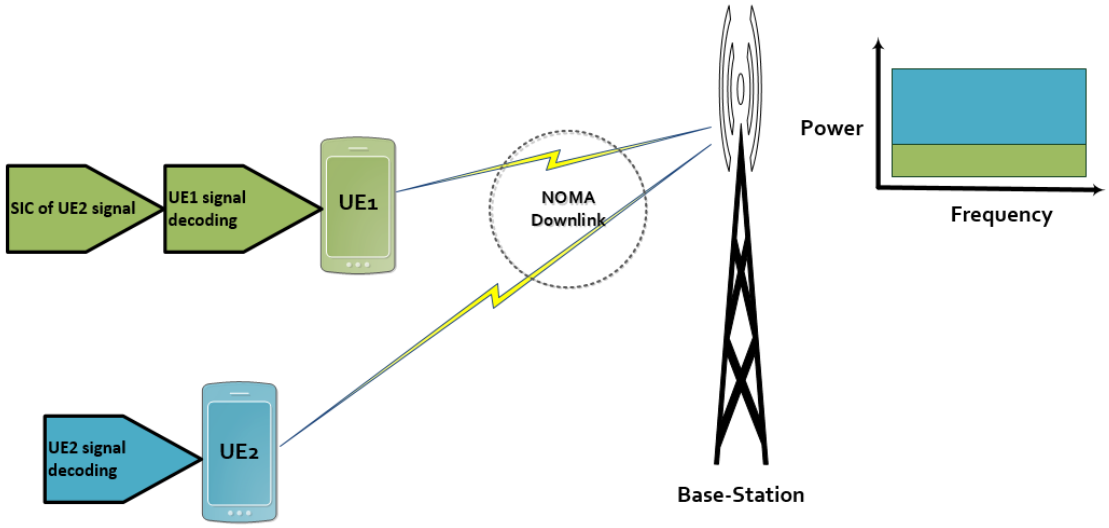


Figure 2.2: Basic Downlink NOMA Illustration with SIC at UE Receivers

sends data to the two UEs simultaneously using superposition coding [53] technique, subject to power constrained in the case of Power Domain NOMA [54]. The UEs wireless channels are assumed to be identically distributed and independent. Further, they are assumed to experience fading and Additive White Gaussian Noise (AWGN). They are also sorted such that UE2 is always the one with the weakest instantaneous channel gain. The UEs use Successive Interference Cancellation (SIC) [55] to decode the signals. Note that for uplink a similar process is followed but SIC is applied at the base-station receiver to decode UEs signals.

2.1.3 Energy Harvesting (EH)

Recent emphasis on green communication and insufficient energy storage capability has generated a great interest in the investigation of energy harvesting communications and networking. Energy harvesting from ambient energy sources can potentially reduce the dependence on the supply of grid or battery energy, providing many attractive benefits to the environment and beyond [56]. Generally, energy harvesting sources can be divided into four types, these are: solar/light [57], thermoelectric power [58], mechanical motion [59] and electromagnetic radiation [60]. The principal goal of EH is a self-sustainable, maintenance free network communication devices.

Energy harvesting refers to harnessing energy from the environment or other energy sources and converting it to electrical energy which is then used to power

the device [61]. The typical energy harvesting device consists of EH module that converts ambient energy to electrical energy, which is in turn stored in the storage element, typically a rechargeable battery or a super capacitor [62].

2.1.4 Queueing Statistical Modeling

Queueing theory is a powerful tool for performing traffic analysis in communication networks to make accurate prediction of their performance. In applying queueing theory to communication networks, the server(s) are modelled as the network nodes in a communication system and the buffer on the network nodes as the data queue, then queuing theory concepts are applied to analyse the system behaviour. For this research work, our system model adopts a single queue used to analytically model energy stored in the secondary user battery storage, this energy is used to facilitate transmission of the data packets. The battery energy in the energy queue is quantized to be able to analytically model it as the energy queue, where each quantization represent an energy level in the battery. Data packets transmission depends on available energy in the secondary user energy queue and the transmission channel characteristics.

2.2 Relevant Research Work

2.2.1 Cognitive Radio NOMA-aided (CR-NOMA) Networks

To leverage the benefits of both CR and NOMA technologies, researchers have proposed multiple designs of CR-NOMA based system models. Within these works, the researchers have analysed and optimised some of the key performance indicators of CR-NOMA networks to ensure optimal performance. Below, we cover some of the work done around CR-NOMA system models.

2.2.1.1 Performance Analysis

In order to understand the performance limits and propose the potential applications for CR-NOMA networks, it is of out-most importance that researchers model and analyse the performance of these networks. The following discussion covers research works that engulf this aspect.

Authors in [4–7], study the performance analysis of different CR-NOMA network designs by investigating different performance parameters such as error rate, transmission rates, and network outage. The study in [4] investigates NOMA

transmission with 5G enabled cognitive femtocell to attain higher spectral efficiency and to maximize the sum rate of the femto users with guaranteed QoS. They then, propose a paring algorithm between strong and weak users to reduce NOMA interference between different femto users. In [5] authors investigate error rate performance of relay-assisted NOMA with partial relay selection in an underlay CR network. In their set-up, relays are used to assist transmission between secondary NOMA users and secondary base station, where the relay with the strongest link with the secondary base station is selected to amplify-and-forward received signals to the secondary users. The authors then derive an accurate approximation for the Pairwise Error Probability (PEP) of the secondary users with imperfect SIC. They then, subsequently utilize PEP expression to deduce a union bound, which is considered an upper bound on the bit error rate. Finally, an optimization problem is formulated to calculate the optimum power coefficients that minimize the derived union bound. Authors in [6], study performance of a CR network in the context of Vehicle-to-Everything (V2X), NOMA is applied to their system model which they refer to as CR-assisted NOMA-V2X. In their proposed system, they consider two schemes related to Vehicle-to-Vehicle (V2V) transmissions to enhance the performance of the vehicle that needs higher QoS. The research work in [7], studies the down-link outage and throughput performance in the secondary networks of CR-NOMA systems and investigates both OMA and NOMA with respect to the status of decoding operation of each user. Depending on the transmit Signal-to-Noise Ratio (SNR) at the primary source and interference constraints from the primary network, the closed-form expressions for outage probability of the two users are obtained and compared in terms of performance.

The studies in [8–10] focus on the aspect of outage probability in CR-NOMA networks. Paper [8], investigates the Outage Probability (OP) gap among NOMA users which is due to different power allocation factors. Multiple existing NOMA schemes consider power allocation factors, while the authors in [8] propose a paradigm which exhibits optimal outage scenario of Device to Device (D2D) transmissions. They first derive outage probability, from which approximate outage performance can be achieved. The authors in [9], study the outage probability of the cooperative underlay CR networks consisting of a secondary relay node and k NOMA Secondary Destinations Users (SDUs) under imperfect Channel State Information (CSI) conditions. They derive generalized closed-form expressions for the OP of NOMA-enabled SDUs. Their numerical results show that a superior performance is obtained from their considered system relative to cooperative OMA scheme in terms of OP. Article [10], investigates outage and throughput performance of CR-NOMA network under Partial Relay Selection (PRS) scheme. The authors derive an analytical expression for outage probability experienced by the

secondary users under imperfect Successive Interference Cancellation (i-SIC) conditions. They also consider the interference threshold constraint of the primary receiver and the maximum transmit power constraint of the secondary nodes.

Authors in [29–31], carried out performance analysis of cognitive NOMA-based EH harvesting networks. Authors in [29] study a novel wireless powered cognitive NOMA-based IoT relay networks to improve the performance of a cell-edge user under perfect and imperfect SIC. To analyse the considered system performance, an exact closed-form analytical expressions for downlink outage probability of NOMA users and the overall system throughput are derived. To provide further insights, a performance floor analysis is carried out considering two power-setting scenarios: 1) the transmit powers at the power beacon going to infinity. 2) maximum allowable power constraint going to infinity. They then, develop two iterative algorithms for minimizing outage probability of the users and maximizing system throughput subject to time-switching and power-allocation factors in two-hop transmission. Authors in [30] propose a relaying scheme in an underlay cognitive radio network. The power required for the relay operation is based on applying energy harvesting from the the base station. The mathematical expression for analysis of outage probability for different users is derived, while also discussing linear model for perfect SIC at the receiver. Using fixed power allocation process, they simulate different output parameters such as Bit Error Rate (BER), NOMA capability, and the outage probability. The study in [31], investigates the outage performance of a multihop energy harvesting cognitive relay network, in which the secondary nodes are powered by the dedicated power beacons based on the time splitting strategy. The authors derive an analytical expression for the outage probability experienced by the secondary user taking into account the effect of interference from the primary source. The developed outage probability model is then used to assess the impact of some key parameters on the reliability of the secondary user's link in the considered system model.

2.2.1.2 Resource Allocation (RA) and Optimization

RA is one of the critical factors that need a serious consideration to achieve optimal performance for CR-NOMA systems. Multiple research works have studied the issue of resource allocation in CR-NOMA wireless networks.

Studies in [63–67], researchers propose different efficient power allocation techniques or strategies for CR-NOMA networks. Authors in [63] propose a dynamic up-link power allocation scheme for CR-NOMA networks using deep reinforcement learning algorithm. In their case, Deep Q learning is used to maximize the long-term throughput of the system. The study in [64] proposes a novel heuristic Power

Allocation (PA) method called k-scaled PA. The authors further establish the relation between the power coefficients in order to mitigate the probability of symbol errors at the users due to multiplexing using NOMA at the transmitter. Authors in [65], explore resource allocation technique for a hybrid Orthogonal Frequency Division Multiple Access (OFDMA) CR-NOMA system to further elaborate on the capabilities of the system. The authors develop a power minimization resource allocation, in which the aim is to serve the CR users with minimum possible total transmission power, while achieving a set of relevant NOMA and CR constraints.

Authors in [66] propose a power allocation strategy based on an actor-critic reinforcement learning, where a cluster of cognitive users can access simultaneously the same primary spectrum of the primary users using NOMA. In [67], the authors propose a robust RA algorithm which takes into account imperfect CSI. This algorithm is designed to maximize the sum energy efficiency of secondary users under channel uncertainties. To cater for efficient spectrum usage as one of the principal design principles to consider in wireless communication networks, authors in [68] developed a mathematical model of teletraffic for resource allocation using Power Domain NOMA (PD-NOMA) in a CR environment, specifically in the interweave spectrum sharing scheme. Their mathematical results are validated through simulations considering three different scenarios. In these scenarios, a comparison between PD-NOMA and OMA schemes is presented considering the blocking probability and the average number of users. Their proposed mathematical model shows convergence to the performed simulations.

In attempt to achieve optimal performance of CR-NOMA networks, a number of research works such as in [11–14] have formulated optimization problems that aim to improve the overall performance of CR-NOMA systems. The study in [11] proposes a game theory-based joint energy-efficient optimization of resources in CR networks consisting of secondary networks and primary networks through Hybrid Non-Orthogonal Multiple Access (HNOMA). HNOMA provides freedom for users clustering to utilise either NOMA or OMA. The proposed clustering (priority and non-priority) and power allocation schemes are jointly optimized to enhance the system sum rate. The existence, stability, and uniqueness criteria for the proposed schemes are derived and proved. The study in [12], proposes a joint power allocation and secondary user assignment problem for NOMA downlink transmission in an underlay CR network, in which the worst-case achievable rate for NOMA secondary users is maximized.

In [13], study the energy minimization problem for NOMA computation offloading in CR networks, the solution is obtained by deploying the block coordination

descent method and successive convex approximation. The authors in [14], first analyse the achievable rate regions on three different assumptions for the SIC, these assumptions being: 1) the primary network performs the SIC, 2) the secondary network performs the SIC, and 3) either of the two networks adaptively performs the SIC depending on channel conditions. The authors then, optimize the power allocation to different layers of the superimposed signal by maximizing the achievable rate for the secondary network under QoS constraints of the primary network.

2.2.2 Queuing Analysis of Coupled Data-Energy Queues

Queuing analysis of coupled data-energy queues has been applied in different energy-harvesting network system designs to analyse the performance of these networks.

The studies in [15–18] perform performance analysis and/or optimization of CR networks with energy harvesting deploying queuing analysis. Authors in [15], present a cross-layer perspective on data transmission in energy harvesting CR networks in which the physical layer power allocation and network layer delay are jointly considered. Then stochastic stackelberg game approach is used to study the optimal power allocation for cases where; there is intermittent energy harvesting, data generation is random and finally, where there is uncertainty in the grid power price. The research study in [16] investigates the maximum throughput for a rechargeable SU sharing spectrum with the PU plugged to a reliable power supply. In their proposed system model, the secondary user maintains a finite energy queue and harvests energy from natural resources and primary RF transmissions. The authors then propose a power allocation policy at the PU and analyse its effect on the throughput of both the PU and SU. The study also considers the impact of busty arrivals at the PU on the energy harvested by the SU from RF transmissions and the impact of the rate of energy harvesting from natural resources on the SU throughput.

Authors in [17] consider a network where the secondary user can perform channel access to transmit a packet or to harvest RF energy when the selected channel is idle or occupied by the primary user, respectively. The authors then present an optimization formulation to obtain the channel access policy for the secondary user to maximize the user's throughput. In [18], a multi-hop cellular D2D communication system with EH in underlay CR networks is constructed. The authors consider the locations of primary user equipment (PUEs) and cellular base stations as a Poisson point process and assume that the transmit power of the secondary devices is collected from the power beacon with time-switching EH policy. Fur-

ther, the authors propose two optimal charging policies, one for identical charging channels and the other for varying charging channels and then analyse the end-to-end outage probability for the proposed system using Monte Carlo simulations.

The authors in [19–21] consider simple network designs with one user device with energy harvesting capability and one base station. In [19], the authors analyse the stationery distribution of packets for an Energy Packet Network (EPN) model with multiclass data packets and the energy queues are multiserver queueus. Moreover, it is assumed that when a data packet arrives to a data queue, it routes a job of a given class according to one of the following disciplines: FCFS, preemptive Last Come First Served (LCFS), and Processor Sharing (PS). The authors then show that all the disciplines admit a product form solution for a given value of the probability at which an energy packet is sent to the data queue in case of jump-over blocking. For queueing networks whose routing matrix is a directed tree, the authors show that there exists a stochastic ordering to the probability at which an energy packet is sent to each data queue in case of jump-over blocking. Authors in [20], provide a mathematical framework to tackle the resource allocations problems for energy harvesting systems with delay QoS constraints to optimize the resources. Authors in [21], consider a two-queue model for optimising the value of information (VoI) in energy-harvesting sensor networks, with the focus on optimal transmission policy, the authors formulate the optimal control problem as a Markov Decision Process (MDP) with a level-dependent block-triangular transition probability matrix. They then, find the optimal policy which maximizes the mean VoI transmitted from the node in the long run and numerically show that it is of threshold type.

2.3 Summary

This chapter covered literature review of the background concepts considered in this research work. The concepts covered include; CR, NOMA, EH, and queueing theory. Apart from the background concepts, the chapter also reviews the relevant work that has already been done in literature and is of similar nature to the one done in this dissertation. The works presented have modelled and analysed the performance of different systems that incorporate a combination of the mentioned background concepts or technologies. System models covered include; CR-NOMA systems, CR-NOMA systems with EH, and queueing systems EH. Though a number of these system models have been studied in literature, to the best knowledge of the author, no work has been done around performance analysis of EH CR-NOMA aided IoT system, which caters for the stochastic nature of energy harvesting and the residual energy from one transmission frame to the next.

Chapter 3

Energy-Harvesting Cognitive Radio NOMA IoT Network

3.1 Introduction

This chapter presents the considered EH CR-NOMA IoT system in Fig. 3.1. The assumed frame structure for the considered system model is shown in Fig. 3.2. For ease of analysis, a simplified system model is presented in Fig. 3.3 with two CR-NOMA users and one primary network user. To cater for the stochastic nature of energy harvesting process and its evolution from one transmission frame to the next, energy levels are discretized in steps of Δ_p. Then, queuing theory is deployed to statistically represent each CR-NOMA Secondary User (SU) energy state from one transmission frame to the next. Each SU uplink transmit power P_n^s is chosen as the minimum between the evolved battery energy power and the primary network interference constraint.

Studies in literature that performed outage probability analysis are presented in Chapter 2, these include works in [5, 7, 9, 10]. The difference in outage analysis done in these studies as opposed to the one done in this dissertation is that; their system models do not include EH. The other related works include studies in [29–31], these studies considered system models with CR, NOMA, and EH as it is done in this dissertation. The primary difference aside from the studies focus on downlink analysis is that, the authors did not account for the resultant residual energy from one transmission frame to the next. This assumption does not consider the possible availability of residual energy from the previous transmission frame. In their case, the residual would occur when the harvested energy in the previous frame was not used up because of the interference constraint set to protect the primary network QoS.

In this dissertation, queueing theory and Markovian analysis concepts are used to cater for the residual energy from one transmission frame to the next. Markovian state transitions for each SU are on the basis of harvested energy, consumed energy for transmission power, and the residual energy left from previous frame. This is presented later in this chapter using battery energy evolution equation. Harvested energy is modelled in two ways: where the SU harvests from SBS and when energy harvesting is from both the SBS and MBS. To mathematically represent both scenarios, cumulative distribution function (CDF) expressions for energy harvesting of either case are computed to be able to accurately derive relevant state transition probability expressions. Once the state transition probabilities are derived, closed-form expressions for the probability of being in a particular energy level/state at each frame is computed to complete Markovian analysis of each SU.

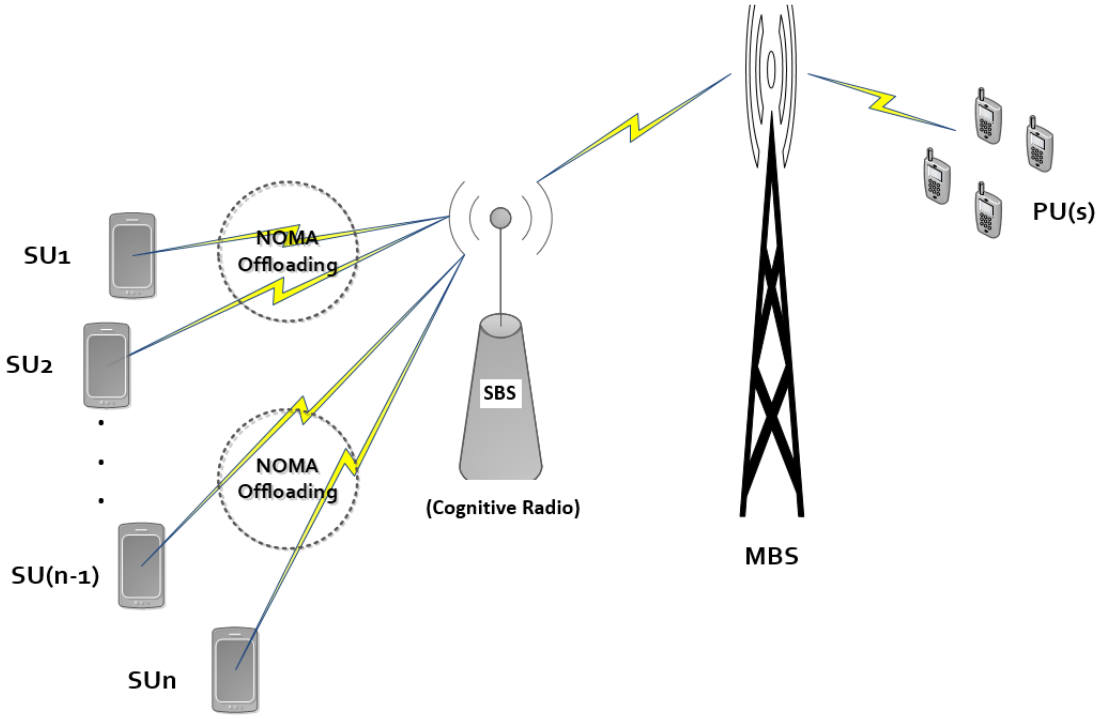


Figure 3.1: CR-NOMA IoT System

Key for Figure 3.1:

1. PUs: primary network users.
2. SUs: secondary network users.

3. Small Base-station (SBS) for the secondary network.

4. Macro Base-station (MBS) for the primary network.

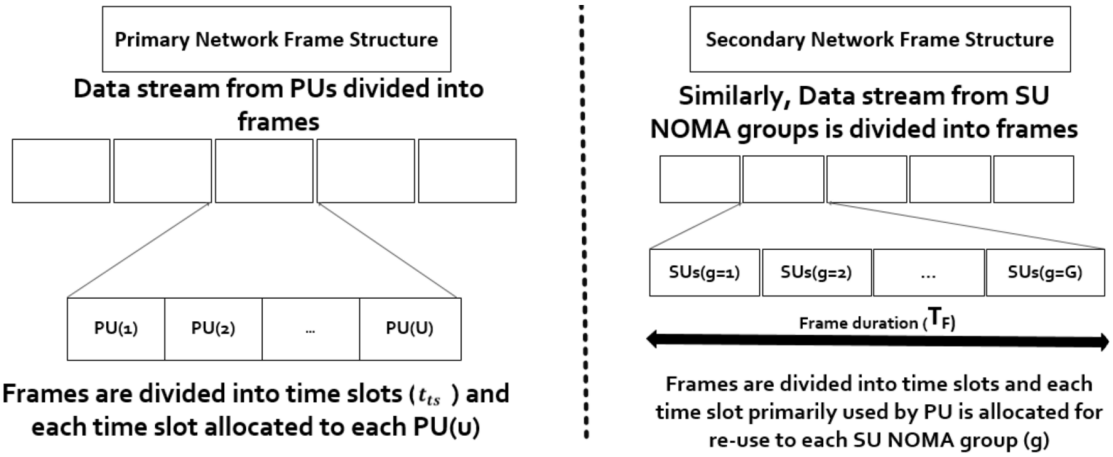


Figure 3.2: CR-NOMA IoT Frame Structure

Key for Figure 3.2:

1. T_F is the frame duration and t_{ts} is the time-slot within the frame duration. Assuming the use of Time Division Multiple Access technique, there are multiple time-slots t_{ts} within the frame duration.

2. g represents the index of the NOMA groups and can take values: {1, 2, . . . , U}, where U is the number of time-slots allocated to PUs in the primary network.

3.2 System Description

This research work considers a system model where an EH CR-NOMA enabled IoT network is studied. The considered system model is built of a primary network and a CR secondary network. The primary network is built of PUs and MBS. In the secondary network, there exists one SBS with cognitive radio capabilities and SUs. Fig. 3.1 represents the system model considered. The PUs are using the same frequency channel which is divided into different time-slots (i.e., Time Division Multiple Access, TDMA) of length t_{ts}, where t_{ts} is an element of {1,...,U}. PUs are allocated one time-slot t_{ts} which they share with a single NOMA group of SUs to perform cellular operations as shown in Fig. 3.2. SUs are assumed to be equipped with an antenna with energy harvesting capabilities. Further, the

Table 3.1: Table of Symbols

Symbol	Description
$\lambda_{H_1^p}$	uplink channel gain rate between SU_1 and MBS.
$\lambda_{H_2^p}$	uplink channel gain rate between SU_2 and MBS.
H_1^p	uplink power channel gain between SU_1 and MBS.
H_2^p	uplink power channel gain between SU_2 and MBS.
λ_{G^s}	uplink channel gain rate between PU and SBS.
G^s	uplink channel gain between PU and SBS.
$\lambda_{G^{SU_1}}$	downlink channel gain rate between SBS and SU_1 for energy harvesting.
$\lambda_{G^{SU_2}}$	downlink channel gain rate between SBS and SU_2 for energy harvesting.
G^{SU_1}	downlink power channel gain between SBS and SU_1 for energy harvesting.
G^{SU_2}	downlink power channel gain between SBS and SU_2 for energy harvesting.
$\lambda_{G_m^{SU_1}}$	downlink channel gain rate between MBS and SU_1 for energy harvesting.
$\lambda_{G_m^{SU_2}}$	downlink channel gain rate between MBS and SU_2 for energy harvesting.
$G_m^{SU_1}$	downlink power channel gain between MBS and SU_1 for energy harvesting.
$G_m^{SU_2}$	downlink power channel gain between MBS and SU_2 for energy harvesting.
$\lambda_{H_1^s}$	uplink channel gain rate between SU_1 and SBS.
$\lambda_{H_2^s}$	uplink channel gain rate between SU_2 and SBS.
H_1^s	uplink power channel gain between SU_1 and SBS.
H_2^s	uplink power channel gain between SU_2 and SBS.
P_n^s	uplink transmit power from SU_n to SBS, where n=1,2.
P^p	uplink transmit power from PU detected at the SBS reciever.
P^e	downlink transmit power from SBS to SUs for energy harvesting.
P^m	downlink transmit power from MBS to SUs for energy harvesting.
η	energy harvesting efficiency
σ^2	Additive White Gaussian Noise (AWGN) variance.
Ω^2	residual noise variance from SIC process.
Δ_p	battery power descritisation steps.
T_f	frame duration.
t_{ts}	transmission time-slot duration.
$(T_f - t_{ts})$	energy harvesting duration.
W	channel bandwidth.
t	frame index.

same SUs are grouped in pairs of two to facilitate NOMA grouping. It is further assumed that the SUs are harvesting energy from SBS and MBS downlink radio frequency transmissions, where the downlink transmissions are considered to be on a separate downlink frequency from the uplink.

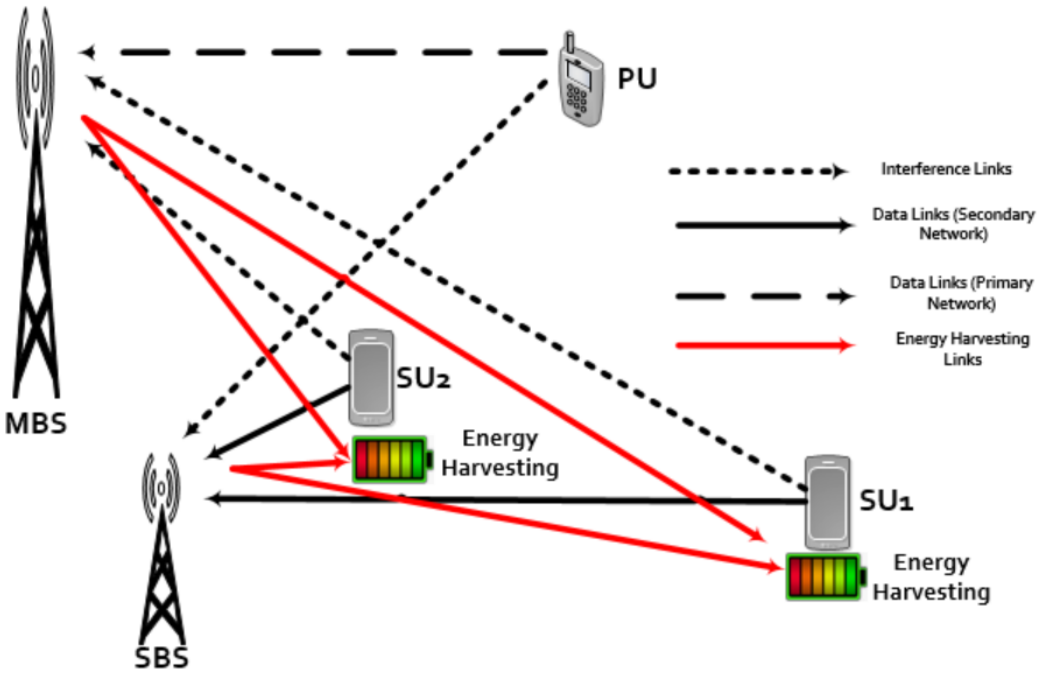


Figure 3.3: Energy Harvesting CR-NOMA IoT Network

For ease of analysis, we assume two SUs are connected to the SBS forming a single CR-NOMA group and one PU connected to the MBS as shown in Fig. 3.3. We also assume that the PU is performing its basic cellular operations and to improve spectrum utilization, SUs re-use the same uplink frequency time-slot allocated to the PU in the primary network. The PU is assumed to have two RF chains, one used for transmission on the allocated time-slot on the uplink frequency and the other used for reception on the allocated slot on the downlink frequency. To enhance spectrum efficiency, the two SUs use NOMA [38] to be able to simultaneously re-use the PU allocated time-slot to perform their uplink transmissions. It is further assumed that the SUs also have two RF chains, one operating on the uplink frequency for transmission in the allocated reused time-slot. The other RF chain operates in the downlink frequency, where it receives data on the allocated time-slot within the downlink frame, and switches to energy harvesting on the remainder of the frame duration. Moreover, we assume quasi-static network scenario, where the state of the PU and SUs remain unchanged for the duration of the time-slot.

In uplink CR-NOMA scenario, the two SUs transmit their signals towards the

SBS in the orthogonal block (using the same frequency and at the same time). Each SU transmits its individual signal x_n where $n = 1$ for SU_1 and $n = 2$ for SU_2. This is done with a transmit power of P_n^s, such that the received signal at the SBS in the t^{th} frame can be defined as shown in Equation (3.1) below. The detected PU transmit power at the SBS is represented as P^p and its signal symbol as x_p:

$$y(t) = \sum_{n=1}^{2} \sqrt{P_n^s(t) H_n^s(t)} x_n + \sqrt{P^p(t) G^s(t)} x_p + w(t), \tag{3.1}$$

where $w(t)$ is AWGN with variance of σ^2.

In CR-NOMA, SUs are operated in power-controlled mode and PUs in full power allocated mode. The SBS receiver must have SIC capability to be able to decode received signals from multiple users by first ordering the received signals in descending order on the basis of their relative signal strength, then apply successive interference cancellation to extract and decode the symbols.

In order to guarantee the QoS requirements for the primary network, the instantaneous transmit power of the SUs must be kept below MBS receiver maximum tolerable interference constraint I_{it}^{tot}. Note that total interference as seen by MBS is the total interference from both SUs. Thus, to guarantee QoS of the primary network, transmit power of SUs is constrained as follows:

$$\sum_{n=1}^{2} P_n^s(t) * H_n^p(t) \leqslant I_{it}^{tot}. \tag{3.2}$$

For simplicity, an assumption is made that the interference from each SU should be constrained by half the total interference component above. Thus decoupling the interference from the SUs, the transmit power of SUs is constrained as follows, where $I_{it} = \frac{I_{it}^{tot}}{2}$:

$$P_n^s(t) * H_n^p(t) \leqslant I_{it}. \tag{3.3}$$

Accordingly, P_n^s is selected as follows:

$$P_n^s(t) = min\left(B_n(t), \frac{I_{it}}{H_n^p(t)}\right), \tag{3.4}$$

where:

- $B_n(t)$ is the available battery power of the n^{th} secondary user in the NOMA group during the t^{th} frame index.

Battery energy evolution for each SU is represented as follows, in which t^{th} indexing is at the beginning of the frame.

$$b_n(t) = min\{max\{b_n(t-1) + e_n^H(t-1) - P_n^s(t-1) \times t_{ts}, 0\}, B^{max}\}, \quad (3.5)$$

where $e_n^H(t-1)$ is the energy harvested by SU_n in frame index $(t-1)$ and the battery power $B_n(t)$ depicted in Equation (3.4) is computed as $B_n(t) = \frac{b_n(t)}{t_{ts}}$. $b_n(t-1)$ represents the available battery energy at the beginning of $(t-1)$ frame, and $P(t-1)$ is transmit power used during $(t-1)$ frame index.

The instantaneous transmission rate R_n for SU_n at frame t is expressed as follows, using Shannon channel capacity theorem [38, 39]:

$$R_n(t) = Wlog_2\left(1 + \delta_{I_n}(t)\right), \quad (3.6)$$

where W is the channel bandwidth and δ_{In} represents instantaneous Signal to Interference and Noise Ratio (SINR) for each CR-NOMA user SU_n.

The generalized expression for instantaneous SINR at the SBS is derived as follows for each user SU_n in the NOMA group. Note that since SU_2 symbol is received with larger power, SBS decodes x_2 first by treating x_1 and x_p in Equation (3.1) as interference. Then, decodes SU_1 symbol x_1 using SIC technique. The received decoded signals for each SU at the SBS is represented as follows, similar to [69]:

Decoded signal for SU_1:

$$y_1(t) = \sqrt{P_1^s(t)H_1^s(t)}x_1 + (x_2 - \bar{x}_2)\sqrt{P_2^s(t)H_2^s(t)}x_2 + \sqrt{P^p(t)G^s(t)}x_p + w(t), \quad (3.7)$$

where:

- $\bar{x}_2$ is the decoded x_2, in which there is imperfect SIC when $\bar{x}_2 \neq x_2$ and perfect SIC when $\bar{x}_2 = x_2$.

Decoded signal for SU_2:

$$y_2(t) = \sqrt{P_2^s(t)H_2^s(t)}x_2 + \sqrt{P_1^s(t)H_1^s(t)}x_1 + \sqrt{P^p(t)G^s(t)}x_p + w(t). \quad (3.8)$$

Using Equations (3.7) and (3.8), instantaneous SINR expressions for each SU are defined as follows:

$$\delta_{I_n}(t) = \begin{cases} \frac{P_1^s(t)H_1^s(t)}{E(|x_2 - \bar{x}_2|^2)P_2^s(t)H_2^s(t) + P^p(t)G^s(t) + \sigma^2}, & n = 1 \\ \\ \frac{P_2^s(t)H_2^s(t)}{P_1^s(t)H_1^s(t) + P^p(t)G^s(t) + \sigma^2}, & n = 2 \end{cases} \quad (3.9)$$

Modelling $E(|x_2-\bar{x}_2|^2)P_2^s(t)H_2^s(t)$ as a Gaussian random variable with variance of Ω^2 as in [70–72], where $E(\cdot)$ denotes the expected value. Equation (3.9) can be reduced to the below expression:

$$\delta_{I_n}(t) = \begin{cases} \frac{P_1^s(t)H_1^s(t)}{P^p(t)G^s(t)+\Omega^2+\sigma^2}, & n=1 \\ \\ \frac{P_2^s(t)H_2^s(t)}{P_1^s(t)H_1^s(t)+P^p(t)G^s(t)+\sigma^2}, & n=2 \end{cases} \tag{3.10}$$

The aim of this work is to accurately determine closed-form expressions for each SU outage probability and mean capacity (which can be computed from Equation (3.6) above). Outage probability is defined as the probability that the instantaneous SINR is less than some set system threshold/target SINR δ_n. Analytically this can be expressed as follows using Equation (3.10) for each SU:

$$P_{out}^n(t) = \begin{cases} \frac{P_1^s(t)H_1^s(t)}{P^p(t)G^s(t)+\Omega^2+\sigma^2} < \delta_1, & n=1 \\ \\ \frac{P_2^s(t)H_2^s(t)}{P_1^s(t)H_1^s(t)+P^p(t)G^s(t)+\sigma^2} < \delta_2, & n=2 \end{cases} \tag{3.11}$$

To be able to mathematically model the considered system outage probability and mean capacity, we need to derive closed-form expressions for both outage probability and mean capacity. For mean capacity analysis, it is assumed that SUs always have data to transmit.

3.2.1 Computing SU_1 Outage Probability and Mean Capacity:

We start with showing the complexity of deducing closed-form analytical expression for outage probability and mean capacity. Then, we present how Markovain analysis approach adopted in this dissertation allows us to derive exact solutions for both performance metrics.

a) Outage Probability:
Using Equation (3.11), outage probability for SU_1 is directly computed as follows:

$$
\begin{aligned}
P^1_{out}(t) &= Pr\left(\frac{P^s_1(t)H^s_1(t)}{P^p(t)G^s(t)+\Omega^2+\sigma^2} < \delta_1\right), \\
&= 1 - Pr\left(P^s_1(t) \geq \frac{\delta_1\left(P^p(t)G^s(t)+\Omega^2+\sigma^2\right)}{H^s_1(t)}\right), \\
&= 1 - \int_0^\infty \int_0^\infty \left(1 - F_{P^s_1(t)}\left(\frac{\delta_1\left(P^p(t)y+\Omega^2+\sigma^2\right)}{x}\right)\right) \\
&\times f_{G^s(t)}(y) f_{H^s_1(t)}(x)\; dydx,
\end{aligned}
\tag{3.12}
$$

where $f_{G^s(t)}(y)$ and $f_{H^s_1(t)}(x)$ are the Probability Density Functions (PDFs) of the exponential random variables $G^s(t)$ and $H^s_1(t)$, respectively. $F_{P^s_1(t)}(\cdot)$ is the Cumulatively Distribution Function (CDF) for the random variable $P^s_1(t)$.

The complication that arises when trying solve Equation (3.12) is that $P^s_1(t)$ is selected as $P^s_1(t) = min\left(\frac{b_1(t)}{t_{ts}}, \frac{I_{it}}{H^p_1}\right)$ in Equation (3.4). This brings a situation in which $P^s_1(t)$ becomes a correlated random variable, where there is dependency between $P^s_1(t)$ and $P^s_1(t-1)$. Equation (3.13) below presents the dependency stated:

$$
\begin{aligned}
P^s_1(t) &= min\left(\frac{b_1(t)}{t_{ts}}, \frac{I_{it}}{H^p_1}\right), \\
&= min\left(\frac{b_1(t-1) + e^{EH}_1(t-1) - P^s_1(t-1)\times t_{ts}}{t_{ts}}, \frac{I_{it}}{H^p_1}\right).
\end{aligned}
\tag{3.13}
$$

The above expression in Equation (3.13) confirming the dependency of $P^s_1(t)$ on $P^s_1(t-1)$ is obtained using battery energy evolution Equation (3.5) as the basis. The dependency of $P^s_1(t)$ on $P^s_1(t-1)$ observed in Equation (3.13) above, makes it very difficult to find the CDF of $P^s_1(t)$ ($F_{P^s_1(t)}(x)$) which is required to solve the expression $P^1_{out}(t)$ for outage probability.

Assuming one is able to find the complex CDF expression for $P^s_1(t)$, that expression would need to be multiplied by the PDFs of the exponential random variables G^s and H^s_1. Then, integrate the resulting product expression twice as shown in Equation (3.12). Overall it would be very complicated to find the exact analytical expression for $P^1_{out}(t)$ following this direct route.

b) Mean Capacity:

Using Equation (3.6), mean capacity for SU_1 is directly computed as follows using similar approach as in [73]:

$$\begin{aligned} C_1(t) =& W \times log_2\left(1+\delta_{I_1}(t)\right), \\ =& W \int_0^\infty log_2\left(1+y\right) f_{\delta_{I_1}(t)}(y)\, dy, \\ =& \frac{W}{log_e(2)} \int_0^\infty \frac{1-F_{\delta_{I_1}(t)}(y)}{1+y}\, dy. \end{aligned} \tag{3.14}$$

Deducing the expression for mean capacity requires finding CDF of SINR $F_{\delta_{I_1}(t)}(y)$. SINR expression for SU_1 contains the random variable $P_1^s(t)$ as shown in Equation (3.10). Finding the CDF of SINR ($F_{\delta_{I_1}(t)}(y)$) requires computing the CDF for $P_1^s(t)$ as shown below:

$$\begin{aligned} F_{\delta_{I_1}(t)}(y) &= Pr\left(\frac{P_1^s(t)H_1^s(t)}{P^p(t)G^s(t)+\Omega^2+\sigma^2} \leqslant y\right), \\ &= 1 - Pr\left(\frac{P_1^s(t)H_1^s(t)}{P^p(t)G^s(t)+\Omega^2+\sigma^2} > y\right), \\ &= 1 - Pr\left(P_1^s(t) > y\left(\frac{P^p(t)G^s(t)+\Omega^2+\sigma^2}{H_1^s(t)}\right)\right), \\ &= 1 - \int_0^\infty \int_0^\infty \left(1 - F_{P_1^s(t)}\left(y\left(\frac{P^p(t)x+\Omega^2+\sigma^2}{z}\right)\right)\right) \\ &\times f_{G^s(t)}(x) f_{H_1^s(t)}(z)\, dxdz, \end{aligned} \tag{3.15}$$

where $f_{G^s(t)}(x)$ and $f_{H_1^s(t)}(z)$ are the PDFs of the exponential random variables $G^s(t)$ and $H_1^s(t)$, respectively. $F_{P_1^s(t)}(\cdot)$ is the CDF for the random variable $P_1^s(t)$, similar to Equation (3.12).

As shown in Equation (3.15), finding the CDF of $F_{\delta_{I_1}(t)}(y)$ requires computing the CDF of $P_1^s(t)$. Equation (3.13) has already shown the complex probability expression that one would need to solve in order to find the CDF of $P_1^s(t)$. Finding $F_{\delta_{I_1}(t)}(y)$ is further complicated by the double integrals that would need to be applied on the product of the CDF of $P_1^s(t)$ and PDFs of the exponential random variables $G^s(t)$ and $H_1^s(t)$. This highlights how complicated it would be to deduce $F_{\delta_{I_1}(t)}(y)$. Assuming $F_{\delta_{I_1}(t)}(y)$ is deduced, to finally compute closed-form expression for mean capacity, there is still a requirement to integrate one minus the complex $F_{\delta_{I_1}(t)}(y)$ expression divided by $(1+y)$ as shown in Equation (3.14) above.

3.2.2 Computing SU_2 Outage Probability and Mean Capacity:

Similar to SU_1 case, we first show the complexity of directly deducing closed-form analytical expression for outage probability and mean capacity for SU_2.

a) Outage Probability:
SU_2 outage probability is deduced as follows:

$$\begin{aligned}
P^2_{out}(t) &= Pr\left(\frac{P^s_2(t)H^s_2(t)}{P^s_1(t)H^s_1(t)+P^p(t)G^s(t)+\sigma^2} < \delta_2\right), \\
&= 1 - Pr\left(P^s_2(t)H^s_2(t) - \delta_2\left(P^s_1(t)H^s_1(t)+P^p(t)G^s(t)\right) \geq \delta_2\sigma^2\right), \\
&= 1 - Pr\left(P^s_2(t) \geq \delta_2\left(\frac{P^s_1(t)H^s_1(t)+P^p(t)G^s(t)+\sigma^2}{H^s_2(t)}\right)\right), \\
&= 1 - Pr\left(P^s_2(t) \geq \delta_2\left(\frac{P^s_1(t)H^s_1(t)+P^p(t)G^s(t)+\sigma^2}{H^s_2(t)}\right)\right), \\
&= 1 - \int_0^{\frac{I_{it}}{H^p_1}}\left[\int_0^\infty\int_0^\infty\int_0^\infty\left(1 - F_{P^s_2(t)}\left(\delta_2\left(\frac{xy+P^p(t)z+\sigma^2}{w}\right)\right)\right)\right. \\
&\left.\times f_{H^s_1(t)}(y)f_{G^s(t)}(z)f_{H^s_2(t)}(w)\,dydzdw\right] f_{P^s_1(t)}(x)\,dx,
\end{aligned} \tag{3.16}$$

where $f_{P^s_1(t)}(x)$, $f_{H^s_1(t)}(y)$, $f_{G^s(t)}(z)$ and $f_{H^s_2(t)}(w)$ are the PDFs of the random variables $P^s_1(t)$, $H^s_1(t)$, $G^s(t)$ and $H^s_2(t)$, respectively. $F_{P^s_2(t)}(\cdot)$ is the CDF for the random variable $P^s_2(t)$. Note that the random variable $P^s_1(t)$ can take range of values $\left[0, \frac{I_{it}}{H^p_1}\right]$ on the basis of Equation (3.4), hence x integration limits are $\left[0, \frac{I_{it}}{H^p_1}\right]$.

To find the closed-form expression for $P^2_{out}(t)$, it is required that the CDF of $P^s_2(t)$ and the PDFs of $P^s_1(t)$, $H^s_1(t)$, $G^s(t)$, and $H^s_2(t)$ are derived as shown in Equation (3.16). Using the same argument as in SU_1 outage probability, directly finding the CDF expression for $P^s_2(t)$ is very complicated. The complication is brought by the dependency of $P^s_2(t)$ on $P^s_2(t-1)$, this is the similar case for SU_1 as articulated in the previous section for $P^s_1(t)$. Deducing SU_2 outage probability is further complicated by the fact that we would still need to find the PDF for $P^s_1(t)$, which similar to its CDF is very complicated to derive. SU_2 outage probability is overly complicated by the need to solve for the four specified integrals in Equation (3.16).

b) Mean Capacity:

Using Equation (3.6), mean capacity expression for SU_2 is computed directly as follows, using similar approach as in [73]:

$$\begin{aligned} C_2(t) =& W \times log_2\left(1+\delta_{I_2}(t)\right), \\ =& W \int_0^{\infty} log_2\left(1+y\right) f_{\delta_{I_2}(t)}(y)\, dy, \\ =& \frac{W}{log_e(2)} \int_0^{\infty} \frac{1-F_{\delta_{I_2}(t)}(y)}{1+y}\, dy. \end{aligned} \tag{3.17}$$

To find an exact solution for SU_2 mean capacity as shown in Equation (3.17) requires finding the CDF expression for SINR of SU_2. CDF of SINR for SU_2 is derived as follows:

$$\begin{aligned} F_{\delta_{I_2}(t)}(y) &= Pr\left(\frac{P_2^s(t)H_2^s(t)}{P_1^s(t)H_1^s(t)+P^p(t)G^s(t)+\sigma^2} \leqslant y\right), \\ &= 1 - Pr\left(P_2^s(t) > y\left(\frac{P_1^s(t)H_1^s(t)+P^p(t)G^s(t)+\sigma^2}{H_2^s(t)}\right)\right), \\ &= 1 - \int_0^{\frac{I_{it}}{H_1^p}} \Bigg[\int_0^{\infty}\int_0^{\infty}\int_0^{\infty}\left(1-F_{P_2^s(t)}\left(y\left(\frac{xv+P^p(t)z+\sigma^2}{w}\right)\right)\right) \\ &\times f_{H_1^s(t)}(v) f_{G^s(t)}(z) f_{H_2^s(t)}(w)\; dvdzdw\Bigg] f_{P_1^s(t)}(x)\; dx, \end{aligned} \tag{3.18}$$

where $f_{P_1^s(t)}(x)$, $f_{H_1^s(t)}(v)$, $f_{G^s(t)}(z)$ and $f_{H_2^s(t)}(w)$ are the PDFs of the random variables $P_1^s(t)$, $H_1^s(t)$, $G^s(t)$ and $H_2^s(t)$, respectively. $F_{P_2^s(t)}(\cdot)$ is the CDF for the random variable $P_2^s(t)$. Note that the random variable $P_1^s(t)$ can take range of values $\left[0, \frac{I_{it}}{H_1^p}\right]$ on the basis of Equation (3.4), hence x integration limits are $\left[0, \frac{I_{it}}{H_1^p}\right]$.

Finding the CDF for SINR of SU_2, $F_{\delta_{I_2}(t)}(y)$, requires us to find the CDF of $P_2^s(t)$ as well as the PDF of $P_1^s(t)$ as shown in Equation (3.18). Due to the dependency of $P_1^s(t)$ and $P_2^s(t)$ on $P_1^s(t-1)$ and $P_2^s(t-1)$, respectively, it is very difficult to derive the distributions for $P_1^s(t)$ and $P_2^s(t)$ as it has already been explained in the previous paragraphs in this chapter. Deriving exact solution for $F_{\delta_{I_2}(t)}(y)$ is further complicated by the need to solve for the four integrals shown in Equation (3.18). To find the final closed-form expression for mean capacity, it required that the integral of one minus $F_{\delta_{I_2}(t)}(y)$ divided by $(1+y)$ is computed,

this final integral further complicates finding the exact solution for SU_2 mean capacity.

3.2.3 Assumptions Made in Literature

Multiple similar works in literature have made some assumptions to simplify their derivations of outage probability closed-form expressions. Authors in [5, 7, 9, 10], considered system models with CR and NOMA without the consideration of EH. In their analysis power selection was defined as: $P_t = min\left(\frac{I_{it}}{H}, P_{max}\right)$, where H is the channel power gain and P_{max} is the maximum possible transmit power that can be attained by the transmitter. Different to our case, P_{max} is a constant. Substituting P_{max} for P_1^s and P_2^s in our SINR expressions for SUs result in the following simpler expressions to deal with for both SU_1 and SU_2 outage probabilities:

For SU_1:

$$\begin{aligned} P_{out}^1(t) &= Pr\left(\frac{P_{max}(t)H_1^s(t)}{P^p(t)G^s(t)+\Omega^2+\sigma^2} < \delta_1\right), \\ &= 1 - Pr\left(H_1^s(t) > \frac{\delta_1\left(P^p(t)G^s(t)+\Omega^2+\sigma^2\right)}{P_{max}(t)}\right), \\ &= 1 - \int_0^\infty \left(1 - F_{H_1^s(t)}\left(\frac{\delta_1\left(P^p(t)y+\Omega^2+\sigma^2\right)}{P_{max}(t)}\right)\right) f_{G^s(t)}(y)\ dy. \end{aligned} \tag{3.19}$$

For SU_2:

$$\begin{aligned} P_{out}^2(t) &= Pr\left(\frac{P_{max}(t)H_2^s(t)}{P_{max}(t)H_1^s(t)+P^p(t)G^s(t)+\sigma^2} < \delta_2\right), \\ &= 1 - Pr\left(P_{max}(t)H_2^s(t) - \delta_2\left(P_{max}(t)H_1^s(t)+P^p(t)G^s(t)\right) > \delta_2\sigma^2\right), \\ &= 1 - Pr\left(H_2^s(t) > \delta_2\left(\frac{P_{max}(t)H_1^s(t)+P^p(t)G^s(t)+\sigma^2}{P_{max}(t)}\right)\right), \\ &= 1 - \int_0^\infty\int_0^\infty \left(1 - F_{H_2^s(t)}\left(\delta_2\left(\frac{P_{max}(t)y+P^p(t)x+\sigma^2}{P_{max}(t)}\right)\right)\right) \\ &\times f_{H_1^s(t)}(y) f_{G^s(t)}(x)\ dydx. \end{aligned} \tag{3.20}$$

As shown in Equations (3.19) and (3.20), excluding EH in our system model would have greatly reduced the complexity of our expressions. This is attained by eliminating the requirement to find complex CDFs of recursively dependent random variables P_1^s and P_2^s, while also reducing the number of integrals we would be required to deal with. SU_1 outage is reduced to only finding distributions for simple exponential random variables (H_1^s and G^s) and one integral to solve. Also

for SU_2, the only distributions we would need to find are for simple exponential random variables (H_1^s, H_2^s, and G^s). The integrals to solve would be reduced from four to two integrals of independent random variables. These studies [5,7,9,10] did not work on mean capacity analysis, but by the same token, their assumptions and exclusion of EH would have resulted in less complex mean capacity expressions to solve for our considered system model.

The studies in [29–31] considered system models similar (with CR, NOMA, and EH) to the one considered in this dissertation, though their analyses are on the downlink. Note that, since these studies have considered all the technologies considered in the system model for this dissertation, outage and mean capacity expressions structure will stay the same as in Equations (3.12), (3.14), (3.16), and (3.17). The power selection in these studies is determined as follows: $P_t = min\left(\frac{I_{it}}{H}, P_{EH}\right)$, where in their case P_{EH} is the harvested energy in the current transmission frame, I_{it} is the inteference threshold, and H is the channel power gain. Unlike in the previous discussion where P_{max} is a constant, P_{EH} is an exponential random variable. Different to the work in this dissertation, P_{EH} in these studies is not evolving. Using P_{EH} for $P_1^s(t)$ and $P_2^s(t)$ in our case would render both random variables not dependent on $P_1^s(t-1)$ and $P_2^s(t-1)$, respectively. Removing recursive dependence for the transmit powers ($P_1^s(t)$ and $P_2^s(t)$) will reduce the complexity of finding their distributions. The reduced complexity would be that $P_1^s(t)$ and $P_2^s(t)$ would now be treated as simple exponential random variables. With $P_1^s(t)$ and $P_2^s(t)$ reduced to simple exponential random variables, it becomes easy to find their distributions, thus, reducing overall complexity of solving outage and mean capacity expressions.

3.2.4 This Dissertation Approach

The approach used in this dissertation is to discretize battery energy $b_n(t)$ and then, find the exact expressions for outage probability and mean capacity at the discrete $b_n(t)$ values. Total outage probability and mean capacity are each found by averaging across all the discrete levels of $b_n(t)$. This is achieved by doing Markovian analysis of the battery evolution across the discrete $b_n(t)$ values for each SU. To do this, each discrete battery level is treated as the SU Markovian state for our analysis. With this approach, the final expressions for outage and mean capacity are as follows:

SU_1 Outage Probability and Mean Capacity:

$$P_{out}^{1,total}(t) = \sum_{i=0}^{\frac{B^{max}}{\Delta_p}} P_{out}^{1}(i)\Pi(j), \tag{3.21}$$

$$C_1(t) = \sum_{i=0}^{\frac{B_{max}}{\Delta_p}} C_1(i) \times \Pi(j). \tag{3.22}$$

SU_2 Outage Probability and Mean Capacity:

$$P_{out}^{2,total}(t) = \sum_{i=0}^{\frac{B^{max}}{\Delta_p}} \sum_{j=0}^{\frac{B^{max}}{\Delta_p}} P_{out}^{2}(i,j)\Pi(k,l), \tag{3.23}$$

$$C_2(t) = \sum_{i=0}^{\frac{B_{max}}{\Delta_p}} \sum_{j=0}^{\frac{B_{max}}{\Delta_p}} C_2(i,j) \times \Pi(k,l). \tag{3.24}$$

For SU_1, Equations (3.21) and (3.22) have a variable $\Pi(j)$ in their expressions. $\Pi(j)$ is the probability of SU_1 being in battery state (j). Thus, to find the closed-form expression for SU_1 outage and mean capacity we need to solve for $\Pi(j)$. Similarly for SU_2, the expressions for outage and mean capacity contain $\Pi(k,l)$ as shown in Equations (3.23) and (3.24). Since our considered system uses NOMA, outage and mean capacity expressions for SU_2 depends on both SUs transmit powers, $\Pi(k,l)$ is the joint probability that SU_1 is in state (k) when SU_2 is in state (l). To solve for both outage and mean capacity for SU_2, it is required that $\Pi(k,l)$ is determined. Markovain analysis is used to determine analytical expressions for both $\Pi(j)$ and $\Pi(k,l)$.

The following Section 3.3 performs Markovian analysis for both SU_1 and SU_2 to determine $\Pi(j)$ and $\Pi(k,l)$. Chapter 4 of this dissertation focuses on deriving outage probability for both SUs, using Markovian analysis as the basis. In Chapter 5, closed-form mean capacity expressions for each SU are derived using Markovian analysis as the basis as well.

3.3 System Markov Analysis

The considered system model Markovian analysis for each SU is built by modelling the battery storage of each SU as a queue, where the queue levels are represented

by discretizing the energy within the batteries into multiple energy chunks. Each energy chunk represents SU system state where we index each SU state by the number of chunks in its energy queue. The indexing starts from zero energy chunks to the maximum number of energy chunks that the SU battery capacity can store.

3.3.1 System Markov Analysis With Respect to SU_1

Assuming a time-slotted system, Markovian state of SU_1 is defined by $i = \{0, 1, 2, ..., \left\lceil \frac{B^{max}}{\Delta_p} \right\rceil\}$, where i represents available energy chunks of SU_1 at the frame index t. SU_1 transitions from one state to another are characterized as $\xi(t) = \{0, 1\}$, depending on whether SU_1 transmit power is conditioned on available battery chunks or interference constraint as shown in Equation (3.4). Mathematically SU_1 state transitions are characterized as follows for each condition:

$\xi(t) = \{0, 1\}$,

where:

- $\xi(t) = \xi_0 = 0$ when $\frac{b_n(t)}{t_{ts}} < \frac{I_{it}}{H_n^p(t)}$.
- $\xi(t) = \xi_1 = 1$ when $\frac{b_n(t)}{t_{ts}} \geq \frac{I_{it}}{H_n^p(t)}$.

The above conditions are on the basis of Equation (3.4) for selecting of the appropriate transmit power to use at each frame index. We assume the two possible transmit power selections ($\frac{b_n(t)}{t_{ts}}$ and $\frac{I_{it}}{H_n^p}$) are discretized in steps (or chunks) of Δ_p, then the transmit power for SU_1 is computed as follows for each condition:

for $\xi_0 = 0$:

$$P_n^s = \frac{b_n(t)}{t_{ts}} = \frac{i}{t_{ts}}\Delta_p, \tag{3.25}$$

and for $\xi_1 = 1$:

$$P_n^s = (\frac{I_{it}}{H_n^p}) = \frac{n_{I_1}}{t_{ts}}\Delta_p, \tag{3.26}$$

where:

- n_{I_1} is the battery power conditioned on tolerable interference constraint I_{it} from Equation (3.3).

Modeling battery energy storage at SU_1 as a queuing system, the battery energy evolution can be presented by the below equation:

$$b_1(t) = min\{max\{b_1(t-1) + e_1^H(t-1) - P_1^s(t-1) \times t_{ts}, 0\}, B^{max}\}. \quad (3.27)$$

To build the Markovian model of SU_1, we need to find the closed-form expression for the probability of SU_1 transitioning from one energy state to another. The transition from state i (battery energy index) at frame index $(t-1)$ to state j (battery energy index) at frame index (t) is defined as follows for $\xi_0 = 0$ (where the transmit power is conditioned using available energy chunks): $j = i + \frac{e_1^H}{\Delta_p} - i = \frac{e_1^H}{\Delta_p}$, using energy queue evolution Equation (3.27), in which $P_1^s(t-1) \times t_{ts} = b_1(t-1) = i$ and $b_1(t) = j$. Thus, the state transition probability for $\xi_0 = 0$ is expressed as follows:

$$Q_{\xi_0}(i,j) = Pr(j = \frac{e_1^H}{\Delta_p}, \xi = 0). \quad (3.28)$$

To find closed-form expression for Equation (3.28) above, we need the expression for e_1^H. Since e_1^H is an exponential random variable, we need to derive its CDF to be able to obtained a closed-form expression for the transition probability expression in Equation (3.28). Deriving of e_1^H distribution is done in the following subsections where we derive the CDF expressions when SU_1 is harvesting energy from SBS and also when SU_1 is harvesting from both SBS and MBS.

3.3.1.1 SU_1 Energy Harvesting from SBS

(i) Case: $\xi = 0$

The harvested energy by SU_1 at the t^{th} frame duration T_F is expressed as follows similar to [74]:

$$e_1^H(t) = \eta P^e(t) G^{SU_1}(t)(T_F - t_{ts}). \quad (3.29)$$

From Equation (3.29) above, CDF $F_{e_1^H}(y)$ of energy harvested by SU_1 is derived as follows:

$$\begin{aligned} F_{e_1^H}(y) &= Pr(e_1^H \leqslant y), \\ &= Pr\left(\eta P^e(t) G^{SU_1}(t)(T_F - t_{ts}) \leqslant y\right), \\ &= Pr\left(G^{SU_1}(t) \leqslant \frac{y}{\eta P^e(t)(T_F - t_{ts})}\right), \\ &= F_{G^{SU_1}(t)}\left(\frac{y}{\eta P^e(t)(T_F - t_{ts})}\right). \end{aligned} \quad (3.30)$$

Since $G^{SU_1}(t)$ is an exponentially distributed random variable (RV), $F_{e_1^H}(y)$ is also an exponentially distributed function and can be expressed as follows:

$$F_{e_1^H}(y) = 1 - e^{-\left(\frac{y}{\eta P^e(t)(T_F - t_{ts})}\right)\lambda_{G^{SU_1}}}. \tag{3.31}$$

Thus, using Equations (3.28) and (3.31) we have:

$$\begin{aligned}
Q_{\xi_0}(i,j) &= Pr(j\Delta_p = e_1^H, \xi = 0), \\
&= Pr\left(e_1^H = j\Delta_p\right) Pr\left(i < n_{I1}\right), \\
&= \left(\left(1 - e^{-\left(\frac{(j+1)\Delta_p}{\eta P^e(t)(T_F - t_{ts})}\right)\lambda_{G^{SU_1}}}\right) - \left(1 - e^{-\left(\frac{j\Delta_p}{\eta P^e(t)(T_F - t_{ts})}\right)\lambda_{G^{SU_1}}}\right)\right) \\
&\times \left(1 - e^{-\left(\frac{\lambda_{H_1^p} I_{it} t_{ts}}{i\Delta_p}\right)}\right), \\
&= \left(e^{-\left(\frac{j\Delta_p \lambda_{G^{SU_1}}}{\eta P^e(t)(T_F - t_{ts})}\right)} - e^{-\left(\frac{(j+1)\Delta_p \lambda_{G^{SU_1}}}{\eta P^e(t)(T_F - t_{ts})}\right)}\right) \times \left(1 - e^{-\left(\frac{\lambda_{H_1^p} I_{it} t_{ts}}{i\Delta_p}\right)}\right).
\end{aligned} \tag{3.32}$$

(ii) Case: $\xi = 1$

Similarly, for $\xi = 1$ (when the SU transmit power is conditioned on interference threshold I_{it}): $j = i + \frac{e_1^H}{\Delta_p} - n_{I_1} => j - i = \frac{e_1^H}{\Delta_p} - n_{I_1}$ using energy evolution in Equation (3.27), where in this case: $P_1^s(t-1) \times t_{ts} = n_{I_1}$, $b_1(t-1) = i$ and $b_1(t) = j$. Hence, the state transition probability from i to j for this case is expressed as follows:

$$Q_{\xi_1}(i,j) = Pr(j - i = \frac{e_1^H}{\Delta_p} - n_{I_1}, \xi = 1), \tag{3.33}$$

using Equation (3.33) above, the expression for $Q_{\xi_1}(i,j)$ is derived as follows:

$$
\begin{aligned}
Q_{\xi_1}(i,j) &= Pr(j-i = \frac{e_1^H}{\Delta_p} - n_{I_1}, \xi = 1), \\
&= Pr\left(j-i = \frac{e_1^H}{\Delta_p} - n_{I_1}, i \geq n_{I_1}\right), \\
&= Pr\left(e_1^H = (j-i+n_{I_1})\,\Delta_p, i \geq n_{I_1}\right), \\
&= \sum_{n_{I_1}=0}^{i} Pr\left(e_1^H = (j-i+n_{I_1})\,\Delta_p\right) \\
&\times \left(e^{-\left(\frac{\lambda_{H_1^p} I_{it} t_{ts}}{(n_{I_1}+1)\Delta_p}\right)} - e^{-\left(\frac{\lambda_{H_1^p} I_{it} t_{ts}}{n_{I_1}\Delta_p}\right)} \right), \\
&= \sum_{n_{I_1}=0}^{i} \left(e^{-\left(\frac{(j-i+n_{I_1})\Delta_p \lambda_{G^{SU_1}}}{\eta P^e(t)(T_F - t_{ts})}\right)} - e^{-\left(\frac{(j-i+n_{I_1}+1)\Delta_p \lambda_{G^{SU_1}}}{\eta P^e(t)(T_F - t_{ts})}\right)} \right) \\
&\times \left(e^{-\left(\frac{\lambda_{H_1^p} I_{it} t_{ts}}{(n_{I_1}+1)\Delta_p}\right)} - e^{-\left(\frac{\lambda_{H_1^p} I_{it} t_{ts}}{n_{I_1}\Delta_p}\right)} \right).
\end{aligned}
\tag{3.34}
$$

(iii) Joint Transition:

SU_1 transition probability from state i to state j is the summation of the above derived mutually-exclusive conditional transition probabilities in Equations (3.32) and (3.34) using probability sum rule. Thus, SU_1 transition probability from state i to state j can be expressed as follows:

$$
Q(i,j) = Q_{\xi_0}(i,j) + Q_{\xi_1}(i,j), \tag{3.35}
$$

using Equation (3.35) above and Markovian analysis, we can be able to solve for the steady state probability that SU_1 is in state j as follows:

$$
\Pi(j) = \sum_{i=0}^{\frac{B^{max}}{\Delta_p}} Q(i,j) * \Pi(i), \tag{3.36}
$$

where:

$$
\sum_{j=0}^{\frac{B^{max}}{\Delta_p}} \Pi(j) = 1. \tag{3.37}
$$

Equation (3.37) applies because the sum of all the probabilities in a probability distribution should be equal to 1.

3.3.1.2 SU_1 Energy Harvesting from SBS and MBS

Energy harvested by SU_1 from SBS and MBS at the t^{th} frame duration T_F is expressed as follows using similar approach as in [74] but now harvesting from multiple sources:

$$\bar{e}_1^H(t) = \eta(T_F - t_{ts}) \left(P^e(t) G^{SU_1}(t) + P^m(t) G_m^{SU_1}(t) \right), \tag{3.38}$$

from Equation (3.38) above, CDF $F_{\bar{e}_1^H}(y)$ of energy harvested by SU_1 from both SBS and MBS is attained by first letting $X_1 = \eta(T_F - t_{ts}) P^e(t) G^{SU_1}(t)$ and $X_2 = \eta(T_F - t_{ts}) P^m(t) G_m^{SU_1}(t)$. Then deriving CDF and PDF expressions of X_1 and X_2 as follows:

$$\begin{aligned} F_{X_1}(x) &= Pr\left(X_1 \leqslant x\right), \\ &= Pr\left(\eta(T_F - t_{ts}) P^e G^{SU_1} \leqslant x\right), \\ &= Pr\left(G^{SU_1} \leqslant \frac{x}{P^e \eta(T_F - t_{ts})}\right), \\ &= F_{G^{SU_1}}\left(\frac{x}{P^e \eta(T_F - t_{ts})}\right), \end{aligned} \tag{3.39}$$

since G^{SU_1} is an exponentially distributed random variable, Equation (3.39) reduces to:

$$\begin{aligned} F_{X_1}(x) &= F_{G^{SU_1}}\left(\frac{x}{P^e \eta(T_F - t_{ts})}\right), \\ &= 1 - e^{-\lambda_{G^{SU_1}}\left(\frac{x}{P^e \eta(T_F - t_{ts})}\right)}. \end{aligned} \tag{3.40}$$

PDF of X_1 is derived by differentiating CDF expression of X_1 in Equation (3.40) above:

$$\begin{aligned} f_{X_1}(x) &= \frac{d}{dx} F_{X_1}(x) dx, \\ &= \frac{d}{dx}\left(1 - e^{-\lambda_{G^{SU_1}}\left(\frac{x}{P^e \eta(T_F - t_{ts})}\right)}\right) dx, \\ &= \frac{\lambda_{G^{SU_1}}}{P^e \eta(T_F - t_{ts})} e^{-\lambda_{G^{SU_1}}\left(\frac{x}{P^e \eta(T_F - t_{ts})}\right)}. \end{aligned} \tag{3.41}$$

Similarly, for X_2:

$$
\begin{aligned}
F_{X_2}(x) &= Pr\left(X_2 \leqslant x\right), \\
&= Pr\left(\eta(T_F - t_{ts})P^m G_m^{SU_1} \leqslant x\right), \\
&= Pr\left(G_m^{SU_1} \leqslant \frac{x}{P^m \eta(T_F - t_{ts})}\right), \\
&= F_{G_m^{SU_1}}\left(\frac{x}{P^m \eta(T_F - t_{ts})}\right), \\
&= 1 - e^{-\lambda_{G_m^{SU_1}}\left(\frac{x}{P^m \eta(T_F - t_{ts})}\right)}.
\end{aligned}
\tag{3.42}
$$

PDF of X_2 is derived by differentiating CDF expression of X_1 in Equation (3.42) above:

$$
\begin{aligned}
f_{X_2}(x) &= \frac{d}{dx} F_{X_2}(x) dx, \\
&= \frac{d}{dx}\left(1 - e^{-\lambda_{G_m^{SU_1}}\left(\frac{x}{P^m \eta(T_F - t_{ts})}\right)}\right) dx, \\
&= \frac{\lambda_{G_m^{SU_1}}}{P^m \eta(T_F - t_{ts})} e^{-\lambda_{G_m^{SU_1}}\left(\frac{x}{P^m \eta(T_F - t_{ts})}\right)}.
\end{aligned}
\tag{3.43}
$$

Using the results from Equations (3.41) and (3.43) above, the PDF expression for $\bar{e}_1^H = X_1 + X_2$, is attained as follows, using convolution approach:

$$
\begin{aligned}
f_{\bar{e}_1^H}(y) &= \int_0^y f_{X_1}(x) f_{X_2}(y-x)dx, \\
&= \int_0^y \left(\frac{\lambda_{G^{SU_1}}}{P^e \eta (T_F - t_{ts})} e^{-\lambda_{G^{SU_1}} \left(\frac{x}{P^e \eta (T_F - t_{ts})} \right)} \right) \\
&\times \left(\frac{\lambda_{G_m^{SU_1}}}{P^m \eta (T_F - t_{ts})} e^{-\lambda_{G_m^{SU_1}} \left(\frac{(y-x)}{P^m \eta (T_F - t_{ts})} \right)} \right) dx, \\
&= \left(\frac{\lambda_{G^{SU_1}}}{P^e \eta (T_F - t_{ts})} \right) \left(\frac{\lambda_{G_m^{SU_1}}}{P^m \eta (T_F - t_{ts})} \right) e^{-\left(\frac{\lambda_{G_m^{SU_1}} y}{P^m \eta (T_F - t_{ts})} \right)} \\
&\times \int_0^y e^{-x \left(\frac{P^m \lambda_{G^{SU_1}} - P^e \lambda_{G_m^{SU_1}}}{P^e P^m \eta (T_F - t_{ts})} \right)} dx, \\
&= \frac{\lambda_{G^{SU_1}} \lambda_{G_m^{SU_1}} \left(e^{-\left(\frac{y \lambda_{G_m^{SU_1}}}{P^m \eta (T_F - t_{ts})} \right)} - e^{-\left(\frac{y \lambda_{G^{SU_1}}}{P^e \eta (T_F - t_{ts})} \right)} \right)}{\eta (T_F - t_{ts}) \left(P^m \lambda_{G^{SU_1}} - P^e \lambda_{G_m^{SU_1}} \right)}.
\end{aligned}
\tag{3.44}
$$

Thus, the CDF of energy harvesting from both SBS and MBS is derived as follows by finding the integral of Equation (3.44) above:

$$
\begin{aligned}
F_{\bar{e}_1^H}(z) &= \int_0^z f_{\bar{e}_1^H}(y)dy, \\
&= \frac{\lambda_{G^{SU_1}} \lambda_{G_m^{SU_1}}}{\eta (T_F - t_{ts}) \left(P^m \lambda_{G^{SU_1}} - P^e \lambda_{G_m^{SU_1}} \right)} \\
&\times \int_0^z \left(e^{-\left(\frac{y \lambda_{G_m^{SU_1}}}{P^m \eta (T_F - t_{ts})} \right)} - e^{-\left(\frac{y \lambda_{G^{SU_1}}}{P^e \eta (T_F - t_{ts})} \right)} \right) dy, \\
&= \frac{P^m \lambda_{G^{SU_1}}}{P^m \lambda_{G^{SU_1}} - P^e \lambda_{G_m^{SU_1}}} \left(1 - e^{-\left(\frac{z \lambda_{G_m^{SU_1}}}{P^m \eta (T_F - t_{ts})} \right)} \right) \\
&- \frac{P^e \lambda_{G_m^{SU_1}}}{P^m \lambda_{G^{SU_1}} - P^e \lambda_{G_m^{SU_1}}} \left(1 - e^{-\left(\frac{z \lambda_{G^{SU_1}}}{P^e \eta (T_F - t_{ts})} \right)} \right), \\
&= 1 - \frac{P^m \lambda_{G^{SU_1}} e^{-\left(\frac{z \lambda_{G_m^{SU_1}}}{P^m \eta (T_F - t_{ts})} \right)}}{P^m \lambda_{G^{SU_1}} - P^e \lambda_{G_m^{SU_1}}} + \frac{P^e \lambda_{G_m^{SU_1}} e^{-\left(\frac{z \lambda_{G^{SU_1}}}{P^e \eta (T_F - t_{ts})} \right)}}{P^m \lambda_{G^{SU_1}} - P^e \lambda_{G_m^{SU_1}}}.
\end{aligned}
\tag{3.45}
$$

(i) Case: $\xi = 0$

Using Equations (3.28) and (3.45), SU_1 state transition probability expressions are attained as follows for $\xi = 0$ where $j = i + \frac{\bar{e}_1^H}{\Delta_p} - i => j = \frac{\bar{e}_1^H}{\Delta_p}$

$$
\begin{aligned}
\bar{Q}_{\xi_0}(i,j) &= Pr(j\Delta_p = \bar{e}_1^H, \xi = 0), \\
&= Pr\left(\bar{e}_1^H = j\Delta_p\right) Pr\left(i < n_{I1}\right), \\
&= \left(\left(1 - \frac{P^m \lambda_{G^{SU_1}} e^{-\left(\frac{(j+1)\Delta_p \lambda_{G_m^{SU_1}}}{P^m \eta (T_F - t_{ts})}\right)}}{P^m \lambda_{G^{SU_1}} - P^e \lambda_{G_m^{SU_1}}} + \frac{P^e \lambda_{G_m^{SU_1}} e^{-\left(\frac{(j+1)\Delta_p \lambda_{G^{SU_1}}}{P^e \eta (T_F - t_{ts})}\right)}}{P^m \lambda_{G^{SU_1}} - P^e \lambda_{G_m^{SU_1}}} \right) \right. \\
&\quad \left. - \left(1 - \frac{P^m \lambda_{G^{SU_1}} e^{-\left(\frac{j\Delta_p \lambda_{G_m^{SU_1}}}{P^m \eta (T_F - t_{ts})}\right)}}{P^m \lambda_{G^{SU_1}} - P^e \lambda_{G_m^{SU_1}}} + \frac{P^e \lambda_{G_m^{SU_1}} e^{-\left(\frac{j\Delta_p \lambda_{G^{SU_1}}}{P^e \eta (T_F - t_{ts})}\right)}}{P^m \lambda_{G^{SU_1}} - P^e \lambda_{G_m^{SU_1}}} \right) \right) \\
&\quad \times \left(1 - e^{-\left(\frac{\lambda_{H_1^p} I_{it} t_{ts}}{i\Delta_p}\right)} \right), \\
&= \left(\frac{P^e \lambda_{G_m^{SU_1}} e^{-\left(\frac{(j+1)\Delta_p \lambda_{G^{SU_1}}}{P^e \eta (T_F - t_{ts})}\right)}}{P^m \lambda_{G^{SU_1}} - P^e \lambda_{G_m^{SU_1}}} + \frac{P^m \lambda_{G^{SU_1}} e^{-\left(\frac{j\Delta_p \lambda_{G_m^{SU_1}}}{P^m \eta (T_F - t_{ts})}\right)}}{P^m \lambda_{G^{SU_1}} - P^e \lambda_{G_m^{SU_1}}} \right) \\
&\quad - \left(\frac{P^m \lambda_{G^{SU_1}} e^{-\left(\frac{(j+1)\Delta_p \lambda_{G_m^{SU_1}}}{P^m \eta (T_F - t_{ts})}\right)}}{P^m \lambda_{G^{SU_1}} - P^e \lambda_{G_m^{SU_1}}} + \frac{P^e \lambda_{G_m^{SU_1}} e^{-\left(\frac{j\Delta_p \lambda_{G^{SU_1}}}{P^e \eta (T_F - t_{ts})}\right)}}{P^m \lambda_{G^{SU_1}} - P^e \lambda_{G_m^{SU_1}}} \right) \\
&\quad \times \left(1 - e^{-\left(\frac{\lambda_{H_1^p} I_{it} t_{ts}}{i\Delta_p}\right)} \right).
\end{aligned}
\tag{3.46}
$$

(ii) Case: $\xi = 1$

Similarly, for $\xi = 1$: $j = i + \frac{\bar{e}_1^H}{\Delta_p} - n_{I_1} => j - i = \frac{\bar{e}_1^H}{\Delta_p} - n_{I_1}$. The state transition probability for this case is expressed as follows:

$$\bar{Q}_{\xi_1}(i,j) = Pr(j - i = \frac{\bar{e}_1^H}{\Delta_p} - n_{I_1}, \xi = 1), \tag{3.47}$$

using Equation (3.47) above, the expression for $\bar{Q}_{\xi_1}(i,j)$ is derived as follows:

$$\begin{aligned}
\bar{Q}_{\xi_1}(i,j) &= Pr(j - i = \frac{\bar{e}_1^H}{\Delta_p} - n_{I_1}, \xi = 1), \\
&= Pr\left(j - i = \frac{\bar{e}_1^H}{\Delta_p} - n_{I_1}, i \geq n_{I_1}\right), \\
&= Pr\left(\bar{e}_1^H = (j - i + n_{I_1})\,\Delta_p, i \geq n_{I_1}\right), \\
&= \sum_{n_{I_1}=0}^{i} Pr\left(\bar{e}_1^H = (j - i + n_{I_1})\,\Delta_p\right) \times \left(e^{-\left(\frac{\lambda_{H_1^p} I_{it} t_{ts}}{(n_{I_1}+1)\Delta_p}\right)} - e^{-\left(\frac{\lambda_{H_1^p} I_{it} t_{ts}}{n_{I_1}\Delta_p}\right)}\right), \\
&= \sum_{n_{I_1}=0}^{i} \left(\frac{P^e \lambda_{G_m^{SU_1}} e^{-\left(\frac{((j-i+n_{I_1})+1)\Delta_p \lambda_{G^{SU_1}}}{P^e \eta (T_F - t_{ts})}\right)}}{P^m \lambda_{G^{SU_1}} - P^e \lambda_{G_m^{SU_1}}} + \frac{P^m \lambda_{G^{SU_1}} e^{-\left(\frac{(j-i+n_{I_1})\Delta_p \lambda_{G_m^{SU_1}}}{P^m \eta (T_F - t_{ts})}\right)}}{P^m \lambda_{G^{SU_1}} - P^e \lambda_{G_m^{SU_1}}}\right) \\
&\quad - \left(\frac{P^m \lambda_{G^{SU_1}} e^{-\left(\frac{((j-i+n_{I_1})+1)\Delta_p \lambda_{G_m^{SU_1}}}{P^m \eta (T_F - t_{ts})}\right)}}{P^m \lambda_{G^{SU_1}} - P^e \lambda_{G_m^{SU_1}}} + \frac{P^e \lambda_{G_m^{SU_1}} e^{-\left(\frac{(j-i+n_{I_1})\Delta_p \lambda_{G^{SU_1}}}{P^e \eta (T_F - t_{ts})}\right)}}{P^m \lambda_{G^{SU_1}} - P^e \lambda_{G_m^{SU_1}}}\right) \\
&\quad \times \left(e^{-\left(\frac{\lambda_{H_1^p} I_{it} t_{ts}}{(n_{I_1}+1)\Delta_p}\right)} - e^{-\left(\frac{\lambda_{H_1^p} I_{it} t_{ts}}{n_{I_1}\Delta_p}\right)}\right).
\end{aligned} \tag{3.48}$$

(iii) Joint Transition:

From Equations (3.46) and (3.48), the state transition probability from state i to state i is as follows using probability sum rule for the above two mutually-exclusive transition probability conditions (ξ_0, ξ_1):

$$\bar{Q}(i,j) = \bar{Q}_{\xi_0}(i,j) + \bar{Q}_{\xi_1}(i,j), \tag{3.49}$$

from Equation (3.49) above, the probability of SU_1 being in state j can be deduced as follows using Markovian analysis:

$$\bar{\Pi}(j) = \sum_{i=0}^{\frac{B^{max}}{\Delta_p}} \bar{Q}(i,j) * \bar{\Pi}(i), \tag{3.50}$$

where:

$$\sum_{j=0}^{\frac{B^{max}}{\Delta_p}} \bar{\Pi}(j) = 1. \tag{3.51}$$

3.3.2 System Markov Analysis with respect to SU_2

Since the two SUs (SU_1 and SU_2) are in a NOMA group, decoding the transmissions of the stronger user (SU_2) at the SBS considers the signal from the weaker user (SU_1) as interference because SIC is only applied when decoding the carrier signal of the weaker user (SU_1). Therefore, Markovian analysis of SU_2 considers the state transitions for SU_1 as well to be able to cater for its transmission as part of the interference. Thus, the states of the system to solve for SU_2 Markovian analysis is now defined by (i, j) where $i = \{0, 1, 2, ..., \left\lceil \frac{B^{max}}{\Delta_p} \right\rceil\}$ and $j = \{0, 1, 2, 3, ..., \left\lceil \frac{B^{max}}{\Delta_p} \right\rceil\}$. The states i and j represent the available energy chunks at the t^{th} frame index for SU_1 and SU_2, respectively. We have already presented battery energy evolution expression for SU_1 in Equation (3.27). Similarly, below is the battery energy evolution expression for SU_2:

$$b_2(t) = min\{max\{b_2(t-1) + e_2^H(t-1) - P_2^s(t-1) \times t_{ts}, 0\}, B^{max}\}. \tag{3.52}$$

At any point in time (t), the state transition event from (i, j) to (k, l) can be characterized by the following state transition conditions considering the transitions that each SU can take:

$ST = \{ST1, ST2, ST3, ST4\}$,
where:

- $ST = ST1$ when $\frac{b_1(t)}{t_{ts}} < \frac{I_{it}}{H_1^p}$ and $\frac{b_2(t)}{t_{ts}} < \frac{I_{it}}{H_2^p}$.
- $ST = ST2$ when $\frac{b_1(t)}{t_{ts}} < \frac{I_{it}}{H_1^p}$ and $\frac{b_2(t)}{t_{ts}} \geq \frac{I_{it}}{H_2^p}$.
- $ST = ST3$ when $\frac{b_1(t)}{t_{ts}} \geq \frac{I_{it}}{H_2^p}$ and $\frac{b_2(t)}{t_{ts}} < \frac{I_{it}}{H_2^p}$.
- $ST = ST4$ when $\frac{b_1(t)}{t_{ts}} \geq \frac{I_{it}}{H_1^p}$ and $\frac{b_2(t)}{t_{ts}} \geq \frac{I_{it}}{H_2^p}$.

Having defined system state transition events above, to build the Markovian model for these system made up of states for both SUs, we need to derive expressions for transition probabilities for moving from state (i,j) to state (k,l), where SU_1 would be transition from state i to k and SU_2 would be making a transition from state j to l. Similar to what was done with modeling of SU_1 transitions

in the previous section, we first have to derive energy harvesting distributions of SU_2 for harvesting from the SBS and when harvesting from both SBS and MBS. Following the similar approach as done for SU_1, below are SU_2 energy harvesting expressions and their corresponding CDF distributions for harvesting from SBS and also for harvesting from both SBS and MBS, respectively:

SU_2 energy harvesting from SBS:

$$e_2^H(t) = \eta P^e(t) G^{SU_2}(t)(T_F - t_{ts}), \tag{3.53}$$

using Equation (3.53) above, the CDF expression of SU_2 energy harvesting is as follows following the similar approach as when deriving energy harvesting for SU_1:

$$F_{e_2^H}(y) = 1 - e^{-\left(\frac{y}{\eta P^e(t)(T_F - t_{ts})}\right)\lambda_{G^{SU_2}}}. \tag{3.54}$$

SU_2 energy harvesting from both SBS and MBS:

$$\bar{e}_2^H(t) = \eta(T_F - t_{ts}) \left(P^e(t) G^{SU_2}(t) + P^m(t) G_m^{SU_2}(t)\right), \tag{3.55}$$

using Equation (3.55) above and the approach followed in the previous section when deriving energy harvesting CDF for SU_1 harvesting from both SBS and MBS. Below is the CDF expression for SU_2 when harvesting from both SBS and MBS:

$$F_{\bar{e}_2^H}(z) = 1 - \frac{P^m \lambda_{G^{SU_2}} e^{-\left(\frac{z\lambda_{G_m^{SU_2}}}{P^m \eta (T_F - t_{ts})}\right)}}{P^m \lambda_{G^{SU_2}} - P^e \lambda_{G_m^{SU_2}}} + \frac{P^e \lambda_{G_m^{SU_2}} e^{-\left(\frac{z\lambda_{G^{SU_2}}}{P^e \eta (T_F - t_{ts})}\right)}}{P^m \lambda_{G^{SU_2}} - P^e \lambda_{G_m^{SU_2}}}. \tag{3.56}$$

Once we have the above energy harvesting distribution expressions for SU_2, we should be able to find closed-form expressions for SU_1 and SU_2 combined state transition probabilities following similar approach as done in the previous section for SU_1. In the following sub-sections we derive state transition probabilities for the defined state transition events (ST1, ST2, ST3 and ST4), considering cases when both SUs are harvesting from SBS and when both SUs are harvesting from the two sources (SBS and MBS).

3.3.2.1 SU_1 and SU_2 Energy Harvesting from SBS

Assuming that SU_1 and SU_2 are both harvesting from SBS. The transitions from state (i,j) at frame index $(t-1)$ to (k,l) at frame index (t) are derived using SU_1 and SU_2 energy evolution Equations (3.27 and 3.52) for the defined state transition events. Below we derive state transition probabilities for each of the state transition events (ST1, ST2, ST3 and ST4):

For $ST = ST1$: $k = i + \frac{e_1^H}{\Delta_p} - i => k = \frac{e_1^H}{\Delta_p}$ and $l = j + \frac{e_2^H}{\Delta_p} - j => l = \frac{e_2^H}{\Delta_p}$:

$$\begin{aligned}
Q_{ST1}((i,j),(k,l)) &= Pr\left(k = \frac{e_1^H}{\Delta_p}, l = \frac{e_2^H}{\Delta_p}, ST1\right), \\
&= Pr\left(k = \frac{e_1^H}{\Delta_p}, l = \frac{e_2^H}{\Delta_p}, i < n_{I_1}, j < n_{I_2}\right), \\
&= \left(e^{-\left(\frac{k\Delta_p \lambda_{G^{SU_1}}}{\eta P^e (T_F - t_{ts})}\right)} - e^{-\left(\frac{(k+1)\Delta_p \lambda_{G^{SU_1}}}{\eta P^e (T_F - t_{ts})}\right)}\right) \times \left(1 - e^{-\left(\frac{\lambda_{H_1^p I_{it} t_{ts}}}{i\Delta_p}\right)}\right) \\
&\times \left(e^{-\left(\frac{l\Delta_p \lambda_{G^{SU_2}}}{\eta P^e (T_F - t_{ts})}\right)} - e^{-\left(\frac{(l+1)\Delta_p \lambda_{G^{SU_2}}}{\eta P^e (T_F - t_{ts})}\right)}\right) \times \left(1 - e^{-\left(\frac{\lambda_{H_2^p I_{it} t_{ts}}}{j\Delta_p}\right)}\right).
\end{aligned} \tag{3.57}$$

For $ST = ST2$: $k = i + \frac{e_1^H}{\Delta_p} - i => k = \frac{e_1^H}{\Delta_p}$ and $l = j + \frac{e_2^H}{\Delta_p} - n_{I_2} => l - j = \frac{e_2^H}{\Delta_p} - n_{I_2}$:

$$\begin{aligned}
Q_{ST2}((i,j),(k,l)) &= Pr\left(k = \frac{e_1^H}{\Delta_p}, l - j = \frac{e_2^H}{\Delta_p} - n_{I_2}, k < n_{I_1}, l \geq n_{I_2}\right), \\
&= Pr\left(e_1^H = k\Delta_p, i < n_{I_1}\right) \times Pr\left(e_2^H = (l - j + n_{I_2})\Delta_p, j \geq n_{I_2}\right), \\
&= \left(e^{-\left(\frac{k\Delta_p \lambda_{G^{SU_1}}}{\eta P^e (t)(T_F - t_{ts})}\right)} - e^{-\left(\frac{(k+1)\Delta_p \lambda_{G^{SU_1}}}{\eta P^e (t)(T_F - t_{ts})}\right)}\right) \times \left(1 - e^{-\left(\frac{\lambda_{H_1^p I_{it} t_{ts}}}{i\Delta_p}\right)}\right) \\
&\times \left(\sum_{n_{I_2}=0}^{j} \left(e^{-\left(\frac{(l-j+n_{I_2})\Delta_p \lambda_{G^{SU_2}}}{\eta P^e (t)(T_F - t_{ts})}\right)} - e^{-\left(\frac{(l-j+n_{I_2}+1)\Delta_p \lambda_{G^{SU_2}}}{\eta P^e (t)(T_F - t_{ts})}\right)}\right)\right. \\
&\times \left.\left(e^{-\left(\frac{\lambda_{H_2^p I_{it} t_{ts}}}{(n_{I_2}+1)\Delta_p}\right)} - e^{-\left(\frac{\lambda_{H_2^p I_{it} t_{ts}}}{n_{I_2}\Delta_p}\right)}\right)\right).
\end{aligned} \tag{3.58}$$

For $ST = ST3$: $k = i + \frac{e_1^H}{\Delta_p} - n_{I_1} => k - i = \frac{e_1^H}{\Delta_p} - n_{I_1}$ and $l = j + \frac{e_2^H}{\Delta_p} - j => l = \frac{e_2^H}{\Delta_p}$:

$$
\begin{aligned}
Q_{ST3}((i,j),(k,l)) &= Pr\left(k - i = \frac{e_1^H}{\Delta_p} - n_{I_1}, l = \frac{e_2^H}{\Delta_p}, i \geq n_{I_1}, j < n_{I_2}\right), \\
&= Pr(e_1^H = (k - i + n_{I_1})\,\Delta_p, i \geq n_{I_1}) Pr\left(e_2^H = l\Delta_p, j < n_{I_2}\right), \\
&= \left(\sum_{n_{I_1}=0}^{i} \left(e^{-\left(\frac{(k-i+n_{I_1})\Delta_p \lambda_{GSU_1}}{\eta P^e(t)(T_F - t_{ts})}\right)} - e^{-\left(\frac{(k-i+n_{I_1}+1)\Delta_p \lambda_{GSU_1}}{\eta P^e(t)(T_F - t_{ts})}\right)}\right)\right. \\
&\times \left.\left(e^{-\left(\frac{\lambda_{H_1^p I_{it} t_{ts}}}{(n_{I_1}+1)\Delta_p}\right)} - e^{-\left(\frac{\lambda_{H_1^p I_{it} t_{ts}}}{n_{I_1}\Delta_p}\right)}\right)\right) \\
&\times \left(e^{-\left(\frac{l\Delta_p \lambda_{GSU_2}}{\eta P^e(t)(T_F - t_{ts})}\right)} - e^{-\left(\frac{(l+1)\Delta_p \lambda_{GSU_2}}{\eta P^e(t)(T_F - t_{ts})}\right)}\right) \times \left(1 - e^{-\left(\frac{\lambda_{H_2^p I_{it} t_{ts}}}{j\Delta_p}\right)}\right).
\end{aligned}
\tag{3.59}
$$

For $ST = ST4$: $k = i + \frac{e_1^H}{\Delta_p} - n_{I_1} => k - i = \frac{e_1^H}{\Delta_p} - n_{I_1}$ and $l = j + \frac{e_2^H}{\Delta_p} - n_{I_2} => l - j = \frac{e_2^H}{\Delta_p} - n_{I_2}$:

$$
\begin{aligned}
Q_{ST4}((i,j),(k,l)) &= Pr(k - i = \frac{e_1^H}{\Delta_p} - n_{I_1}, l - j = \frac{e_2^H}{\Delta_p} - n_{I_2}, i \geq n_{I_1}, j \geq n_{I_2}), \\
&= Pr\left(e_1^H = (k - i + n_{I_1})\,\Delta_p, i \geq n_{I_1}\right) \\
&\times Pr\left(e_2^H = (l - j + n_{I_2})\,\Delta_p, j \geq n_{I_2}\right), \\
&= \left(\sum_{n_{I_1}=0}^{i} \left(e^{-\left(\frac{(k-i+n_{I_1})\Delta_p \lambda_{GSU_1}}{\eta P^e(t)(T_F - t_{ts})}\right)} - e^{-\left(\frac{(k-i+n_{I_1}+1)\Delta_p \lambda_{GSU_1}}{\eta P^e(t)(T_F - t_{ts})}\right)}\right)\right. \\
&\times \left.\left(e^{-\left(\frac{\lambda_{H_1^p I_{it} t_{ts}}}{(n_{I_1}+1)\Delta_p}\right)} - e^{-\left(\frac{\lambda_{H_1^p I_{it} t_{ts}}}{n_{I_1}\Delta_p}\right)}\right)\right) \\
&\times \left(\sum_{n_{I_2}=0}^{j} \left(e^{-\left(\frac{(l-j+n_{I_2})\Delta_p \lambda_{GSU_2}}{\eta P^e(t)(T_F - t_{ts})}\right)} - e^{-\left(\frac{(l-j+n_{I_2}+1)\Delta_p \lambda_{GSU_2}}{\eta P^e(t)(T_F - t_{ts})}\right)}\right)\right. \\
&\times \left.\left(e^{-\left(\frac{\lambda_{H_2^p I_{it} t_{ts}}}{(n_{I_2}+1)\Delta_p}\right)} - e^{-\left(\frac{\lambda_{H_2^p I_{it} t_{ts}}}{n_{I_2}\Delta_p}\right)}\right)\right).
\end{aligned}
\tag{3.60}
$$

Using probability sum rule, state transition probability expression for moving from (i,j) to (k,l) is the sum of all the conditional state transition probabilities derived for each transition event in Equations (3.57), (3.58), (3.59), and (3.60):

$$\begin{aligned} Q((i,j),(k,l)) = Q_{ST1}((i,j),(k,l)) + Q_{ST2}((i,j),(k,l)) \\ +Q_{ST3}((i,j),(k,l)) + Q_{ST4}((i,j),(k,l)), \end{aligned} \tag{3.61}$$

with reference to Equation (3.61) above, the probability of being in any state (k,l) at t^{th} frame index is computed as follows using Markovian analysis approach:

$$\Pi(k,l) = \sum_{i=0}^{\frac{B^{max}}{\Delta_p}} \sum_{j=0}^{\frac{B^{max}}{\Delta_p}} Q((i,j),(k,l))\Pi(i,j), \tag{3.62}$$

where:

$$\sum_{k=0}^{\frac{B^{max}}{\Delta_p}} \sum_{l=0}^{\frac{B^{max}}{\Delta_p}} \Pi(k,l) = 1. \tag{3.63}$$

3.3.2.2 SU_1 and SU_2 Energy Harvesting from SBS and MBS

Similar to when both SUs are harvesting from only the SBS, transitioning from state (i,j) at $(t-1)$ to (k,l) at (t) is defined as follows when both SUs are harvesting from SBS and MBS for each of the state transition events (ST1, ST2, ST3 and ST4):

For $ST = ST1$: $k = i + \frac{\bar{e}_1^H}{\Delta_p} - i => k = \frac{\bar{e}_1^H}{\Delta_p}$ and $l = j + \frac{\bar{e}_2^H}{\Delta_p} - j => l = \frac{\bar{e}_2^H}{\Delta_p}$:

$$
\begin{aligned}
\bar{Q}_{ST1}((i,j),(k,l)) &= Pr\left(k = \frac{\bar{e}_1^H}{\Delta_p}, l = \frac{\bar{e}_2^H}{\Delta_p}, ST1\right), \\
&= Pr\left(k = \frac{\bar{e}_1^H}{\Delta_p}, l = \frac{\bar{e}_2^H}{\Delta_p}, i < n_{I_1}, j < n_{I_2}\right), \\
&= Pr\left(k = \frac{\bar{e}_1^H}{\Delta_p}, i < n_{I_1}, l = \frac{\bar{e}_2^H}{\Delta_p}, j < n_{I_2}\right), \\
&= \left(\left(\frac{P^e \lambda_{G_m^{SU_1}} e^{-\left(\frac{(k+1)\Delta_p \lambda_{G^{SU_1}}}{P^e \eta (T_F - t_{ts})}\right)}}{P^m \lambda_{G^{SU_1}} - P^e \lambda_{G_m^{SU_1}}} + \frac{P^m \lambda_{G^{SU_1}} e^{-\left(\frac{k\Delta_p \lambda_{G_m^{SU_1}}}{P^m \eta (T_F - t_{ts})}\right)}}{P^m \lambda_{G^{SU_1}} - P^e \lambda_{G_m^{SU_1}}} \right) \right. \\
&\quad \left. - \left(\frac{P^m \lambda_{G^{SU_1}} e^{-\left(\frac{(k+1)\Delta_p \lambda_{G_m^{SU_1}}}{P^m \eta (T_F - t_{ts})}\right)}}{P^m \lambda_{G^{SU_1}} - P^e \lambda_{G_m^{SU_1}}} + \frac{P^e \lambda_{G_m^{SU_1}} e^{-\left(\frac{k\Delta_p \lambda_{G^{SU_1}}}{P^e \eta (T_F - t_{ts})}\right)}}{P^m \lambda_{G^{SU_1}} - P^e \lambda_{G_m^{SU_1}}} \right) \right) \\
&\quad \times \left(1 - e^{-\left(\frac{\lambda_{H_1^p} I_{it} t_{ts}}{i\Delta_p}\right)} \right) \\
&\quad \times \left(\left(\frac{P^e \lambda_{G_m^{SU_2}} e^{-\left(\frac{(l+1)\Delta_p \lambda_{G^{SU_2}}}{P^e \eta (T_F - t_{ts})}\right)}}{P^m \lambda_{G^{SU_2}} - P^e \lambda_{G_m^{SU_2}}} + \frac{P^m \lambda_{G^{SU_2}} e^{-\left(\frac{l\Delta_p \lambda_{G_m^{SU_2}}}{P^m \eta (T_F - t_{ts})}\right)}}{P^m \lambda_{G^{SU_2}} - P^e \lambda_{G_m^{SU_2}}} \right) \right. \\
&\quad \left. - \left(\frac{P^m \lambda_{G^{SU_2}} e^{-\left(\frac{(l+1)\Delta_p \lambda_{G_m^{SU_2}}}{P^m \eta (T_F - t_{ts})}\right)}}{P^m \lambda_{G^{SU_2}} - P^e \lambda_{G_m^{SU_2}}} + \frac{P^e \lambda_{G_m^{SU_2}} e^{-\left(\frac{l\Delta_p \lambda_{G^{SU_2}}}{P^e \eta (T_F - t_{ts})}\right)}}{P^m \lambda_{G^{SU_2}} - P^e \lambda_{G_m^{SU_2}}} \right) \right) \\
&\quad \times \left(1 - e^{-\left(\frac{\lambda_{H_2^p} I_{it} t_{ts}}{j\Delta_p}\right)} \right).
\end{aligned}
\tag{3.64}
$$

For $ST = ST2$: $k = i + \frac{\bar{e}_1^H}{\Delta_p} - i => k = \frac{\bar{e}_1^H}{\Delta_p}$ and $l = j + \frac{\bar{e}_2^H}{\Delta_p} - n_{I_2} => l - j = \frac{\bar{e}_2^H}{\Delta_p} - n_{I_2}$:

$$
\begin{aligned}
\bar{Q}_{ST2}((i,j),(k,l)) &= Pr\left(k = \frac{\bar{e}_1^H}{\Delta_p}, l - j = \frac{\bar{e}_2^H}{\Delta_p} - n_{I_2}, k < n_{I_1}, l \geq n_{I_2}\right), \\
&= Pr\left(\bar{e}_1^H = k\Delta_p, i < n_{I_1}\right) \times Pr\left(\bar{e}_2^H = (l - j + n_{I_2})\,\Delta_p, j \geq n_{I_2}\right), \\
&= \left(\left(\frac{P^e \lambda_{G_m^{SU_1}} e^{-\left(\frac{(k+1)\Delta_p \lambda_{G_m^{SU_1}}}{P^e \eta (T_F - t_{ts})}\right)}}{P^m \lambda_{G^{SU_1}} - P^e \lambda_{G_m^{SU_1}}} + \frac{P^m \lambda_{G^{SU_1}} e^{-\left(\frac{k\Delta_p \lambda_{G_m^{SU_1}}}{P^m \eta (T_F - t_{ts})}\right)}}{P^m \lambda_{G^{SU_1}} - P^e \lambda_{G_m^{SU_1}}} \right) \right. \\
&\quad \left. - \left(\frac{P^m \lambda_{G^{SU_1}} e^{-\left(\frac{(k+1)\Delta_p \lambda_{G_m^{SU_1}}}{P^m \eta (T_F - t_{ts})}\right)}}{P^m \lambda_{G^{SU_1}} - P^e \lambda_{G_m^{SU_1}}} + \frac{P^e \lambda_{G_m^{SU_1}} e^{-\left(\frac{k\Delta_p \lambda_{G^{SU_1}}}{P^e \eta (T_F - t_{ts})}\right)}}{P^m \lambda_{G^{SU_1}} - P^e \lambda_{G_m^{SU_1}}} \right) \right) \\
&\quad \times \left(1 - e^{-\left(\frac{\lambda_{H_1^p} I_{it} t_{ts}}{i\Delta_p}\right)} \right) \\
&\quad \times \left(\sum_{n_{I_2}=0}^{j} \left(\left[\frac{P^e \lambda_{G_m^{SU_2}} e^{-\left(\frac{((l-j+n_{I_2})+1)\Delta_p \lambda_{G^{SU_2}}}{P^e \eta (T_F - t_{ts})}\right)}}{P^m \lambda_{G^{SU_2}} - P^e \lambda_{G_m^{SU_2}}} \right.\right.\right. \\
&\quad \left. + \frac{P^m \lambda_{G^{SU_2}} e^{-\left(\frac{(l-j+n_{I_2}) Delta_p \lambda_{G_m^{SU_2}}}{P^m \eta (T_F - t_{ts})}\right)}}{P^m \lambda_{G^{SU_2}} - P^e \lambda_{G_m^{SU_2}}} \right] \\
&\quad - \left[\frac{P^m \lambda_{G^{SU_2}} e^{-\left(\frac{((l-j+n_{I_2})+1)\Delta_p \lambda_{G_m^{SU_2}}}{P^m \eta (T_F - t_{ts})}\right)}}{P^m \lambda_{G^{SU_2}} - P^e \lambda_{G_m^{SU_2}}} \right. \\
&\quad \left.\left. + \frac{P^e \lambda_{G_m^{SU_2}} e^{-\left(\frac{(l-j+n_{I_2}) Delta_p \lambda_{G^{SU_2}}}{P^e \eta (T_F - t_{ts})}\right)}}{P^m \lambda_{G^{SU_2}} - P^e \lambda_{G_m^{SU_2}}} \right] \right) \\
&\quad \left. \times \left(e^{-\left(\frac{\lambda_{H_2^p} I_{it} t_{ts}}{(n_{I_2}+1)\Delta_p}\right)} - e^{-\left(\frac{\lambda_{H_2^p} I_{it} t_{ts}}{n_{I_2}\Delta_p}\right)} \right) \right).
\end{aligned}
\tag{3.65}
$$

For $ST = ST3$: $k = i + \frac{\bar{e}_1^H}{\Delta_p} - n_{I_1} => k - i = \frac{\bar{e}_1^H}{\Delta_p} - n_{I_1}$ and $l = j + \frac{\bar{e}_2^H}{\Delta_p} - j => l = \frac{\bar{e}_2^H}{\Delta_p}$:

$$
\begin{aligned}
\bar{Q}_{ST3}((i,j),(k,l)) &= Pr\left(k - i = \frac{\bar{e}_1^H}{\Delta_p} - n_{I_1}, l = \frac{\bar{e}_2^H}{\Delta_p}, i \geq n_{I_1}, j < n_{I_2}\right), \\
&= Pr(\bar{e}_1^H = (k - i + n_{I_1})\,\Delta_p, i \geq n_{I_1}) Pr\left(\bar{e}_2^H = l\Delta_p, j < n_{I_2}\right), \\
&= \left(\sum_{n_{I_1}=0}^{i} \left(\left[\frac{P^e \lambda_{G_m^{SU_1}} e^{-\left(\frac{((k-i+n_{I_1})+1)\Delta_p \lambda_{G^{SU_1}}}{P^e \eta (T_F - t_{ts})}\right)}}{P^m \lambda_{G^{SU_1}} - P^e \lambda_{G_m^{SU_1}}} \right.\right. \right. \\
&\quad \left. + \frac{P^m \lambda_{G^{SU_1}} e^{-\left(\frac{(k-i+n_{I_1})\Delta_p \lambda_{G_m^{SU_1}}}{P^m \eta (T_F - t_{ts})}\right)}}{P^m \lambda_{G^{SU_1}} - P^e \lambda_{G_m^{SU_1}}} \right] \\
&\quad - \left[\frac{P^m \lambda_{G^{SU_1}} e^{-\left(\frac{((k-i+n_{I_1})+1)\Delta_p \lambda_{G_m^{SU_1}}}{P^m \eta (T_F - t_{ts})}\right)}}{P^m \lambda_{G^{SU_1}} - P^e \lambda_{G_m^{SU_1}}} \right. \\
&\quad \left. \left. + \frac{P^e \lambda_{G_m^{SU_1}} e^{-\left(\frac{(k-i+n_{I_1})\Delta_p \lambda_{G^{SU_1}}}{P^e \eta (T_F - t_{ts})}\right)}}{P^m \lambda_{G^{SU_1}} - P^e \lambda_{G_m^{SU_1}}} \right] \right) \\
&\quad \left. \times \left(e^{-\left(\frac{\lambda_{H_1^p} I_{it} t_{ts}}{(n_{I_1}+1)\Delta p}\right)} - e^{-\left(\frac{\lambda_{H_1^p} I_{it} t_{ts}}{n_{I_1} \Delta_p}\right)} \right) \right) \\
&\quad \times \left(\left(\frac{P^e \lambda_{G_m^{SU_2}} e^{-\left(\frac{(l+1)\Delta_p \lambda_{G^{SU_2}}}{P^e \eta (T_F - t_{ts})}\right)}}{P^m \lambda_{G^{SU_2}} - P^e \lambda_{G_m^{SU_2}}} + \frac{P^m \lambda_{G^{SU_2}} e^{-\left(\frac{l\Delta_p \lambda_{G_m^{SU_2}}}{P^m \eta (T_F - t_{ts})}\right)}}{P^m \lambda_{G^{SU_2}} - P^e \lambda_{G_m^{SU_2}}} \right) \right. \\
&\quad \left. - \left(\frac{P^m \lambda_{G^{SU_2}} e^{-\left(\frac{(l+1)\Delta_p \lambda_{G_m^{SU_2}}}{P^m \eta (T_F - t_{ts})}\right)}}{P^m \lambda_{G^{SU_2}} - P^e \lambda_{G_m^{SU_2}}} + \frac{P^e \lambda_{G_m^{SU_2}} e^{-\left(\frac{l\Delta_p \lambda_{G^{SU_2}}}{P^e \eta (T_F - t_{ts})}\right)}}{P^m \lambda_{G^{SU_2}} - P^e \lambda_{G_m^{SU_2}}} \right) \right) \\
&\quad \times \left(1 - e^{-\left(\frac{\lambda_{H_2^p} I_{it} t_{ts}}{j\Delta_p}\right)} \right).
\end{aligned}
\tag{3.66}
$$

For $ST = ST4$: $k = i + \frac{\bar{e}_1^H}{\Delta_p} - n_{I_1} => k - i = \frac{\bar{e}_1^H}{\Delta_p} - n_{I_1}$ and $l = j + \frac{\bar{e}_2^H}{\Delta_p} - n_{I_2} => l - j = \frac{\bar{e}_2^H}{\Delta_p} - n_{I_2}$:

$$\bar{Q}_{ST4}((i,j),(k,l)) = Pr(k-i = \frac{\bar{e}_1^H}{\Delta_p} - n_{I_1}, l-j = \frac{\bar{e}_2^H}{\Delta_p} - n_{I_2}, i \geq n_{I_1}, j \geq n_{I_2}),$$

$$= \left(\sum_{n_{I_1}=0}^{i} \left(\left[\frac{P^e \lambda_{G_m^{SU_1}} e^{-\left(\frac{((k-i+n_{I_1})+1)\Delta_p \lambda_{G^{SU_1}}}{P^e \eta (T_F - t_{ts})} \right)}}{P^m \lambda_{G^{SU_1}} - P^e \lambda_{G_m^{SU_1}}} \right. \right.$$

$$\left. + \frac{P^m \lambda_{G^{SU_1}} e^{-\left(\frac{(k-i+n_{I_1})\Delta_p \lambda_{G_m^{SU_1}}}{P^m \eta (T_F - t_{ts})} \right)}}{P^m \lambda_{G^{SU_1}} - P^e \lambda_{G_m^{SU_1}}} \right]$$

$$- \left[\frac{P^m \lambda_{G^{SU_1}} e^{-\left(\frac{((k-i+n_{I_1})+1)\Delta_p \lambda_{G_m^{SU_1}}}{P^m \eta (T_F - t_{ts})} \right)}}{P^m \lambda_{G^{SU_1}} - P^e \lambda_{G_m^{SU_1}}} \right.$$

$$\left. \left. + \frac{P^e \lambda_{G_m^{SU_1}} e^{-\left(\frac{(k-i+n_{I_1})\Delta_p \lambda_{G^{SU_1}}}{P^e \eta (T_F - t_{ts})} \right)}}{P^m \lambda_{G^{SU_1}} - P^e \lambda_{G_m^{SU_1}}} \right] \right)$$

$$\times \left(e^{-\left(\frac{\lambda_{H_1^p} I_{it} t_{ts}}{(n_{I_1}+1)\Delta_p} \right)} - e^{-\left(\frac{\lambda_{H_1^p} I_{it} t_{ts}}{n_{I_1} \Delta_p} \right)} \right) \Bigg)$$

$$\times \left(\sum_{n_{I_2}=0}^{i} \left(\left[\frac{P^e \lambda_{G_m^{SU_2}} e^{-\left(\frac{((l-j+n_{I_2})+1)\Delta_p \lambda_{G^{SU_2}}}{P^e \eta (T_F - t_{ts})} \right)}}{P^m \lambda_{G^{SU_2}} - P^e \lambda_{G_m^{SU_2}}} \right. \right.$$

$$\left. + \frac{P^m \lambda_{G^{SU_2}} e^{-\left(\frac{(l-j+n_{I_2}) Delta_p \lambda_{G_m^{SU_2}}}{P^m \eta (T_F - t_{ts})} \right)}}{P^m \lambda_{G^{SU_2}} - P^e \lambda_{G_m^{SU_2}}} \right]$$

$$- \left[\frac{P^m \lambda_{G^{SU_2}} e^{-\left(\frac{((l-j+n_{I_2})+1)\Delta_p \lambda_{G_m^{SU_2}}}{P^m \eta (T_F - t_{ts})} \right)}}{P^m \lambda_{G^{SU_2}} - P^e \lambda_{G_m^{SU_2}}} \right.$$

$$\left. \left. + \frac{P^e \lambda_{G_m^{SU_2}} e^{-\left(\frac{(l-j+n_{I_2}) Delta_p \lambda_{G^{SU_2}}}{P^e \eta (T_F - t_{ts})} \right)}}{P^m \lambda_{G^{SU_2}} - P^e \lambda_{G_m^{SU_2}}} \right] \right)$$

$$\times \left(e^{-\left(\frac{\lambda_{H_2^p} I_{it} t_{ts}}{(n_{I_2}+1)\Delta_p} \right)} - e^{-\left(\frac{\lambda_{H_2^p} I_{it} t_{ts}}{n_{I_2} \Delta_p} \right)} \right) \Bigg). \tag{3.67}$$

Similarly, the state transition probability expression is the sum the above condi-

tional transition probability expressions derived in Equations (3.64), (3.65), (3.66), and (3.67):

$$\begin{aligned}\bar{Q}((i,j),(k,l)) = \bar{Q}_{ST1}((i,j),(k,l)) + \bar{Q}_{ST2}((i,j),(k,l)) \\ +\bar{Q}_{ST3}((i,j),(k,l)) + \bar{Q}_{ST4}((i,j),(k,l)),\end{aligned} \tag{3.68}$$

using Equation (3.68) above, the probability of being in state (k,l) at t^{th} frame index is computed as follows, using Markovian analysis:

$$\bar{\Pi}(k,l) = \sum_{i=0}^{\frac{B^{max}}{\Delta_p}} \sum_{j=0}^{\frac{B^{max}}{\Delta_p}} \bar{Q}((i,j),(k,l))\bar{\Pi}(i,j), \tag{3.69}$$

where:

$$\sum_{k=0}^{\frac{B^{max}}{\Delta_p}} \sum_{l=0}^{\frac{B^{max}}{\Delta_p}} \bar{\Pi}(k,l) = 1. \tag{3.70}$$

3.4 Simulation Results and Discussion

Table 3.2: Table of Simulation Parameters

Symbol	**Description**
λ_{G^s}	500 Watts/meter
$\lambda_{G^s_{SU1}}$	120 Watts/meter
$\lambda_{G^s_{SU2}}$	70 Watts/meter
$\lambda_{H^s_1}$	120 Watts/meter
$\lambda_{H^s_2}$	70 Watts/meter
$\lambda_{G^{SU1}}$	300 Watts/meter
$\lambda_{G^{SU2}_m}$	250 Watts/meter
$\lambda_{H^p_1}$	300 Watts/meter
$\lambda_{H^p_2}$	250 Watts/meter
Δ_p	0.01 Watts
σ^2	0.05 Watts
T_f	20×10^{-3} seconds
t_{ts}	2×10^{-3} seconds
η	1

In this section, simulations of the derived Markovian analysis are presented using matlab. First we present the confirmations of the derived CDFs that are used to build closed-form expressions for SUs state transition probabilities, which are in turn used to derive long term (steady state) probabilities of SUs being in each state of their Markovian models. To generate required validation results, battery level discretization factor is set to 0.01 watts (Δ_p=0.01). The channel gains between respective transmitter-receiver antenna pairs are generated from the rates set as follows: $\lambda_{G^s} = 500, \lambda_{G^s_{SU1}} = 120, \lambda_{G^s_{SU2}} = 70, \lambda_{H^s_1} = 120, \lambda_{H^s_2} = 70, \lambda_{G^{SU1}} = 300, \lambda_{G^{SU2}_m} = 250, \lambda_{H^p_1} = 300$, and $\lambda_{H^p_2} = 250$. Additive white Gaussian noise is set to $\sigma^2 = 0.05$. Since the proposed system is modelled as a time division multi-access system, frame duration is set as $T_f = 20 \times 10^{-3}$ seconds and the frame time-slot as $t_{ts} = 2 \times 10^{-3}$ seconds. For energy harvesting purposes, the energy conversion coefficient is set to $\eta = 1$. The above initial settings are shown in Table 3.2. On the result graphs, we denote "Sim" and "Analysis" as simulation and analytical result curves, respectively. Matlab simulations are used to verify the derived analytical expressions and to provide system performance evaluation intuitively. The simulation parameters are chosen to evaluate the robustness of the proposed system model. To achieve this, relatively high transmit powers are picked to assess system performance under conditions of excessive interference.

3.4.1 Distributions Confirmations

This sub-section covers confirmation of some major distributions that contribute to the analytical derivations of the subsequent analytical expressions for each SU Markovian analysis. Fig. 3.4 presents distribution validation for the random variable n_i depicted in Equation (3.26). This distribution is one of the distributions used to analytically derive transition probabilities for Markovian analysis done in this research work. Fig. 3.5 shows CDF results confirmation for simulation and analysis of the derived energy harvesting CDF expression for energy harvesting from SBS as shown in Equation (3.30), this distribution is also used in the system Markovian analysis derivations. Similarly, energy harvesting from both SBS and MBS derived CDF expression confirmation is shown in Fig. 3.6. The results presented in this subsection reveal a match between analytical and simulation results. Therefore, the associated analytical expressions can be considered valid.

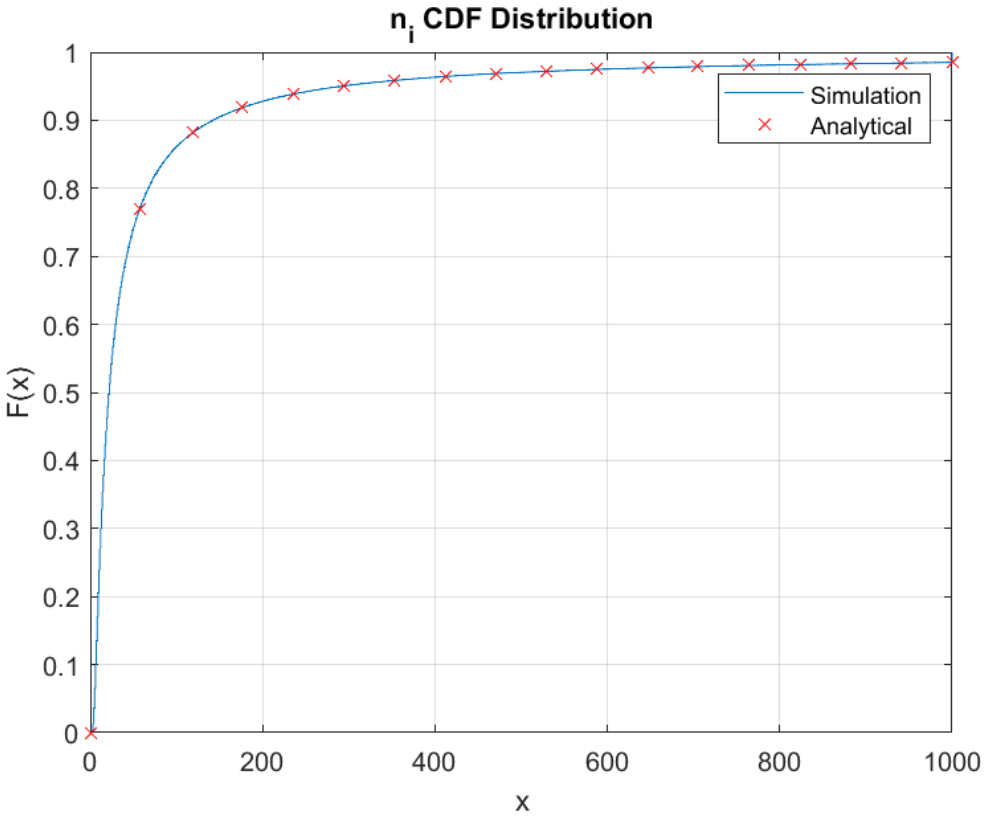


Figure 3.4: n_i Distribution: Battery Power Conditioned on I_{it}

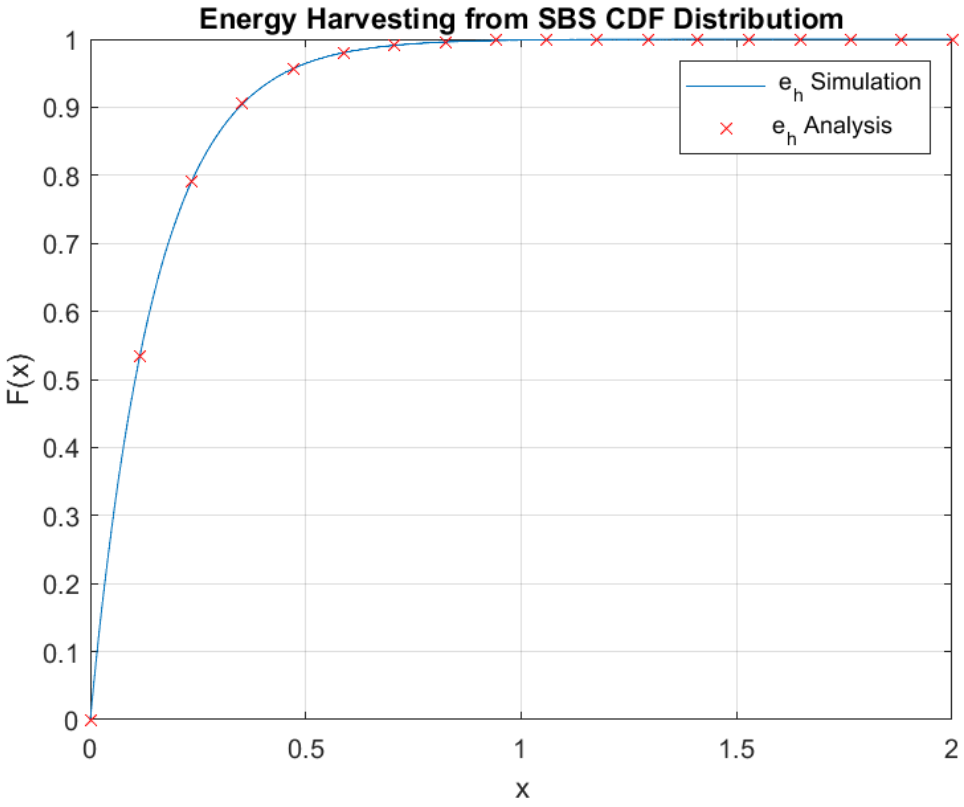


Figure 3.5: SBS: Energy Harvesting CDF Distribution

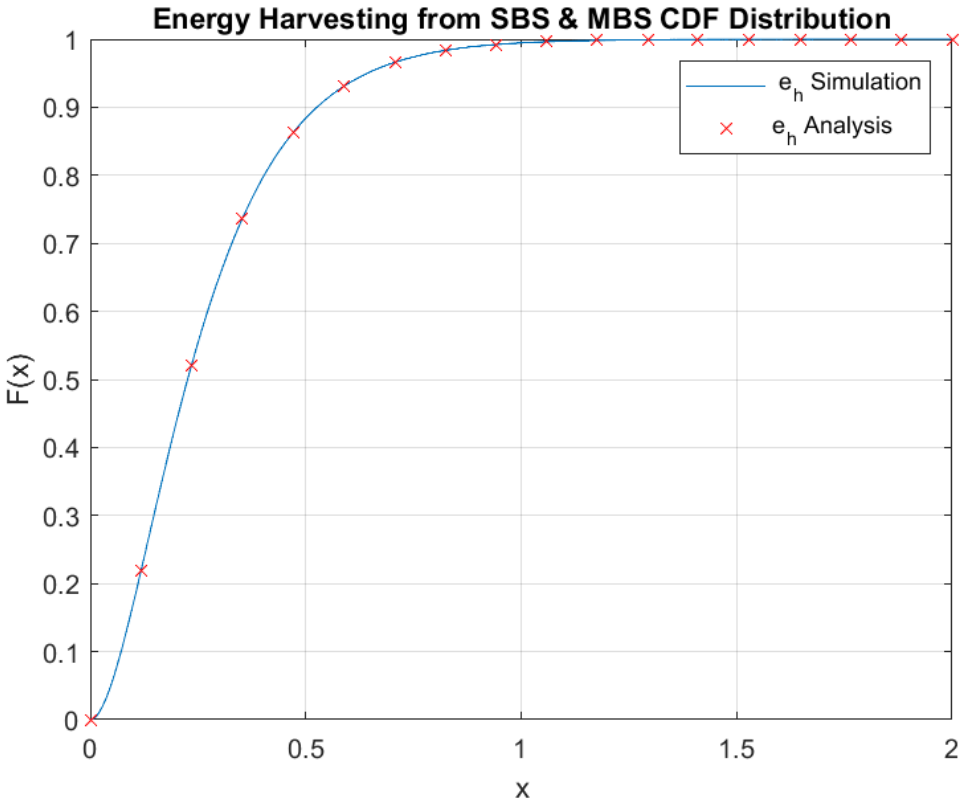


Figure 3.6: SBS and MBS: Energy Harvesting CDF Distribution

3.4.2 Markovian Analysis

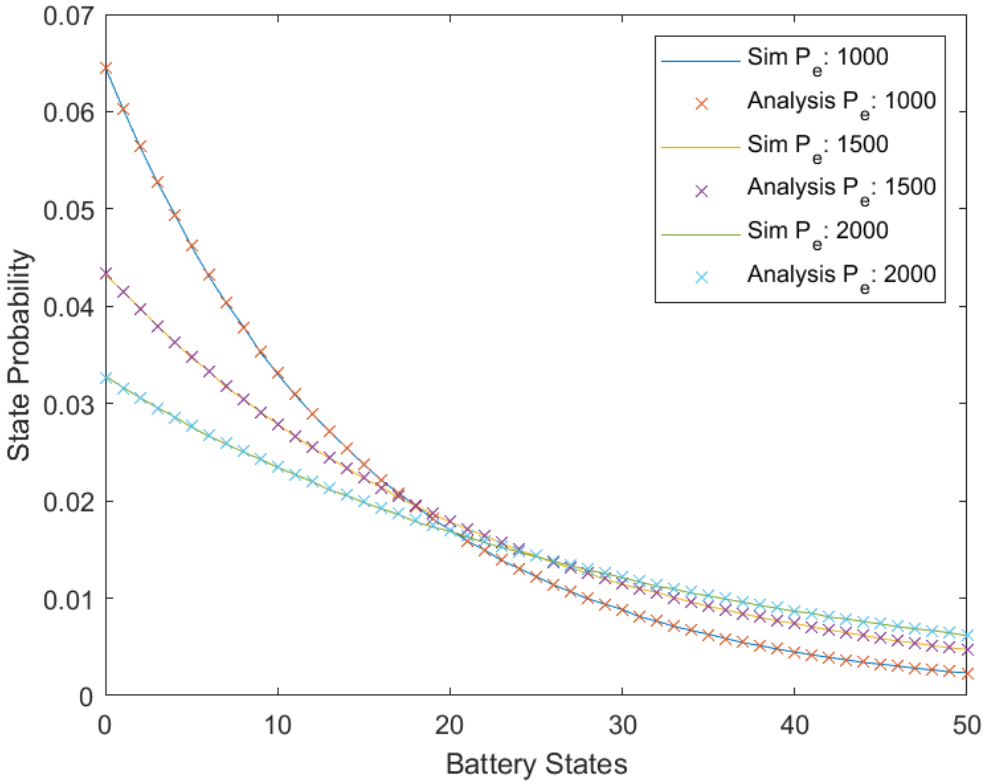


Figure 3.7: SBS: State Probability vs Battery States for Different Values of Primary Transmit Power P_p

Fig. 3.7 illustrates the Markovian analysis of the proposed energy harvesting CR-NOMA system model in this dissertation. The figure shows simulation and corresponding analytical graphs representing probabilities of an SU being in a particular Markovian state. State transitions depend on the energy consumed by the SUs to facilitate transmission, the energy harvested from the SBS downlink transmissions during a particular frame duration, and the residual energy from the previous transmission frame. The simulations and analysis curves were compared for different values of SBS downlink transmit power (watts), $P_e = (1000 : 500 : 2000)$. Similarly, Fig. 3.8 shows state probability simulation and analytical results, but this time around with energy harvesting from both SBS and MBS. For this case, SBS downlink transmit power (watts) is varied as it was when harvesting was done only from the SBS ($P_e = (1000 : 500 : 2000)$), while the MBS downlink transmit power is fixed at $P_m = 1500$ watts. It is observed from the two results

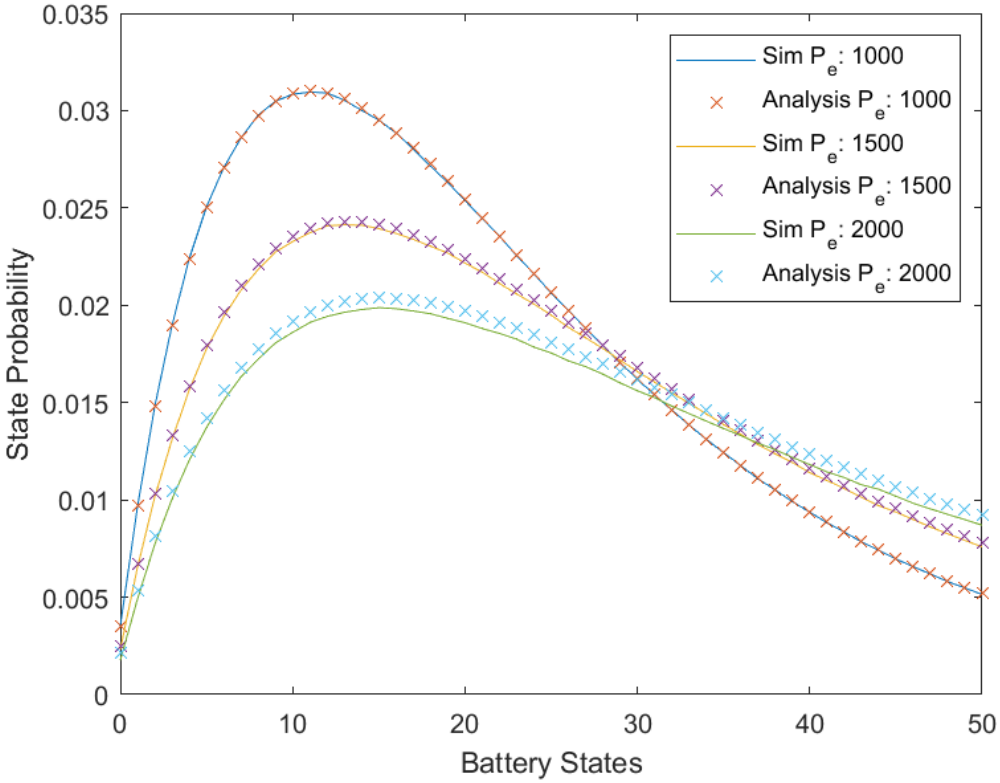


Figure 3.8: SBS and MBS: State Probability vs Battery States for Different Values of Primary Transmit Power P_p

that when harvesting from both sources (SBS and MBS), the SUs spend more time in higher energy states than when harvesting from a single source (SBS) as expected.Good agreement exists between the results obtained from simulation and analytical results. Thus, we can confirm that analytical Markovian expressions for SUs state transitions were derived correctly.

3.5 Summary

In this chapter, the considered system model has been presented, Markovian analysis for each SU when harvesting energy from the SBS and when harvesting from both the SBS and MBS were accurately performed. The derived Markovian analysis expressions for each SU were verified by simulations in Matlab and the obtained results show a close agreement between simulation and analysis results. Thus confirming the validity of the derived analytical expressions.

Chapter 4

Outage Probability Analysis

4.1 Introduction

This chapter investigates outage probability experienced by SU_1 and SU_2 in the proposed energy harvesting CR-NOMA IoT system model. Outage probability is the probability that the instantaneous SINR as shown in Equation (4.1) is less than target SINR as presented in Equation (3.11), where the target SINRs for successful decoding of transmissions from SU_1 and SU_2 at the SBS are denoted as δ_1 and δ_2, respectively.

$$P_{out}^{n}(t) = \begin{cases} \frac{P_1^s(t)H_1^s(t)}{P^p(t)G^s(t)+\Omega^2+\sigma^2} < \delta_1, & n = 1 \\ \\ \frac{P_2^s(t)H_2^s(t)}{P_1^s(t)H_1^s(t)+P^p(t)G^s(t)+\sigma^2} < \delta_2, & n = 2 \end{cases} \tag{4.1}$$

To derive closed-form expressions of outage probability for each SU, CDF for SINRs of each SU has to be derived. To analytically derive closed-form expression for SINR CDF, Markovian models build for each SU in Chapter 3 are adopted to be able to derive SINR CDF expression for an SU at the particular state i (represented by the number of energy chunks in the battery). The closed-form expression for total outage probability of each SU at any state is computed by multiplying the outage probability at any state i by the probability of being in that state.

4.2 Outage Probability Experienced by SU_1

For SBS to reliably receive transmissions from SU_1 (weaker user), both uplink transmissions from SU_1 and SU_2 (stronger user) should be successfully decoded

by SBS during the SIC process. Using Markovian analysis done in Chapter 3 as our basis, outage probability experienced by SU_1 can be derived as follows for the two possible transition events, $\xi = 0$ and $\xi = 1$:

4.2.1 Case 1

Outage probability for SU_1 given $\xi = 0$ at any system state j is given by:

$$\begin{aligned} P^1_{out}(j)|_{\xi=0} &= 1 - Pr\left(\frac{\frac{j}{t_{ts}}\Delta_p H_1^s}{P^p G^s + \sigma^2 + \Omega^2} > \delta_1\right), \\ &= 1 - Pr\left(\frac{j}{t_{ts}}\Delta_p H_1^s - \delta_1 P^p G^s > \delta_1\left(\sigma^2 + \Omega^2\right)\right), \end{aligned} \tag{4.2}$$

letting $Y = \frac{j}{t_{ts}}\Delta_p H_1^s - \delta_1 P^p G^s$, then Equation (4.2) simplifies to:

$$\begin{aligned} P^1_{out}(j)|_{\xi=0} &= 1 - Pr\left(Y > \delta_1\left(\sigma^2 + \Omega^2\right)\right), \\ &= 1 - \left(1 - F_Y\left(\delta_1\left(\sigma^2 + \Omega^2\right)\right), \right. \\ &= F_Y\left(\delta_1\left(\sigma^2 + \Omega^2\right)\right). \end{aligned} \tag{4.3}$$

To solve Equation (4.3), we need to find the CDF of $Y = \frac{j}{t_{ts}}\Delta_p H_1^s - \delta_1 P^p G^s$, which is the difference of two exponential random variables $\frac{j}{t_{ts}}\Delta_p H_1^s$ and $\delta_1 P^p G^s$. The expression for the CDF of Y is derived as follows using the approach defined in [40]:

$$
\begin{aligned}
F_Y(y)|_{j,\xi=0} &= Pr\left(Y \leq y\right), \\
&= Pr\left(\frac{j}{t_{ts}}\Delta_p H_1^s - \delta_1 P^p G^s \leq y\right), \\
&= Pr\left(H_1^s \leq \frac{\delta_1 P^p G^s}{\frac{j}{t_{ts}}\Delta_p} + \frac{y}{\frac{j}{t_{ts}}\Delta_p}\right), \\
&= \int_0^\infty F_{H_1^s}\left(\frac{1}{\frac{j}{t_{ts}}\Delta_p}\left(\delta_1 P^p x + y\right)\right) f_{G^s}(x)\, dx, \\
&= \int_0^\infty \left(1 - e^{-\lambda_{H_1^s}\left(\frac{1}{\frac{j}{t_{ts}}\Delta_p}(\delta_1 P^p x + y)\right)}\right) \lambda_{G^s} e^{-\lambda_{G^s} x}\, dx, \\
&= 1 - \frac{\frac{j}{t_{ts}}\Delta_p \lambda_{G^s} e^{-\left(\frac{\lambda_{H_1^s} y}{\frac{j}{t_{ts}}\Delta_p}\right)}}{\lambda_{H_1^s}\delta_1 P^p + \frac{j}{t_{ts}}\Delta_p \lambda_{G^s}}.
\end{aligned}
\tag{4.4}
$$

Using Equation (4.4) above, outage probability at j given $\xi = 0$, is expressed as follows for imperfect and perfect SIC scenarios:

4.2.1.1 Imperfect SIC Scenario:

This considers scenario where there is some residual interference at the SBS caused by imperfect SIC which is modelled as Ω^2:

$$
\begin{aligned}
P_{out}^1(j)|_{\xi=0} &= \left(1 - Pr\left(\frac{\frac{j}{t_{ts}}\Delta_p H_1^s}{P^p G^s + \sigma^2 + \Omega^2} > \delta_1\right)\right) \times Pr\left(j < n_{I_1}\right), \\
&= \left(1 - \frac{\frac{j}{t_{ts}}\Delta_p \lambda_{G^s} e^{-\left(\frac{\lambda_{H_1^s}\delta_1\left(\sigma^2+\Omega^2\right)}{\frac{j}{t_{ts}}\Delta_p}\right)}}{\lambda_{H_1^s}\delta_1 P^p + \frac{j}{t_{ts}}\Delta_p \lambda_{G^s}}\right) \\
&\times \left(1 - e^{-\left(\frac{\lambda_{H_1^p} I_{it} t_{ts}}{j\Delta_p}\right)}\right).
\end{aligned}
\tag{4.5}
$$

4.2.1.2 Perfect SIC Scenario:

In this scenario, Ω^2 goes to zero because the assumption is that there is no SIC error:

$$
\begin{aligned}
P^1_{out}(j)|_{\xi=0} &= \left(1 - Pr\left(\frac{\frac{j}{t_{ts}}\Delta_p H_1^s}{P^p G^s + \sigma^2 + \Omega^2} > \delta_1\right)\right) \times Pr\left(j < n_{I_1}\right), \\
&= \left(1 - \frac{\frac{j}{t_{ts}}\Delta_p \lambda_{G^s} e^{-\left(\frac{\lambda_{H_1^s}\delta_1\sigma^2}{\frac{j}{t_{ts}}\Delta_p}\right)}}{\lambda_{H_1^s}\delta_1 P^p + \frac{j}{t_{ts}}\Delta_p\lambda_{G^s}}\right) \times \left(1 - e^{-\left(\frac{\lambda_{H_1^p} I_{it} t_{ts}}{j\Delta_p}\right)}\right).
\end{aligned} \tag{4.6}
$$

4.2.2 Case 2

Similarly, outage probability of SU_1 given $\xi = 1$ is derived as follows:

$$
\begin{aligned}
P^1_{out}(j)|_{\xi=1} &= 1 - Pr\left(\frac{\frac{n_{I_1}}{t_{ts}}\Delta_p H_1^s}{P^p G^s + \sigma^2 + \Omega^2} > \delta_1\right), \\
&= 1 - Pr\left(\frac{n_{I_1}}{t_{ts}}\Delta_p H_1^s - \delta_1 P^p G^s > \delta_1\left(\sigma^2 + \Omega^2\right)\right).
\end{aligned} \tag{4.7}
$$

Now let $Y = \frac{n_{I_1}}{t_{ts}}\Delta_p H_1^s - \delta_1 P^p G^s$, then Equation (4.7) above simplifies to:

$$
\begin{aligned}
P^1_{out}(j)|_{\xi=1} &= 1 - Pr\left(Y > \delta_1\left(\sigma^2 + \Omega^2\right)\right), \\
&= 1 - \left(1 - F_Y\left(\delta_1\left(\sigma^2 + \Omega^2\right)\right)\right), \\
&= F_Y\left(\delta_1\left(\sigma^2 + \Omega^2\right)\right).
\end{aligned} \tag{4.8}
$$

To solve Equation (4.8) above, we need to find the CDF of $Y = \frac{n_{I_1}}{t_{ts}}\Delta_p H_1^s - \delta_1 P^p G^s$:

$$
\begin{aligned}
F_Y(y)|_{n_{I_1}} &= Pr\left(Y \leq y\right), \\
&= Pr\left(\frac{n_{I_1}}{t_{ts}}\Delta_p H_1^s - \delta_1 P^p G^s \leq y\right), \\
&= Pr\left(H_1^s \leq \frac{\delta_1 P^p G^s}{\frac{n_{I_1}}{t_{ts}}\Delta_p} + \frac{y}{\frac{n_{I_1}}{t_{ts}}\Delta_p}\right), \\
&= \int_0^\infty F_{H_1^s}\left(\frac{1}{\frac{n_{I_1}}{t_{ts}}\Delta_p}\left(\delta_1 P^p x + y\right)\right) f_{G^s}(x)\, dx, \\
&= \int_0^\infty \left(1 - e^{-\lambda_{H_1^s}\left(\frac{1}{\frac{n_{I_1}}{t_{ts}}\Delta_p}(\delta_1 P^p x + y)\right)}\right) \lambda_{G^s} e^{-\lambda_{G^s} x}\, dx, \\
&= 1 - \frac{\frac{n_{I_1}}{t_{ts}}\Delta_p \lambda_{G^s} e^{-\left(\frac{\lambda_{H_1^s} y}{\frac{n_{I_1}}{t_{ts}}\Delta_p}\right)}}{\lambda_{H_1^s}\delta_1 P^p + \frac{n_{I_1}}{t_{ts}}\Delta_p \lambda_{G^s}}.
\end{aligned}
\tag{4.9}
$$

Un-conditioning on n_{I_1} in Equation (4.9) above, outage probability of SU_1 given $\xi = 1$ at state j is given by the below expressions for imperfect and perfect SIC scenarios:

4.2.2.1 Imperfect SIC Scenario:

In this case, SIC process results in residual interference that is not considered insignificant.

$$
\begin{aligned}
P_{out}^1(j)|_{\xi=1} &= 1 - Pr\left(\frac{\frac{n_{I_1}}{t_{ts}}\Delta_p H_1^s}{P^p G^s + \sigma^2 + \Omega^2} > \delta_1, j \geq n_{I_1}\right), \\
&= \sum_{n_{I_1}=0}^{j} \left(1 - \frac{\frac{n_{I_1}}{t_{ts}}\Delta_p \lambda_{G^s} e^{-\left(\frac{\lambda_{H_1^s}\left(\sigma^2+\Omega^2\right)}{\frac{n_{I_1}}{t_{ts}}\Delta_p}\right)}}{\lambda_{H_1^s}\delta_1 P^p + \frac{n_{I_1}}{t_{ts}}\Delta_p \lambda_{G^s}}\right) \\
&\quad \times \left(e^{-\left(\frac{\lambda_{H_1^p} I_{it} t_{ts}}{(n_{I_1}+1)\Delta_p}\right)} - e^{-\left(\frac{\lambda_{H_1^p} I_{it} t_{ts}}{n_{I_1}\Delta_p}\right)}\right).
\end{aligned}
\tag{4.10}
$$

4.2.2.2 Perfect SIC Scenario:

In this case, it is assumed that SIC process was able to cancel out interference such that the residual interference is considered negligible. Thus Ω is set to zero.

$$\begin{aligned} P_{out}^{1}(j)|_{\xi=1} &= 1 - Pr\left(\frac{\frac{n_{I_1}}{t_{ts}}\Delta_p H_1^s}{P^p G^s + \sigma^2 + \Omega^2} > \delta_1, j \geq n_{I_1}\right), \\ &= \sum_{n_{I_1}=0}^{j} \left(1 - \frac{\frac{n_{I_1}}{t_{ts}}\Delta_p \lambda_{G^s} e^{-\left(\frac{\lambda_{H_1^s}\sigma^2}{\frac{n_{I_1}}{t_{ts}}\Delta_p}\right)}}{\lambda_{H_1^s}\delta_1 P^p + \frac{n_{I_1}}{t_{ts}}\Delta_p \lambda_{G^s}}\right) \\ &\times \left(e^{-\left(\frac{\lambda_{H_1^p} I_{it} t_{ts}}{(n_{I_1}+1)\Delta_p}\right)} - e^{-\left(\frac{\lambda_{H_1^p} I_{it}\, t_{ts}}{n_{I_1}\Delta_p}\right)}\right). \end{aligned} \tag{4.11}$$

Using results from Equations (3.36),(3.50),(4.5), and (4.10), total outage probability for SU_1 is given by the following expressions using probability sum rule and considering both cases of harvesting from SBS as well as when harvesting from both the SBS and MBS:

Case 1: With energy harvesting from SBS

$$P_{out}^{1,total} = \sum_{j=0}^{\frac{B^{max}}{\Delta_p}} \left(P_{out}^{1}(j)|_{\xi=0} + P_{out}^{1}(j)|_{\xi=1}\right) \Pi(j). \tag{4.12}$$

Case 2: With energy harvesting from SBS and MBS:

$$P_{out}^{1,total} = \sum_{j=0}^{\frac{B^{max}}{\Delta_p}} \left(P_{out}^{1}(j)|_{\xi=0} + P_{out}^{1}(j)|_{\xi=1}\right) \bar{\Pi}(j). \tag{4.13}$$

4.3 Outage Probability Experienced by User 2

For SU_2 transmissions to be reliably decoded by the SBS, SBS will only need to decode SU_2 (strong user) signal and treat SU_1 (weak user) signal as part of the interference. Outage probability for SU_2 will occur when its instantaneous SINR is less than target SINR as shown in equation (3.11). We built from that as follows, to find closed-form expression for SU_2 outage probability:

$$P^2_{out}(i,j)|_{P^s_1(i),P^s_2(j)} = Pr\left(\frac{P^s_2(j)H^s_2}{P^s_1(i)H^s_1 + P^pG^s + \sigma^2} < \delta_2\right), \\ = Pr\left(P^s_2(j)H^s_2 - (\delta_2 P^s_1(i)H^s_1 + \delta_2 P^pG^s) < \delta_2\sigma^2\right). \tag{4.14}$$

Letting $T = \delta_2 P^s_1(i)H^s_1 + \delta_2 P^pG^s$, then the PDF of ,$T$, is derived by first, deriving PDFs for $\delta_2 P^s_1(i)H^s_1$ and $\delta_2 P^pG^s$ as follows:

$$F_{H^s_1}(z)|_{P^s_1(i)} = Pr\left(\delta_2 P^s_1(i)H^s_1 \leq z\right), \\ = Pr\left(H^s_1 \leq \frac{z}{\delta_2 P^s_1(i)}\right), \\ = 1 - e^{-\left(\frac{\lambda_{H^s_1} z}{\delta_2 P^s_1(i)}\right)}, \tag{4.15}$$

$$F_{G^s(z)} = Pr\left(\delta_2 P^pG^s \leq z\right), \\ = Pr\left(G^s \leq \frac{z}{\delta_2 P^p}\right), \\ = 1 - e^{-\left(\frac{\lambda^s_G z}{\delta_2 P^p}\right)}. \tag{4.16}$$

Using Equations (4.15) and (4.16), the PDF expressions of the above random variables are derived as follows:

$$f_{H^s_1}(z)|_{P^s_1(i)} = \frac{\partial F_{H^s_1}(z)}{\partial z}, \\ = \left(\frac{\lambda_{H^s_1}}{\delta_2 P^s_1(i)}\right) e^{-\left(\frac{\lambda_{H^s_1} z}{\delta_2 P^s_1(i)}\right)}, \tag{4.17}$$

$$f_{G^s}(z) = \frac{\partial F_{G^s}(z)}{\partial z}, \\ = \left(\frac{\lambda_{G^s}}{\delta_2 P^p}\right) e^{-\left(\frac{\lambda_{G^s} z}{\delta_2 P^p}\right)}. \tag{4.18}$$

Deploying convolution approach as in [75], the PDF of T is then derived as follows using the above derivations in Equations (4.17) and (4.18):

$$
\begin{aligned}
f_T(t)|_{P_1^s(i)} &= \int_0^t f_{H_1^s}(z) f_{G^s}(t-z)\, dz, \\
&= \int_0^t \left(\frac{\lambda_{H_1^s}}{\delta_2 P_1^s(i)}\right) e^{-\left(\frac{\lambda_{H_1^s} z}{\delta_2 P_1^s(i)}\right)} \times \left(\frac{\lambda_{G^s}}{\delta_2 P^p}\right) e^{-\left(\frac{\lambda_{G^s}(t-z)}{\delta_2 P^p}\right)} dz, \\
&= \left(\frac{\lambda_{H_1^s}}{\delta_2 P_1^s(i)}\right)\left(\frac{\lambda_{G^s}}{\delta_2 P^p}\right) \int_0^t e^{-\left(\frac{z\left(\delta_2 P^p \lambda_{H_1^s} - \delta_2 P_1^s(i)\lambda_{G^s}\right) + \delta_2 P_1^s(i)\lambda_{G^s} t}{(\delta_2)^2 P_1^s(i) P^p}\right)} dz, \\
&= \frac{\lambda_{H_1^s}\lambda_{G^s}}{\delta_2\left(P^p\lambda_{H_1^s} - P_1^s(i)\lambda_{G^s}\right)}\left(e^{-\left(\frac{t\lambda_{G^s}}{\delta_2 P_p}\right)} - e^{-\left(\frac{t\lambda_{H_1^s}}{\delta_2 P_1^s(i)}\right)}\right).
\end{aligned}
\tag{4.19}
$$

Substituting T back in Equation (4.14), SU_2 outage probability expression is derived as follows:

$$
\begin{aligned}
P_{out}^2(i,j)|_{P_1^s(i),P_2^s(j)} &= Pr\left(P_2^s(j)H_2^s - T \le \delta_2\sigma^2\right), \\
&= Pr\left(H_2^s \le \frac{\delta_2\sigma^2 + T}{P_2^s(j)}\right), \\
&= \int_0^\infty F_{H_2^s}\left(\frac{\delta_2\sigma^2 + T}{P_2^s(j)}\right) f_T(t)\, dt, \\
&= \int_0^\infty \left(1 - e^{-\lambda_{H_2^s}\left(\frac{\delta_2\sigma^2 + t}{P_2^s(j)}\right)}\right) \\
&\times \left(\frac{\lambda_{H_1^s}\lambda_{G^s}}{\delta_2\left(P^p\lambda_{H_1^s} - P_1^s(i)\lambda_{G^s}\right)}\left(e^{-\left(\frac{t\lambda_{H_1^s}}{\delta_2 P_1^s(i)}\right)} - e^{-\left(\frac{t\lambda_{G^s}}{\delta_2 P_p}\right)}\right)\right) dt, \\
&= \frac{\lambda_{H_1^s}\lambda_{G^s}}{\delta_2\left(P^p\lambda_{H_1^s} - P_1^s(i)\lambda_{G^s}\right)} \\
&\times \int_0^\infty \left(1 - e^{-\lambda_{H_2^s}\left(\frac{\delta_2\sigma^2 + t}{P_2^s(j)}\right)}\right)\left(e^{-\left(\frac{t\lambda_{H_1^s}}{\delta_2 P_1^s(i)}\right)} - e^{-\left(\frac{t\lambda_{G^s}}{\delta_2 P^p}\right)}\right) dt, \\
&= 1 + \left(\frac{P_2^s(j)P_1^s(i)\lambda_{H_1^s}\lambda_{G^s} e^{-\left(\frac{\lambda_{H_2^s}\delta_2\sigma^2}{P_2^s(j)}\right)}}{\left(P^p\lambda_{H_1^s} - P_1^s(i)\lambda_{G^s}\right)\left(\delta_2 P_1^s(i)\lambda_{H_2^s} + P_2^s(j)\lambda_{H_1^s}\right)}\right. \\
&\left. - \frac{P_2^s(j)P^p\lambda_{H_1^s}\lambda_{G^s} e^{-\left(\frac{\lambda_{H_2^s}\delta_2\sigma^2}{P_2^s(j)}\right)}}{\left(P^p\lambda_{H_1^s} - P_1^s(i)\lambda_{G^s}\right)\left(\delta_2 P^p\lambda_{H_2^s} + P_2^s(j)\lambda_{G^s}\right)}\right).
\end{aligned}
\tag{4.20}
$$

Un-conditioning Equation (4.20) with respect to $P_1^s(i)$ and $P_2^s(j)$ since this are random variables, P_{out}^2 is expressed as follows for different values that can be taken by P_1^s and P_2^s:

Case 1: $P_1^s(i) = \frac{i}{t_{ts}}\Delta_p$ for $i < n_{I_1}$ and $P_2^s(j) = \frac{j}{t_{ts}}\Delta_p$ for $j < n_{I_2}$:

$$\begin{aligned}
P_{out}^2(i,j)|_{case1} =& Pr\left(\frac{P_2^s(j)H_2^s}{P_1^s(i)H_1^s + P^pG^s + \sigma^2} < \delta_2\right) \times Pr\left(i < n_{I_1}\right) Pr\left(j < n_{I_2}\right), \\
=& \left(1 + \left(\frac{\frac{j}{t_{ts}}\Delta_p \frac{i}{t_{ts}}\Delta_p \lambda_{H_1^s}\lambda_{G^s} e^{-\left(\frac{\lambda_{H_2^s}\delta_2\sigma^2}{\frac{j}{t_{ts}}\Delta_p}\right)}}{\left(P^p\lambda_{H_1^s} - \frac{i}{t_{ts}}\Delta_p\lambda_{G^s}\right)\left(\delta_2\frac{i}{t_{ts}}\Delta_p\lambda_{H_2^s} + \frac{j}{t_{ts}}\Delta_p\lambda_{H_1^s}\right)}\right.\right. \\
& \left.\left. - \frac{\frac{j}{t_{ts}}\Delta_p P^p\lambda_{H_1^s}\lambda_{G^s} e^{-\left(\frac{\lambda_{H_2^s}\delta_2\sigma^2}{\frac{j}{t_{ts}}\Delta_p}\right)}}{\left(P^p\lambda_{H_1^s} - \frac{i}{t_{ts}}\Delta_p\lambda_{G^s}\right)\left(\delta_2 P^p\lambda_{H_2^s} + \frac{j}{t_{ts}}\Delta_p\lambda_{G^s}\right)}\right)\right) \\
& \times \left(1 - e^{-\left(\frac{\lambda_{H_1^p} I_{it} t_{ts}}{i\Delta_p}\right)}\right)\left(1 - e^{-\left(\frac{\lambda_{H_2^p} I_{it} t_{ts}}{j\Delta_p}\right)}\right).
\end{aligned} \tag{4.21}$$

Case 2: $P_1^s = \frac{n_{I_1}}{t_{ts}}\Delta_p$ for $i \geq n_{I_1}$ and $P_2^s = \frac{j}{t_{ts}}\Delta_p$ for $j < n_{I_2}$:

$$\begin{aligned}
P_{out}^2(i,j)|_{case2} =& Pr\left(\frac{P_2^s(j)H_2^s}{P_1^s(i)H_1^s + P^pG^s + \sigma^2} \leq \delta_2, i \geq n_{I_1}\right) Pr\left(j < n_{I_2}\right), \\
=& \sum_{n_{I_1}=0}^{i} \left(1 + \left(\frac{\frac{j}{t_{ts}}\Delta_p \frac{n_{I_1}}{t_{ts}}\Delta_p \lambda_{H_1^s}\lambda_{G^s} e^{-\left(\frac{\lambda_{H_2^s}\delta_2\sigma^2}{\frac{j}{t_{ts}}\Delta_p}\right)}}{\left(P^p\lambda_{H_1^s} - \frac{n_{I_1}}{t_{ts}}\Delta_p\lambda_{G^s}\right)\left(\delta_2\frac{n_{I_1}}{t_{ts}}\Delta_p\lambda_{H_2^s} + \frac{j}{t_{ts}}\Delta_p\lambda_{H_1^s}\right)}\right.\right. \\
& \left.\left. - \frac{\frac{j}{t_{ts}}\Delta_p P^p\lambda_{H_1^s}\lambda_{G^s} e^{-\left(\frac{\lambda_{H_2^s}\delta_2\sigma^2}{\frac{j}{t_{ts}}\Delta_p}\right)}}{\left(P^p\lambda_{H_1^s} - \frac{n_{I_1}}{t_{ts}}\Delta_p\lambda_{G^s}\right)\left(\delta_2 P^p\lambda_{H_2^s} + \frac{j}{t_{ts}}\Delta_p\lambda_{G^s}\right)}\right)\right) \\
& \times \left(e^{-\left(\frac{\lambda_{H_1^p} I_{it} t_{ts}}{(n_{I_1}+1)\Delta_p}\right)} - e^{-\left(\frac{\lambda_{H_1^p} I_{it} t_{ts}}{n_{I_1}\Delta_p}\right)}\right) \times \left(1 - e^{-\left(\frac{\lambda_{H_2^p} I_{it} t_{ts}}{j\Delta_p}\right)}\right).
\end{aligned} \tag{4.22}$$

Case 3: $P_1^s = \frac{i}{t_{ts}}\Delta_p$ for $i < n_{I_1}$ and $P_2^s = \frac{n_{I_2}}{t_{ts}}\Delta_p$ for $j \geq n_{I_2}$:

$$
\begin{aligned}
P^2_{out}(i,j)|_{case3} =& Pr\left(\frac{P^s_2(j)H^s_2}{P^s_1(i)H^s_1+P^pG^s+\sigma^2}\leq\delta_2, j\geq n_{I_2}\right)Pr\left(i<n_{I_1}\right),\\
=&\sum_{n_{I_2}=0}^{j}\left(1+\left(\frac{\frac{n_{I_2}}{t_{ts}}\Delta_p\frac{i}{t_{ts}}\Delta_p\lambda_{H^s_1}\lambda_{G^s}e^{-\left(\frac{\lambda_{H^s_2}\delta_2\sigma^2}{\frac{n_{I_2}}{t_{ts}}\Delta_p}\right)}}{\left(P^p\lambda_{H^s_1}-\frac{i}{t_{ts}}\Delta_p\lambda_{G^s}\right)\left(\delta_2\frac{i}{t_{ts}}\Delta_p\lambda_{H^s_2}+\frac{n_{I_2}}{t_{ts}}\Delta_p\lambda_{H^s_1}\right)}\right.\right.\\
&\left.\left.-\frac{\frac{n_{I_2}}{t_{ts}}\Delta_pP^p\lambda_{H^s_1}\lambda_{G^s}e^{-\left(\frac{\lambda_{H^s_2}\delta_2\sigma^2}{\frac{n_{I_2}}{t_{ts}}\Delta_p}\right)}}{\left(P^p\lambda_{H^s_1}-\frac{i}{t_{ts}}\Delta_p\lambda_{G^s}\right)\left(\delta_2P^p\lambda_{H^s_2}+\frac{n_{I_2}}{t_{ts}}\Delta_p\lambda_{G^s}\right)}\right)\right)\\
&\times\left(e^{-\left(\frac{\lambda_{H^p_2}I_{it}t_{ts}}{(n_{I_2}+1)\Delta_p}\right)}-e^{-\left(\frac{\lambda_{H^p_2}I_{it}t_{ts}}{n_{I_2}\Delta_p}\right)}\right)\left(1-e^{-\left(\frac{\lambda_{H^p_1}I_{it}t_{ts}}{i\Delta_p}\right)}\right).
\end{aligned}
\tag{4.23}
$$

Case 4: $P^s_1=\frac{n_{I_1}}{t_{ts}}\Delta_p$ for $i\geq n_{I_1}$ and $P^s_2=\frac{n_{I_2}}{t_{ts}}\Delta_p$ for $j\geq n_{I_2}$:

$$
\begin{aligned}
P^2_{out}(i,j)|_{case4} =& Pr\left(\frac{P^s_2(j)H^s_2}{P^s_1(i)H^s_1+P^pG^s+\sigma^2}\leq\delta_2, i\geq n_{I_1}, j\geq n_{I_2}\right),\\
=&\sum_{n_{I_1}=0}^{i}\sum_{n_{I_2}=0}^{j}\left(1+\left[\left(\frac{\frac{n_{I_2}}{t_{ts}}\Delta_p\frac{n_{I_1}}{t_{ts}}\Delta_p\lambda_{H^s_1}\lambda_{G^s}}{\left(P^p\lambda_{H^s_1}-\frac{n_{I_1}}{t_{ts}}\Delta_p\lambda_{G^s}\right)}\right.\right.\right.\\
&\left.\times\frac{e^{-\left(\frac{\lambda_{H^s_2}\delta_2\sigma^2}{\frac{n_{I_2}}{t_{ts}}\Delta_p}\right)}}{\left(\delta_2\frac{n_{I_1}}{t_{ts}}\Delta_p\lambda_{H^s_2}+\frac{n_{I_2}}{t_{ts}}\Delta_p\lambda_{H^s_1}\right)}\right)\\
&\left.\left.-\frac{\frac{n_{I_2}}{t_{ts}}\Delta_pP^p\lambda_{H^s_1}\lambda_{G^s}e^{-\left(\frac{\lambda_{H^s_2}\delta_2\sigma^2}{\frac{n_{I_2}}{t_{ts}}\Delta_p}\right)}}{\left(P^p\lambda_{H^s_1}-\frac{n_{I_1}}{t_{ts}}\Delta_p\lambda_{G^s}\right)\left(\delta_2P^p\lambda_{H^s_2}+\frac{n_{I_2}}{t_{ts}}\Delta_p\lambda_{G^s}\right)}\right]\right)\\
&\times\left(e^{-\left(\frac{\lambda_{H^p_1}I_{it}t_{ts}}{(n_{I_1}+1)\Delta_p}\right)}-e^{-\left(\frac{\lambda_{H^p_1}I_{it}t_{ts}}{n_{I_1}\Delta_p}\right)}\right)\\
&\times\left(e^{-\left(\frac{\lambda_{H^p_2}I_{it}t_{ts}}{(n_{I_2}+1)\Delta_p}\right)}-e^{-\left(\frac{\lambda_{H^p_2}I_{it}t_{ts}}{n_{I_2}\Delta_p}\right)}\right).
\end{aligned}
\tag{4.24}
$$

Using results from Equations (3.62), (3.69),(4.21), (4.22), (4.24), and (4.24), the total outage probability for SU_2 is given by summing the conditional probabilities derived in the above results using probability sum rule:

Case 1: SU_2 total outage probability with energy harvesting done from SBS for both SUs:

$$P_{out}^{2,total} = \sum_{k=0}^{\frac{B^{max}}{\Delta_p}} \sum_{l=0}^{\frac{B^{max}}{\Delta_p}} \Bigg(P_{out}^{2}(k,l)|_{case1} + P_{out}^{2}(k,l)|_{case2} + P_{out}^{2}(k,l)|_{case3} + P_{out}^{2}(k,l)|_{case4} \Bigg) \Pi(k,l). \tag{4.25}$$

Case 2: SU_2 total outage probability with energy harvesting done from both SBS and MBS by the SUs:

$$P_{out}^{2,total} = \sum_{k=0}^{\frac{B^{max}}{\Delta_p}} \sum_{l=0}^{\frac{B^{max}}{\Delta_p}} \Bigg(P_{out}^{2}(k,l)|_{case1} + P_{out}^{2}(k,l)|_{case2} + P_{out}^{2}(k,l)|_{case3} + P_{out}^{2}(k,l)|_{case4} \Bigg) \bar{\Pi}(k,l). \tag{4.26}$$

4.4 Simulation Results and Discussion

In this section, we generate simulation results to confirm the derived outage probability expressions for each SU. The results generated in this chapter adopted the initial parameter settings presented in Chapter 3, Table 3.2.

In Fig. 4.1 and Fig. 4.2 , outage probability performance versus SINR threshold at the SBS is demonstrated for SU_1 and SU_2, respectively. Different curves are generated for different values of primary user transmit power(100, 200, 300)watts. It can be observed from the curves that outage probability increases as SINR threshold is increased, this is the expected behaviour because as we increase SINR threshold with every parameter fixed, we increase the likely-hood that the instantaneous SINR will be less than the threshold SINR. The curves further demonstrate that overall outage probability increases at higher primary transmit power, because an increase in primary transmit power results in an increase in interference experienced at the SBS receiver resulting in the difficulty to decode the carrier

signal at the SBS receiver.

Fig. 4.3 and Fig. 4.4 demonstrate outage probability versus SINR threshold, while varying energy harvesting efficiency factor *eta* , $\eta = 0.3, 0.6, 09$. Similarly, different plots are generated to demonstrate outage probability behaviour of SU_1 and SU_2 for different values of energy harvesting conversion efficiency factor. It can be observed from both figures that as energy conversion efficiency is improved both users achieve better outage probabilities (outage probability decreases), with the lowest *eta* resulting in the highest outage probability graph for both SUs. This is the expected behaviour because as *eta* increases, SUs are able harvest more energy per frame. More harvested energy implies that the SUs will most of the time have sufficient energy (though constrained by interference threshold) for their instantaneous SINRs to be greater than SINR threshold most of the time, thus decreasing outage likely-hood.

Fig. 4.5 and Fig. 4.6 cover the results for outage probability versus interference constraint while varying different values of primary transmit power P^p. It is observed from the graphs that outage probability decreases as interference constraint power is increasing. This is expected because as the interference power constraint increases, both users are allowed to transmit with relatively high powers which increases the likely-hood of successful decoding of their carrier signals, this is because increasing interference threshold relaxes the constraint on the maximum power that the SUs can transmit with. Simulation and analytical results are matching, thus, this further validates the derived analytical closed-form expression for outage probability of both users.

Fig. 4.7 and Fig. 4.8 show the results for outage probability of each user as we vary battery level for different values of primary transmit power P^p. The results clearly show that outage probability decreases as each user's battery level increases. It is further observed that for both users, the highest value of primary transmit power $P^p = 300$ produces the performance with the highest outage probabilities. This is expected because as we increase primary transmit power, we increase interference, which consequently results in higher outage performance.

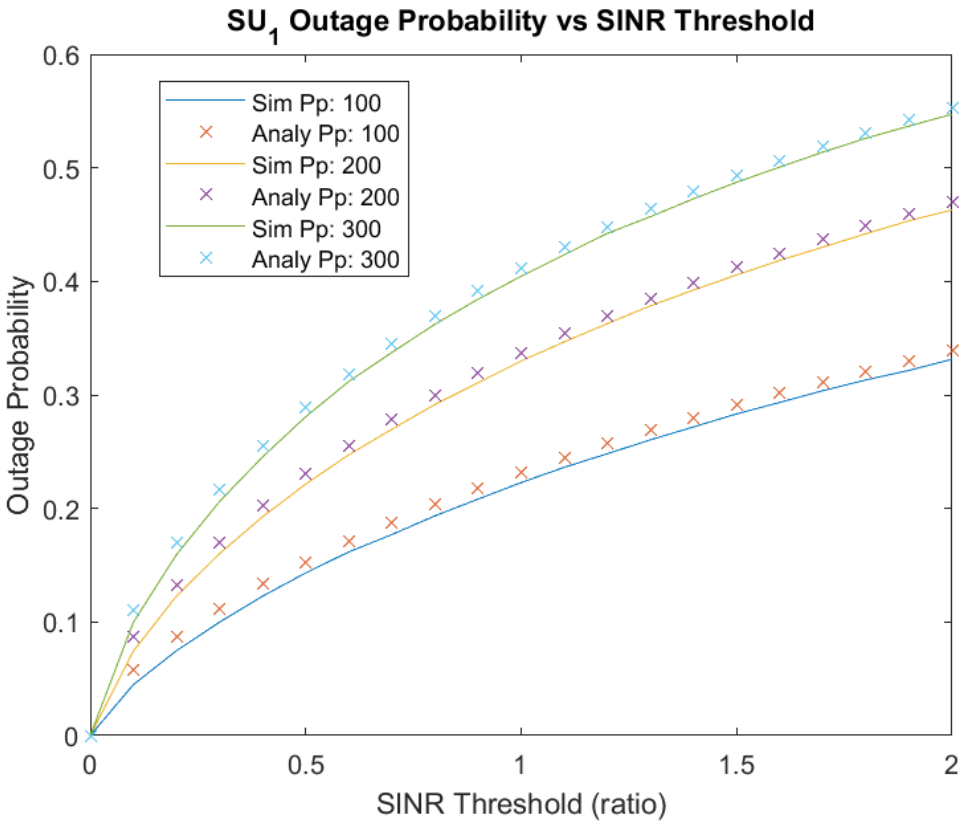


Figure 4.1: Outage Probability vs SINR Threshold for Different Values of Primary Transmit Power P_p (Watts)

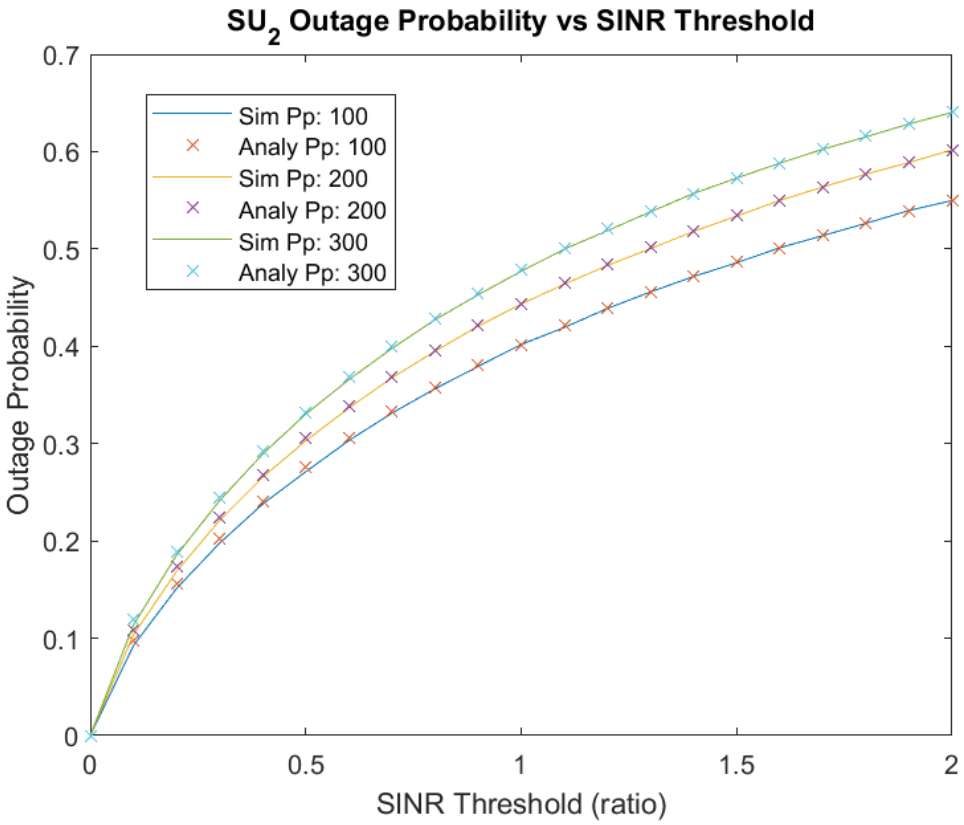


Figure 4.2: Outage Probability vs SINR Threshold for Different Values of Primary Transmit Power P_p (Watts)

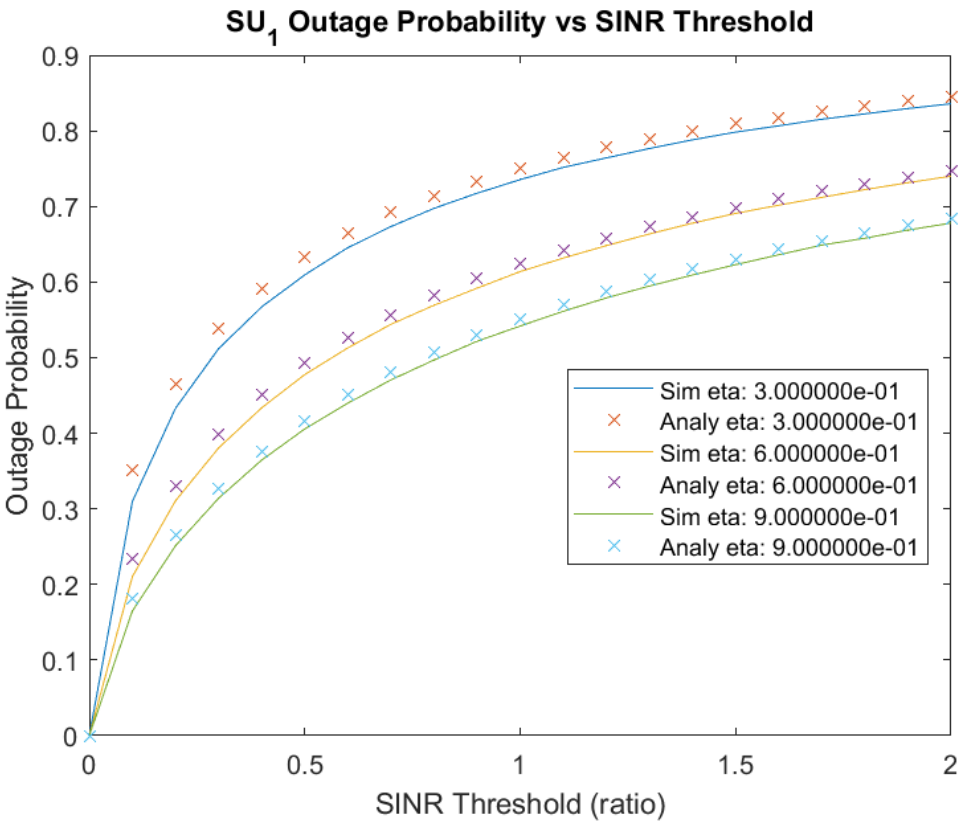


Figure 4.3: Outage Probability vs SINR for Different Values of eta

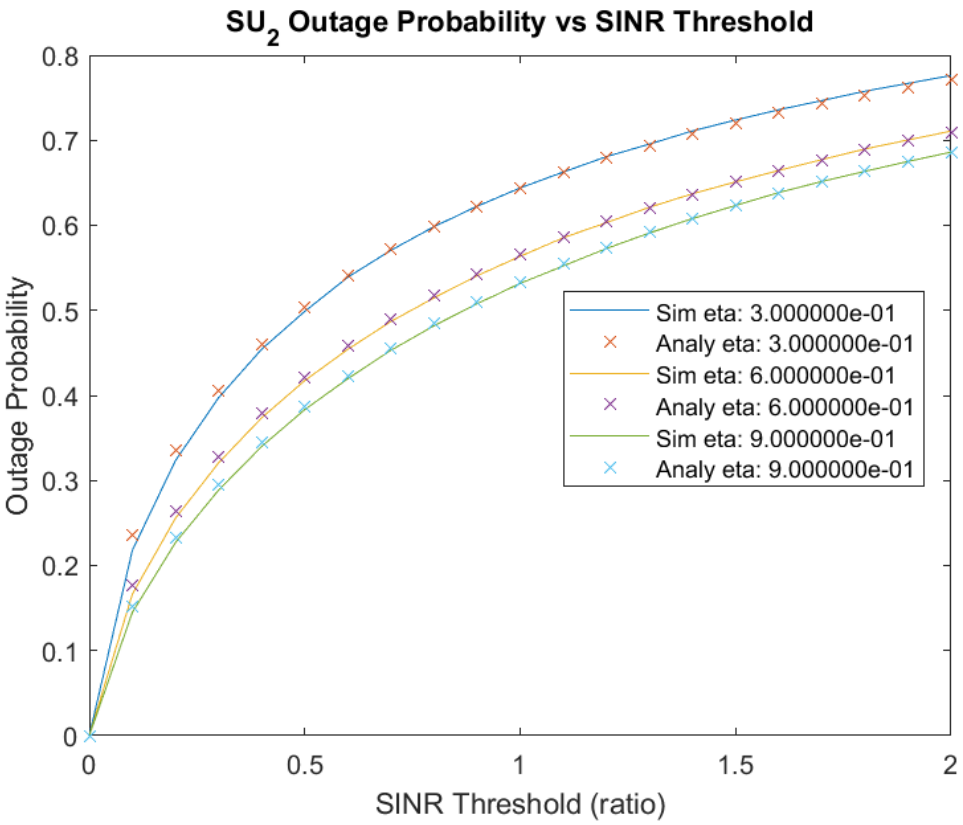


Figure 4.4: Outage Probability vs SINR for Different Values of eta

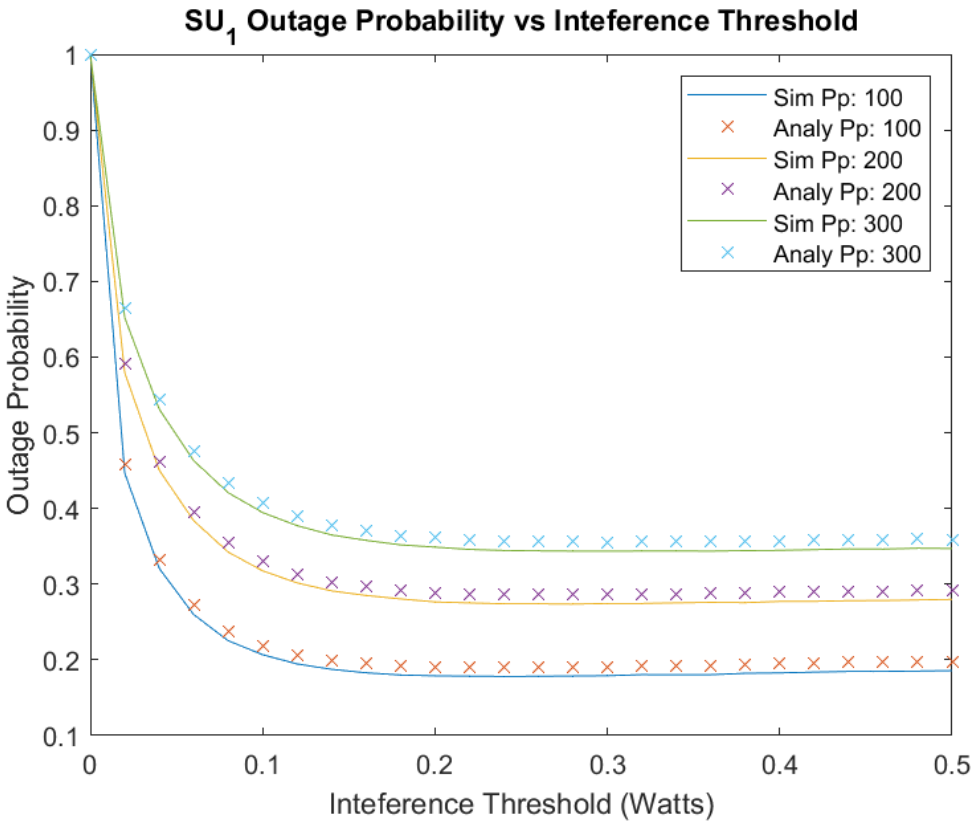


Figure 4.5: Outage Probability vs Interference Threshold for Different Values of Primary Transmit Power P_p (Watts)

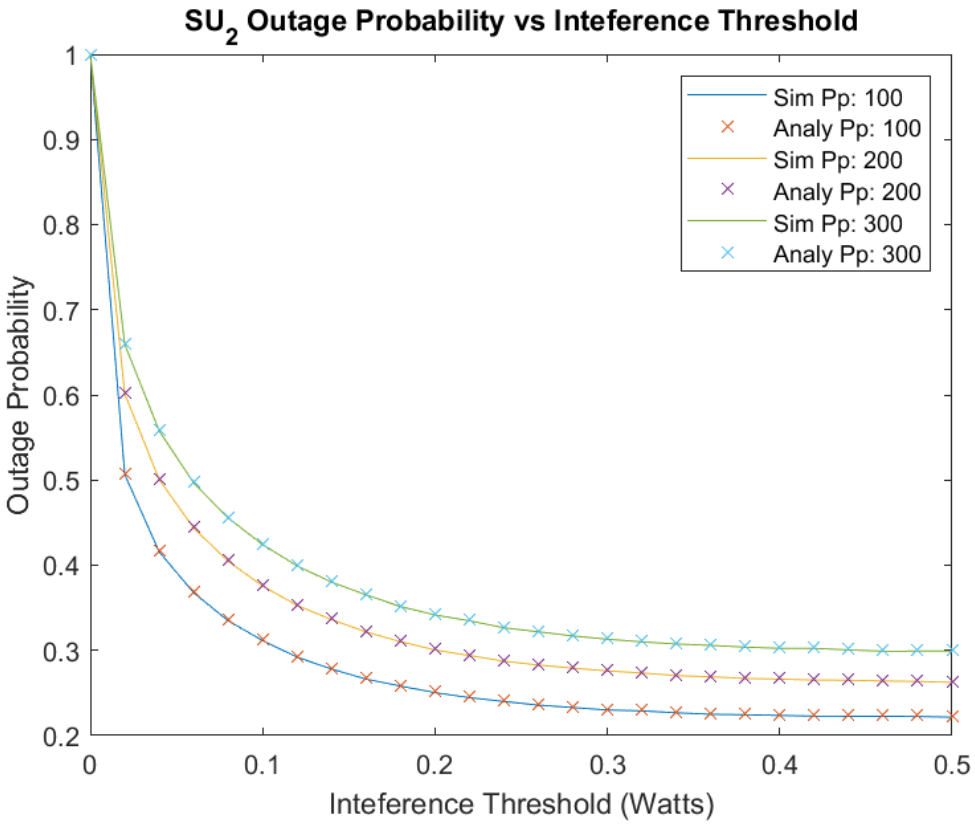


Figure 4.6: Outage Probability vs Interference Threshold for Different Values of Primary Transmit Power P_p (Watts)

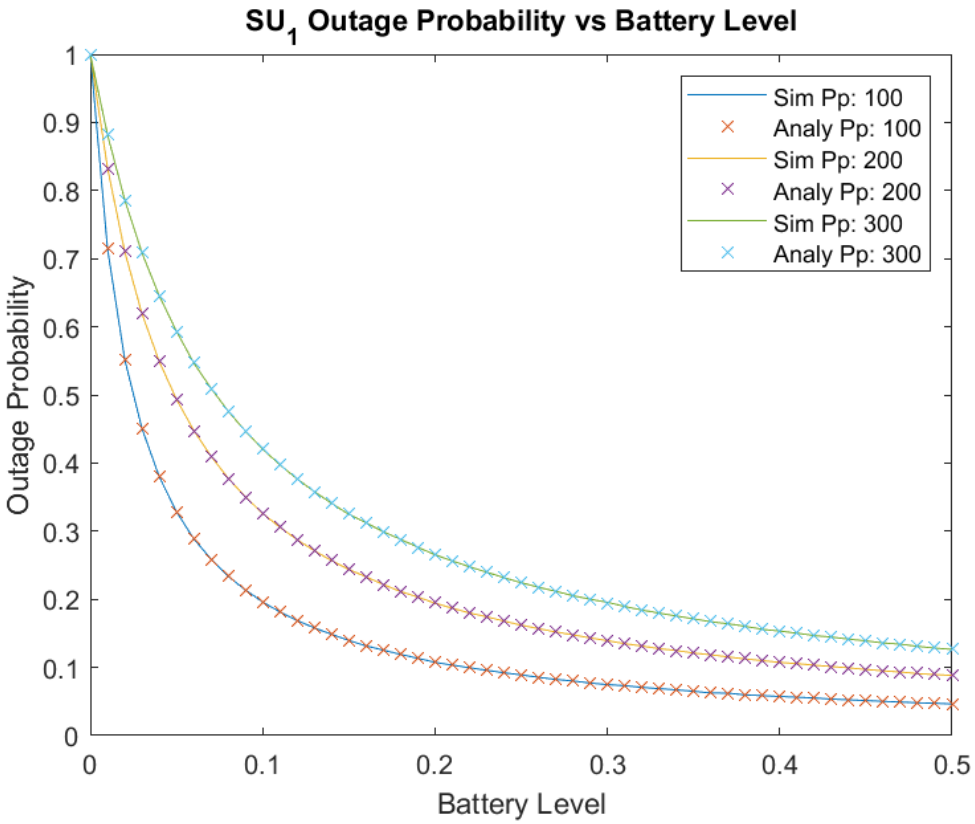


Figure 4.7: Outage Probability vs Battery Level for Different Values of Primary Transmit Power P_p (Watts)

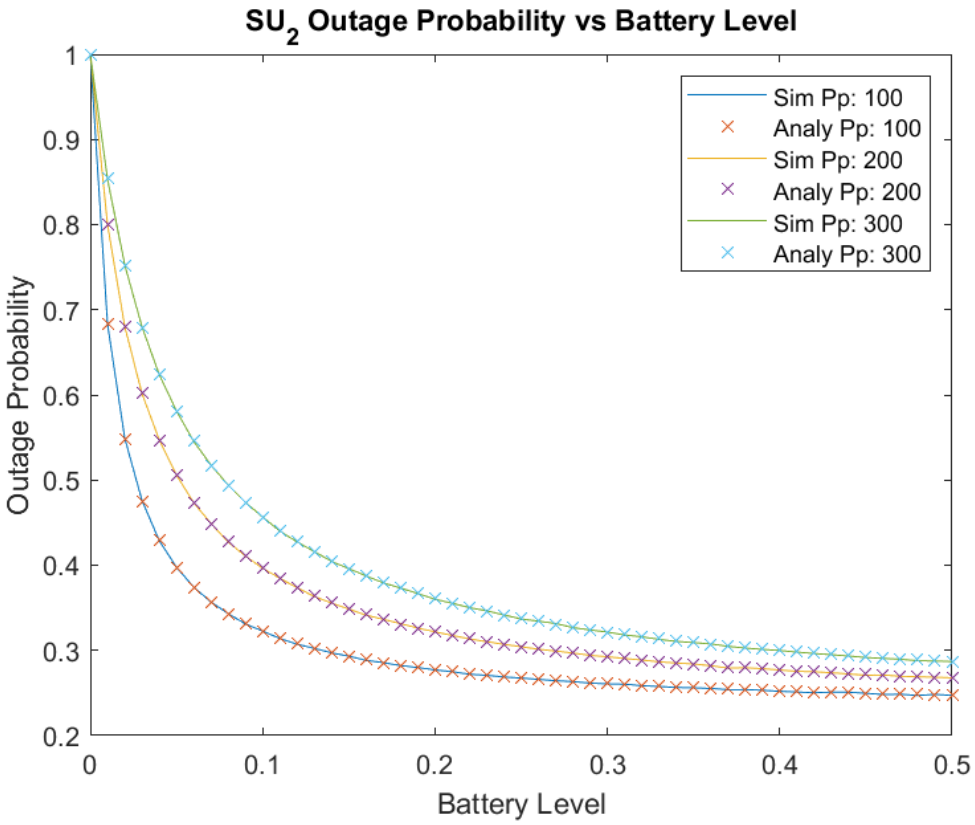


Figure 4.8: Outage Probability vs Battery Level for Different Values of Primary Transmit Power P_p (Watts)

4.5 Summary

This Chapter builds upon the results presented in Chapter 3 to accurately derive close-form expressions for outage probability of each SU in the proposed system model. To confirm that the derived analytical expressions for outage probability are correct, simulation results were presented and they have shown a match between the analytical and simulation results. This results confirmed that the derived outage probability expressions for each SU are valid. Also, the outage results observed when varying different parameters conform to the theoretically expected performance results.

Chapter 5

Mean Capacity Analysis

5.1 Introduction

In this Chapter, we obtain uplink closed-form expression for mean capacity of the SUs in the proposed system model. Mean capacity is determined under peak interference power constraint, I_{it}. This is similar to the assumption made in [73] but in our case instead of assuming maximum transmit power for the SUs, the SUs transmit power is constraint by the user's available battery energy and the interference threshold power as shown in Equation (3.4). It is assumed that the SUs always have data to transmit. Using Shannon capacity formula as expressed in Equation (3.6), mean capacity is calculated as follows, for each SU using the approach similar to the one used in [73]:

$$\begin{aligned} C_n =& W \times log_2\left(1+\delta_n\right), \\ =& W \int_0^{\infty} log_2\left(1+y\right) f_{\delta_n}(y)\, dy, \\ =& \frac{W}{log_e(2)} \int_0^{\infty} \frac{1-F_{\delta_n}(y)}{1+y}\, dy, \end{aligned} \tag{5.1}$$

where W is the bandwidth, $f_{\delta_n}(y)$ and $F_{\delta_n}(y)$ are the PDF and CDF of the random variable δ_n, respectively. δ_n represents the SU SINR as expressed in Equation (4.1). Note that we need to find the expression for CDF of SINR $F_{\delta_n}(y)$ to be able to derive a closed-form expression for mean capacity of each SU.

5.2 Mean Capacity SU_1

To evaluate mean capacity for SU_1, we need to derive the CDF of SINR $F_{\delta_1}(y)$ as observed in the capacity expression in Equation (5.1). To do this, we adopt the Markovian model build for SU_1 in Chapter 3 by finding $F_{\delta_1}(y)$ at SU_1 system state i as follows:

$$\begin{aligned} F_{\delta_1}(y)|_i =& Pr\left(\frac{P_1^s(i)H_1^s}{P^pG^s+\Omega^2+\sigma^2} < y\right), \\ =& 1 - Pr\left(\frac{P_1^s(i)H_1^s}{P^pG^s+\Omega^2+\sigma^2} > y\right), \\ =& 1 - Pr\left(P_1^s(i)H_1^s - yP^pG^s > y\left(\Omega^2+\sigma^2\right)\right). \end{aligned} \tag{5.2}$$

Un-conditioning on $P_1^s(i)$ the above expression for $F_{\delta_1}(y)$ reduces to the below:

$$\begin{aligned} F_{\delta_1}(y)|_i =& 1 - \left(Pr\left(\frac{i\Delta_p}{t_{ts}}H_1^s - yP^pG^s > y\left(\Omega^2+\sigma^2\right)\right) Pr\left(i < n_{I_1}\right) \right. \\ & \left. + \sum_{n_{I_1}=0}^{i} Pr\left(\frac{n_{I_1}\Delta_p}{t_{ts}}H_1^s - yP^pG^s > y\left(\Omega^2+\sigma^2\right)\right) f_{n_{I_1}}(n_{I_1})\right), \\ =& 1 - \left(Pr\left(H_1^s > \frac{y\left(\Omega^2+\sigma^2\right)+yP^pG^s}{\frac{i\Delta_p}{t_{ts}}}\right) Pr\left(i < n_{I_1}\right) \right. \\ & \left. + \sum_{n_{I_1}=0}^{i} Pr\left(H_1^s > \frac{y\left(\Omega^2+\sigma^2\right)+yP^pG^s}{\frac{n_{I_1}\Delta_p}{t_{ts}}}\right) f_{n_{I_1}}(n_{I_1})\right), \\ =& 1 - \left(\left(1 - F_{H_1^s}\left(\frac{y\left(\Omega^2+\sigma^2\right)+yP^pG^s}{\frac{i\Delta_p}{t_{ts}}}\right)\right) Pr\left(i < n_{I_1}\right) \right. \\ & \left. + \sum_{n_{I_1}=0}^{i} \left(1 - F_{H_1^s}\left(\frac{y\left(\Omega^2+\sigma^2\right)+yP^pG^s}{\frac{n_{I_1}\Delta_p}{t_{ts}}}\right)\right) f_{n_{I_1}}(n_{I_1})\right), \\ =& 1 - \left(Pr\left(i < n_{I_1}\right) \times \int_0^\infty \left(1 - \left(1 - e^{-\lambda_{H_1^s}\left(\frac{y\left(\Omega^2+\sigma^2\right)+yP^px}{\frac{i\Delta_p}{t_{ts}}}\right)}\right)\right) f_{G^s}(x)dx \right. \\ & \left. + \sum_{n_{I_1}=0}^{i} f_{n_{I_1}}(n_{I_1}) \times \int_0^\infty \left(1 - \left(1 - e^{-\lambda_{H_1^s}\left(\frac{y\left(\Omega^2+\sigma^2\right)+yP^px}{\frac{n_{I_1}\Delta_p}{t_{ts}}}\right)}\right)\right) f_{G^s}(x)dx\right). \end{aligned} \tag{5.3}$$

Plugging the expressions for $Pr\left(i < n_{I_1}\right)$, $f_{G^s}(x)$ and $f_{n_{I_1}}(n_{I_1})$ in Equation (5.3), then solving the integrals, we get the below result for $F_{\delta_1}(y)|_i$:

$$\begin{aligned}
F_{\delta_1}(y)|_i =& 1 - \Bigg(Pr\left(i < n_{I_1}\right) \int_0^{\infty} e^{-\lambda_{H_1^s}\left(\frac{y\left(\Omega^2+\sigma^2\right)+yP^p x}{\frac{n_{I_1}\Delta_p}{t_{ts}}}\right)} \lambda_{G^s} e^{-(\lambda_{G^s} x)} dx \\
&+ \sum_{n_{I_1}=0}^{i} f_{n_{I_1}}(n_{I_1}) \int_0^{\infty} e^{-\lambda_{H_1^s}\left(\frac{y\left(\Omega^2+\sigma^2\right)+yP^p x}{\frac{n_{I_1}\Delta_p}{t_{ts}}}\right)} \lambda_{G^s} e^{-(\lambda_{G^s} x)} dx \Bigg), \\
=& 1 - \Bigg[\left(1 - e^{-\left(\frac{\lambda_{H_1^s} I_{it} t_{ts}}{i\Delta_p}\right)}\right) \frac{\frac{i\Delta_p}{t_{ts}} \lambda_{G^s} e^{-\left(\frac{y\lambda_{H_1^s}(\Omega^2+\sigma^2)}{\frac{i\Delta_p}{t_{ts}}}\right)}}{yP^p \lambda_{H_1^s} + \frac{i\Delta_p}{t_{ts}} \lambda_{G^s}} \\
&+ \sum_{n_{I_1}=0}^{i} \left(e^{-\left(\frac{\lambda_{H_1^s} I_{it} t_{ts}}{(n_{I_1}+1)\Delta_p}\right)} - e^{-\left(\frac{\lambda_{H_1^s} I_{it} t_{ts}}{n_{I_1}\Delta_p}\right)} \right) \times \frac{\frac{n_{I_1}\Delta_p}{t_{ts}} \lambda_{G^s} e^{-\left(\frac{y\lambda_{H_1^s}(\Omega^2+\sigma^2)}{\frac{n_{I_1}\Delta_p}{t_{ts}}}\right)}}{yP^p \lambda_{H_1^s} + \frac{n_{I_1}\Delta_p}{t_{ts}} \lambda_{G^s}} \Bigg].
\end{aligned} \tag{5.4}$$

Substituting $F_{\delta_1}(y)$ in Equation (5.1), mean capacity for SU_1 is expressed as follows:

$$\begin{aligned}
C_1|_i =& \frac{W}{log_e(2)} \int_0^{\infty} \frac{1 - F_{\delta_1}(y)}{1+y} \, dy, \\
=& \frac{W}{log_e(2)} \Bigg(\left(1 - e^{-\left(\frac{\lambda_{H_1^s} I_{it} t_{ts}}{i\Delta_p}\right)}\right) \frac{i\Delta_p}{t_{ts}} \lambda_{G^s} \\
&\times \int_0^{\infty} \frac{e^{-\left(\frac{y\lambda_{H_1^s}(\Omega^2+\sigma^2)}{\frac{i\Delta_p}{t_{ts}}}\right)}}{(1+y)\left(yP^p \lambda_{H_1^s} + \frac{i\Delta_p}{t_{ts}} \lambda_{G^s}\right)} dy \\
&+ \left(e^{-\left(\frac{\lambda_{H_1^s} I_{it} t_{ts}}{(n_{I_1}+1)\Delta_p}\right)} - e^{-\left(\frac{\lambda_{H_1^s} I_{it} t_{ts}}{n_{I_1}\Delta_p}\right)} \right) \frac{n_{I_1}\Delta_p}{t_{ts}} \lambda_{G^s} \\
&\times \int_0^{\infty} \frac{e^{-\left(\frac{y\lambda_{H_1^s}(\Omega^2+\sigma^2)}{\frac{n_{I_1}\Delta_p}{t_{ts}}}\right)}}{(1+y)\left(yP^p \lambda_{H_1^s} + \frac{n_{I_1}\Delta_p}{t_{ts}} \lambda_{G^s}\right)} dy \Bigg).
\end{aligned} \tag{5.5}$$

Solving the integrals in Equation (5.5) above, the below closed-form expression for SU_1 mean capacity at state i is derived:

$$
\begin{aligned}
C_1|_i =& \frac{W\lambda_{G^s}}{P^p\lambda_{H_1^s} log_e(2)} \Bigg(\left(1 - e^{\left(\frac{\lambda_{H_1^s} I_{it} t_{ts}}{i\Delta_p}\right)}\right) \frac{i\Delta_p}{t_{ts}} \\
& \times \left[\frac{-e^{-\left(\frac{\lambda_{H_1^s}(\Omega^2+\sigma^2)}{\frac{i\Delta_p}{t_{ts}}}\right)} E_i\left(-\frac{\lambda_{H_1^s}(\Omega^2+\sigma^2)}{\frac{i\Delta_p}{t_{ts}}}\right)}{\frac{\frac{i\Delta_p}{t_{ts}}\lambda_{G^s}}{P^p\lambda_{H_1^s}} - 1} + \frac{-e^{\left(\frac{\lambda_{G^s}(\Omega^2+\sigma^2)}{P^p}\right)} E_i\left(-\frac{\lambda_{G^s}(\Omega^2+\sigma^2)}{P^p}\right)}{1 - \frac{\frac{i\Delta_p}{t_{ts}}\lambda_{G^s}}{P^p\lambda_{H_1^s}}} \right] \\
& + \sum_{n_{I_1}=0}^{i} \left(e^{-\left(\frac{\lambda_{H_1^s} I_{it} t_{ts}}{(n_{I_1}+1)\Delta_p}\right)} - e^{-\left(\frac{\lambda_{H_1^s} I_{it} t_{ts}}{n_{I_1}\Delta_p}\right)} \right) \frac{n_{I_1}\Delta_p}{t_{ts}} \\
& \times \left[\frac{-e^{-\left(\frac{\lambda_{H_1^s}(\Omega^2+\sigma^2)}{\frac{n_{I_1}\Delta_p}{t_{ts}}}\right)} E_i\left(-\frac{\lambda_{H_1^s}(\Omega^2+\sigma^2)}{\frac{n_{I_1}\Delta_p}{t_{ts}}}\right)}{\frac{\frac{n_{I_1}\Delta_p}{t_{ts}}\lambda_{G^s}}{P^p\lambda_{H_1^s}} - 1} + \frac{-e^{\left(\frac{\lambda_{G^s}(\Omega^2+\sigma^2)}{P^p}\right)} E_i\left(-\frac{\lambda_{G^s}(\Omega^2+\sigma^2)}{P^p}\right)}{1 - \frac{\frac{n_{I_1}\Delta_p}{t_{ts}}\lambda_{G^s}}{P^p\lambda_{H_1^s}}} \right] \Bigg).
\end{aligned}
\tag{5.6}
$$

Therefore, the overall SU_1 mean capacity is expressed as follows using Markovian analysis:

Case 1: SU_1 harvesting energy from SBS

$$
C_1 = \sum_{i=0}^{\frac{B_{max}}{\Delta_p}} C_1|_i \times \Pi(j). \tag{5.7}
$$

Case 2: SU_1 harvesting energy from SBS and MBS

$$
C_1 = \sum_{i=0}^{\frac{B_{max}}{\Delta_p}} C_1|_i \times \bar{\Pi}(j). \tag{5.8}
$$

5.3 Mean Capacity SU_2

Similar to SU_1, we need to derive the expression for CDF of SINR $F_{\delta_2}(y)$ for SU_2 to be able to evaluate this user's mean capacity. Adopting Markovian analysis presented in Chapter 3 we first derive CDF of SINR where SU_1 is at state i and SU_2 is at state j, $F_{\delta_2}(y)|_{i,j}$:

$$
\begin{aligned}
F_{\delta_2}(y)|_{i,j} =& Pr\left(\frac{P_2^s(j)H_2^s}{P_1^s(i)H_1^s + P^pG^s + \sigma^2} < y\right), \\
=& 1 - Pr\left(\frac{P_2^s(j)H_2^s}{P_1^s(i)H_1^s + P^pG^s + \sigma^2} > y\right), \\
=& 1 - Pr\left(P_2^s(j)H_2^s - (yP_1^s(i)H_1^s + yP^pG^s) > y\sigma^2\right).
\end{aligned} \tag{5.9}
$$

Since SUs transmit powers $P_2^s(j)$ and $P_1^s(i)$ are random variables as shown in Equation (3.4), we need to express $F_{\delta_2}(y)|_{i,j}$ un-conditioned on both $P_2^s(j)$ and $P_1^s(i)$, thus Equation (5.9) becomes:

$$
\begin{aligned}
F_{\delta_2}(y)|_{i,j} =& 1 - Pr\left(P_2^s(j)H_2^s - (yP_1^s(i)H_1^s + yP^pG^s) > y\sigma^2\right), \\
&= 1 - \Bigg(Pr\left(\frac{j\Delta_p}{t_{ts}}H_2^s - \left(y\frac{i\Delta_p}{t_{ts}}H_1^s + yP^pG^s\right) > y\sigma^2\right) \\
&\times Pr\left(i < n_{I_1}\right) Pr\left(j < n_{I_2}\right) \\
&+ \sum_{n_{I_1}=0}^{i} Pr\left(\frac{j\Delta_p}{t_{ts}}H_2^s - \left(y\frac{n_{I1}\Delta_p}{t_{ts}}H_1^s + yP^pG^s\right) > y\sigma^2\right) \\
&\times f_{n_{I_1}}(n_{I1}) Pr\left(j < n_{I_2}\right) \\
&+ \sum_{n_{I_2}=0}^{j} Pr\left(\frac{n_{I_2}\Delta_p}{t_{ts}}H_2^s - \left(y\frac{i\Delta_p}{t_{ts}}H_1^s + yP^pG^s\right) > y\sigma^2\right) \\
&\times f_{n_{I_2}}(n_{I2}) Pr\left(i < n_{I_1}\right) \\
&+ \sum_{n_{I_1}=0}^{i}\sum_{n_{I_1}=0}^{j} Pr\left(\frac{n_{I_2}\Delta_p}{t_{ts}}H_2^s - \left(y\frac{n_{I1}\Delta_p}{t_{ts}}H_1^s + yP^pG^s\right) > y\sigma^2\right) \\
&\times f_{n_{I_1}}(n_{I1}) f_{n_{I_2}}(n_{I2})\Bigg).
\end{aligned} \tag{5.10}
$$

Letting $A = y\frac{i\Delta_p}{t_{ts}}H_1^s + yP^pG^s$ and $B = y\frac{n_{I1}\Delta_p}{t_{ts}}H_1^s + yP^pG^s$, the expressions for PDF of A and B are derived as follows:

$$
\begin{aligned}
f_A(x) &= \int_0^x f_{H_1^s}(r) f_{G^s}(x-r) dr, \\
&= \int_0^x \left(\frac{\lambda_{H_1^s}}{y\frac{i\Delta_p}{t_{ts}}} \right) e^{-\left(\frac{\lambda_{H_1^s} r}{y\frac{i\Delta_p}{t_{ts}}} \right)} \times \left(\frac{\lambda_{G^s}}{yP^p} \right) e^{-\left(\frac{\lambda_{G^s}(x-r)}{yP^p} \right)} dr, \\
&= \frac{\lambda_{H_1^s} \lambda_{G^s}}{y\left(P^p \lambda_{H_1^s} - \frac{i\Delta_p}{t_{ts}} \lambda_{G^s} \right)} \left(e^{-\left(\frac{x\lambda_{G^s}}{yP^p} \right)} - e^{-\left(\frac{x\lambda_{H_1^s}}{y\frac{i\Delta_p}{t_{ts}}} \right)} \right),
\end{aligned}
\tag{5.11}
$$

and the PDF for B is as follows:

$$
\begin{aligned}
f_B(z) &= \int_0^z f_{H_1^s}(r) f_{G^s}(z-r) dr, \\
&= \int_0^z \left(\frac{\lambda_{H_1^s}}{y\frac{n_{I_1}\Delta_p}{t_{ts}}} \right) e^{-\left(\frac{\lambda_{H_1^s} r}{y\frac{n_{I_1}\Delta_p}{t_{ts}}} \right)} \times \left(\frac{\lambda_{G^s}}{yP^p} \right) e^{-\left(\frac{\lambda_{G^s}(z-r)}{yP^p} \right)} dr, \\
&= \frac{\lambda_{H_1^s} \lambda_{G^s}}{y\left(P^p \lambda_{H_1^s} - \frac{n_{I_1}\Delta_p}{t_{ts}} \lambda_{G^s} \right)} \left(e^{-\left(\frac{z\lambda_{G^s}}{yP^p} \right)} - e^{-\left(\frac{z\lambda_{H_1^s}}{y\frac{n_{I_1}\Delta_p}{t_{ts}}} \right)} \right).
\end{aligned}
\tag{5.12}
$$

Further reducing Equation (5.10), $F_{\delta_2}(y)|_{i,j}$ is expressed as follows:

$$
\begin{aligned}
F_{\delta_2}(y)|_{i,j} =& 1 - Pr\left(P_2^s(j)H_2^s - (yP_1^s(i)H_1^s + yP^pG^s) > y\sigma^2\right), \\
&= 1 - \Bigg(Pr\left(\frac{j\Delta_p}{t_{ts}}H_2^s - A > y\sigma^2\right) Pr\left(i < n_{I_1}\right) Pr\left(j < n_{I_2}\right) \\
&+ \sum_{n_{I_1}=0}^{i} Pr\left(\frac{j\Delta_p}{t_{ts}}H_2^s - B > y\sigma^2\right) f_{n_{I_1}}(n_{I1}) Pr\left(j < n_{I_2}\right) \\
&+ \sum_{n_{I_2}=0}^{j} Pr\left(\frac{n_{I_2}\Delta_p}{t_{ts}}H_2^s - A > y\sigma^2\right) f_{n_{I_2}}(n_{I2}) Pr\left(i < n_{I_1}\right) \\
&+ \sum_{n_{I_1}=0}^{i}\sum_{n_{I_1}=0}^{j} Pr\left(\frac{n_{I_2}\Delta_p}{t_{ts}}H_2^s - B > y\sigma^2\right) f_{n_{I_1}}(n_{I1}) f_{n_{I_2}}(n_{I2})\Bigg), \\
=& 1 - \Bigg(Pr\left(H_2^s > \frac{y\sigma^2 + A}{\frac{j\Delta_p}{t_{ts}}}\right) Pr\left(i < n_{I_1}\right) Pr\left(j < n_{I_2}\right) \\
&+ \sum_{n_{I_1}=0}^{i} Pr\left(H_2^s > \frac{y\sigma^2 + B}{\frac{j\Delta_p}{t_{ts}}}\right) f_{n_{I_1}}(n_{I1}) Pr\left(j < n_{I_2}\right) \\
&+ \sum_{n_{I_2}=0}^{j} Pr\left(H_2^s > \frac{y\sigma^2 + A}{\frac{n_{I_2}\Delta_p}{t_{ts}}}\right) f_{n_{I_2}}(n_{I2}) Pr\left(i < n_{I_1}\right) \\
&+ \sum_{n_{I_1}=0}^{i}\sum_{n_{I_1}=0}^{j} Pr\left(H_2^s > \frac{y\sigma^2 + B}{\frac{n_{I_2}\Delta_p}{t_{ts}}}\right) f_{n_{I_1}}(n_{I1}) f_{n_{I_2}}(n_{I2})\Bigg).
\end{aligned}
\tag{5.13}
$$

Equation (5.13) above is further reduced to the below expression:

$$
\begin{aligned}
F_{\delta_2}(y)|_{i,j} =& 1 - \Bigg(Pr\left(i < n_{I_1}\right) Pr\left(j < n_{I_2}\right) \times \int_0^\infty \left(1 - F_{H_2^s}\left(\frac{y\sigma^2 + x}{\frac{j\Delta_p}{t_{ts}}}\right)\right) f_A(x)dx \\
&+ \sum_{n_{I_1}=0}^{i} f_{n_{I_1}}(n_{I1}) Pr\left(j < n_{I_2}\right) \times \int_0^\infty \left(1 - F_{H_2^s}\left(\frac{y\sigma^2 + z}{\frac{j\Delta_p}{t_{ts}}}\right)\right) f_B(z)dz \\
&+ \sum_{n_{I_2}=0}^{j} f_{n_{I_2}}(n_{I2}) Pr\left(i < n_{I_1}\right) \times \int_0^\infty \left(1 - F_{H_2^s}\left(\frac{y\sigma^2 + x}{\frac{n_{I_2}\Delta_p}{t_{ts}}}\right)\right) f_A(x)dx \\
&+ \sum_{n_{I_1}=0}^{i} \sum_{n_{I_1}=0}^{j} f_{n_{I_1}}(n_{I1}) f_{n_{I_2}}(n_{I2}) \times \int_0^\infty \left(1 - F_{H_2^s}\left(\frac{y\sigma^2 + z}{\frac{n_{I_2}\Delta_p}{t_{ts}}}\right)\right) f_B(z)dz \Bigg).
\end{aligned}
\tag{5.14}
$$

Re-arranging Equation (5.14) above we get the below expression for $F_{\delta_2}(y)|_{i,j}$:

$$
\begin{aligned}
F_{\delta_2}(y)|_{i,j} =& 1 - \Bigg(Pr\left(i < n_{I_1}\right) Pr\left(j < n_{I_2}\right) \times \int_0^\infty \left(1 - \left(1 - e^{-\lambda_{H_2^s}\left(\frac{y\sigma^2 + x}{\frac{j\Delta_p}{t_{ts}}}\right)}\right)\right) \\
&\times f_A(x)dx \\
&+ \sum_{n_{I_1}=0}^{i} f_{n_{I_1}}(n_{I1}) Pr\left(j < n_{I_2}\right) \times \int_0^\infty \left(1 - \left(1 - e^{-\lambda_{H_2^s}\left(\frac{y\sigma^2 + z}{\frac{n_{I1}\Delta_p}{t_{ts}}}\right)}\right)\right) \\
&\times f_B(z)dz \\
&+ \sum_{n_{I_2}=0}^{j} f_{n_{I_2}}(n_{I2}) Pr\left(i < n_{I_1}\right) \times \int_0^\infty \left(1 - \left(1 - e^{-\lambda_{H_2^s}\left(\frac{y\sigma^2 + x}{\frac{n_{I_2}\Delta_p}{t_{ts}}}\right)}\right)\right) \\
&\times f_A(x)dx \\
&+ \sum_{n_{I_1}=0}^{i} \sum_{n_{I_1}=0}^{j} f_{n_{I_1}}(n_{I1}) f_{n_{I_2}}(n_{I2}) \times \int_0^\infty \left(1 - \left(1 - e^{-\lambda_{H_2^s}\left(\frac{y\sigma^2 + z}{\frac{n_{I_2}\Delta_p}{t_{ts}}}\right)}\right)\right) \\
&\times f_B(z)dz \Bigg).
\end{aligned}
\tag{5.15}
$$

Plugging expressions for $f_A(x)$ and $F_B(z)$ in Equation (5.15) above, we get the below expression for $F_{\delta_2}(y)|_{i,j}$:

$$
\begin{aligned}
F_{\delta_2}(y)|_{i,j} =& 1 - \Bigg(Pr\left(i < n_{I_1}\right) Pr\left(j < n_{I_2}\right) \\
& \times \int_0^\infty e^{-\lambda_{H_2^s}\left(\frac{y\sigma^2+x}{\frac{j\Delta_p}{t_{ts}}}\right)} \Big(\frac{\lambda_{H_1^s}\lambda_{G^s}\left(e^{-\left(\frac{x\lambda_{G^s}}{yP^p}\right)} - e^{-\left(\frac{x\lambda_{H_1^s}}{y\frac{i\Delta_p}{t_{ts}}}\right)}\right)}{y\left(P^p\lambda_{H_1^s} - \frac{i\Delta_p}{t_{ts}}\lambda_{G^s}\right)} \Big) dx \\
& + \sum_{n_{I_1}=0}^{i} f_{n_{I_1}}(n_{I1}) Pr\left(j < n_{I_2}\right) \\
& \times \int_0^\infty e^{-\lambda_{H_2^s}\left(\frac{y\sigma^2+z}{\frac{n_{I_1}\Delta_p}{t_{ts}}}\right)} \Big(\frac{\lambda_{H_1^s}\lambda_{G^s}\left(e^{-\left(\frac{z\lambda_{G^s}}{yP^p}\right)} - e^{-\left(\frac{z\lambda_{H_1^s}}{y\frac{n_{I_1}\Delta_p}{t_{ts}}}\right)}\right)}{y\left(P^p\lambda_{H_1^s} - \frac{n_{I_1}\Delta_p}{t_{ts}}\lambda_{G^s}\right)} \Big) dz \\
& + \sum_{n_{I_2}=0}^{j} f_{n_{I_2}}(n_{I2}) Pr\left(i < n_{I_1}\right) \\
& \times \int_0^\infty e^{-\lambda_{H_2^s}\left(\frac{y\sigma^2+x}{\frac{n_{I_2}\Delta_p}{t_{ts}}}\right)} \Big(\frac{\lambda_{H_1^s}\lambda_{G^s}\left(e^{-\left(\frac{x\lambda_{G^s}}{yP^p}\right)} - e^{-\left(\frac{x\lambda_{H_1^s}}{y\frac{n_{I2}\Delta_p}{t_{ts}}}\right)}\right)}{y\left(P^p\lambda_{H_1^s} - \frac{n_{I2}\Delta_p}{t_{ts}}\lambda_{G^s}\right)} \Big) dx \\
& + \sum_{n_{I_1}=0}^{i} \sum_{n_{I_1}=0}^{j} f_{n_{I_1}}(n_{I1}) f_{n_{I_2}}(n_{I2}) \\
& \times \int_0^\infty e^{-\lambda_{H_2^s}\left(\frac{y\sigma^2+z}{\frac{n_{I_2}\Delta_p}{t_{ts}}}\right)} \Big(\frac{\lambda_{H_1^s}\lambda_{G^s}\left(e^{-\left(\frac{z\lambda_{G^s}}{yP^p}\right)} - e^{-\left(\frac{z\lambda_{H_1^s}}{y\frac{n_{I_1}\Delta_p}{t_{ts}}}\right)}\right)}{y\left(P^p\lambda_{H_1^s} - \frac{n_{I_1}\Delta_p}{t_{ts}}\lambda_{G^s}\right)} \Big) dz \Bigg).
\end{aligned}
\tag{5.16}
$$

Solving the integrals in Equation (5.16), we get the below expression for $F_{\delta_2}(y)|_{i,j}$:

$$
\begin{aligned}
F_{\delta_2}(y)|_{i,j} =& 1 - \Bigg[\frac{\left(1 - e^{-\left(\frac{\lambda_{H_2^p} I_{it} t_{ts}}{j\Delta_p}\right)}\right)\left(1 - e^{-\left(\frac{\lambda_{H_1^p} I_{it} t_{ts}}{i\Delta_p}\right)}\right)}{\left(P^p \lambda_{H_1^s} - \frac{i\Delta_p}{t_{ts}} \lambda_{G^s}\right)} \\
&\times \lambda_{H_1^s} \lambda_{G^s} e^{-\left(\frac{\lambda_{H_2^s} y \sigma^2 t_{ts}}{j\Delta_p}\right)} \left(\frac{P^p \frac{j\Delta_p}{t_{ts}}}{y P^p \lambda_{H_2^s} + \frac{j\Delta_p}{t_{ts}} \lambda_{G^s}} - \frac{\frac{i\Delta_p}{t_{ts}} \frac{j\Delta_p}{t_{ts}}}{y \frac{i\Delta_p}{t_{ts}} \lambda_{H_2^s} + \frac{j\Delta_p}{t_{ts}} \lambda_{H_1^s}} \right) \\
&+ \sum_{n_{I_1}=0}^{i} \frac{\left(1 - e^{-\left(\frac{\lambda_{H_2^p} I_{it} t_{ts}}{j\Delta_p}\right)}\right)\left(e^{-\left(\frac{\lambda_{H_1^p} I_{it} t_{ts}}{(n_{I_1}+1)\Delta_p}\right)} - e^{-\left(\frac{\lambda_{H_1^p} I_{it} t_{ts}}{n_{I_1}\Delta_p}\right)}\right)}{\left(P^p \lambda_{H_1^s} - \frac{n_{I_1}\Delta_p}{t_{ts}} \lambda_{G^s}\right)} \\
&\times \lambda_{H_1^s} \lambda_{G^s} e^{-\left(\frac{\lambda_{H_2^s} y \sigma^2 t_{ts}}{j\Delta_p}\right)} \left(\frac{P^p \frac{j\Delta_p}{t_{ts}}}{y P^p \lambda_{H_2^s} + \frac{j\Delta_p}{t_{ts}} \lambda_{G^s}} - \frac{\frac{n_{I_1}\Delta_p}{t_{ts}} \frac{j\Delta_p}{t_{ts}}}{y \frac{n_{I_1}\Delta_p}{t_{ts}} \lambda_{H_2^s} + \frac{j\Delta_p}{t_{ts}} \lambda_{H_1^s}} \right) \\
&+ \sum_{n_{I_2}=0}^{j} \frac{\left(e^{-\left(\frac{\lambda_{H_2^p} I_{it} t_{ts}}{(n_{I_2}+1)\Delta_p}\right)} - e^{-\left(\frac{\lambda_{H_2^p} I_{it} t_{ts}}{n_{I_2}\Delta_p}\right)}\right)\left(1 - e^{-\left(\frac{\lambda_{H_1^p} I_{it} t_{ts}}{i\Delta_p}\right)}\right)}{\left(P^p \lambda_{H_1^s} - \frac{i\Delta_p}{t_{ts}} \lambda_{G^s}\right)} \\
&\times \lambda_{H_1^s} \lambda_{G^s} e^{-\left(\frac{\lambda_{H_2^s} y \sigma^2 t_{ts}}{n_{I_2}\Delta_p}\right)} \left(\frac{P^p \frac{n_{I_2}\Delta_p}{t_{ts}}}{y P^p \lambda_{H_2^s} + \frac{n_{I_2}\Delta_p}{t_{ts}} \lambda_{G^s}} - \frac{\frac{i\Delta_p}{t_{ts}} \frac{n_{I_2}\Delta_p}{t_{ts}}}{y \frac{i\Delta_p}{t_{ts}} \lambda_{H_2^s} + \frac{n_{I_2}\Delta_p}{t_{ts}} \lambda_{H_1^s}} \right) \\
&+ \sum_{n_{I_1}=0}^{i} \sum_{n_{I_2}=0}^{j} \frac{\left(e^{-\left(\frac{\lambda_{H_2^p} I_{it} t_{ts}}{(n_{I_2}+1)\Delta_p}\right)} - e^{-\left(\frac{\lambda_{H_2^p} I_{it} t_{ts}}{n_{I_2}\Delta_p}\right)}\right)}{\left(P^p \lambda_{H_1^s} - \frac{n_{I_1}\Delta_p}{t_{ts}} \lambda_{G^s}\right)} \\
&\times \left(e^{-\left(\frac{\lambda_{H_1^p} I_{it} t_{ts}}{(n_{I_1}+1)\Delta_p}\right)} - e^{-\left(\frac{\lambda_{H_1^p} I_{it} t_{ts}}{n_{I_1}\Delta_p}\right)}\right) \lambda_{H_1^s} \lambda_{G^s} e^{-\left(\frac{\lambda_{H_2^s} y \sigma^2 t_{ts}}{n_{I_2}\Delta_p}\right)} \\
&\times \left(\frac{P^p \frac{n_{I_2}\Delta_p}{t_{ts}}}{y P^p \lambda_{H_2^s} + \frac{n_{I_2}\Delta_p}{t_{ts}} \lambda_{G^s}} - \frac{\frac{n_{I_1}\Delta_p}{t_{ts}} \frac{n_{I_2}\Delta_p}{t_{ts}}}{y \frac{n_{I_1}\Delta_p}{t_{ts}} \lambda_{H_2^s} + \frac{n_{I_2}\Delta_p}{t_{ts}} \lambda_{H_1^s}} \right) \Bigg].
\end{aligned}
\tag{5.17}
$$

Plugging $F_{\delta_2}(y)|_{i,j}$ back in Equation (5.1), mean capacity for SU_2 is as follows:

$$\begin{aligned} C_2|_{i,j} =& \frac{W}{log_e(2)} \int_0^\infty \frac{1 - F_{\delta_2}(y)|_{i,j}}{1+y}\, dy, \\ =& \bar{A} + \bar{B} + \bar{C} + \bar{D}. \end{aligned} \tag{5.18}$$

The components ($\bar{A}$, $\bar{B}$, $\bar{C}$, and $\bar{D}$) of Equation (5.18) actual expressions are represented in the below different cases, where each component integrals are solved using partial fraction decomposition approach.

Case 1: for $\bar{A}$

$$\begin{aligned} \bar{A} =& \frac{W\left(1 - e^{-\left(\frac{\lambda_{H_2^p} I_{it} t_{ts}}{j\Delta_p}\right)}\right)\left(1 - e^{-\left(\frac{\lambda_{H_1^p} I_{it} t_{ts}}{i\Delta_p}\right)}\right)\lambda_{H_1^s}\lambda_{G^s}}{log_e(2)\left(P^p\lambda_{H_1^s} - \frac{i\Delta_p}{t_{ts}}\lambda_{G^s}\right)} \\ & \times \left(\int_0^\infty \frac{P^p \frac{j\Delta_p}{t_{ts}} e^{-\left(\frac{\lambda_{H_2^s} y\sigma^2 t_{ts}}{j\Delta_p}\right)}}{(1+y)\left(yP^p\lambda_{H_2^s} + \frac{j\Delta_p}{t_{ts}}\lambda_{G^s}\right)} dy \right. \\ & \left. - \int_0^\infty \frac{\frac{i\Delta_p}{t_{ts}}\frac{j\Delta_p}{t_{ts}} e^{-\left(\frac{\lambda_{H_2^s} y\sigma^2 t_{ts}}{j\Delta_p}\right)}}{(1+y)\left(y\frac{i\Delta_p}{t_{ts}}\lambda_{H_2^s} + \frac{j\Delta_p}{t_{ts}}\lambda_{H_1^s}\right)} dy \right), \\ =& \frac{W\frac{j\Delta_p}{t_{ts}}\left(1 - e^{-\left(\frac{\lambda_{H_2^p} I_{it} t_{ts}}{j\Delta_p}\right)}\right)\left(1 - e^{-\left(\frac{\lambda_{H_1^p} I_{it} t_{ts}}{i\Delta_p}\right)}\right)\lambda_{H_1^s}\lambda_{G^s}}{\lambda_{H_2^s} log_e(2)\left(P^p\lambda_{H_1^s} - \frac{i\Delta_p}{t_{ts}}\lambda_{G^s}\right)} \\ & \times \left(- e^{\left(\frac{\lambda_{H_2^s}\sigma^2 t_{ts}}{j\Delta_p}\right)} E_i\left(-\frac{\lambda_{H_2^s}\sigma^2 t_{ts}}{j\Delta_p}\right) \right. \\ & \times \left[\frac{1}{\frac{j\Delta_p\lambda_{G^s}}{P^p\lambda_{H_2^s} t_{ts}} - 1} - \frac{1}{\frac{j\Delta_p\lambda_{H_1^s}}{i\Delta_p\lambda_{H_2}} - 1} \right] \\ & + \frac{-e^{\left(\frac{\lambda_{G^s}\sigma^2}{P^p}\right)} E_i\left(-\frac{\lambda_{G^s}\sigma^2}{P^p}\right)}{1 - \frac{j\Delta_p\lambda_{G^s}}{P^p\lambda_{H_2^s} t_{ts}}} - \frac{-e^{\left(\frac{\lambda_{H_1^s}\sigma^2 t_{ts}}{i\Delta_p}\right)} E_i\left(-\frac{\lambda_{H_1^s}\sigma^2 t_{ts}}{i\Delta_p}\right)}{1 - \frac{j\Delta_p\lambda_{H_1^s}}{i\Delta_p\lambda_{H_2^s}}} \left. \right). \end{aligned} \tag{5.19}$$

Case 2: for $\bar{B}$

$$\bar{B} = \sum_{n_{I_1}=0}^{i} \frac{W\left(1 - e^{-\left(\frac{\lambda_{H_2^p} I_{it} t_{ts}}{j\Delta_p}\right)}\right)\left(e^{-\left(\frac{\lambda_{H_1^p} I_{it} t_{ts}}{(n_{I_1}+1)\Delta_p}\right)} - e^{-\left(\frac{\lambda_{H_1^p} I_{it} t_{ts}}{n_{I_1}\Delta_p}\right)}\right)}{log_e(2)\left(P^p\lambda_{H_1^s} - \frac{n_{I_1}\Delta_p}{t_{ts}}\lambda_{G^s}\right)}$$

$$\times \lambda_{H_1^s}\lambda_{G^s}\left(\int_0^\infty \frac{P^p\frac{j\Delta_p}{t_{ts}} e^{-\left(\frac{\lambda_{H_2^s} y\sigma^2 t_{ts}}{j\Delta_p}\right)}}{(1+y)\left(yP^p\lambda_{H_2^s} + \frac{j\Delta_p}{t_{ts}}\lambda_{G^s}\right)} dy\right.$$

$$\left. - \int_0^\infty \frac{\frac{n_{I_1}\Delta_p}{t_{ts}}\frac{j\Delta_p}{t_{ts}} e^{-\left(\frac{\lambda_{H_2^s} y\sigma^2 t_{ts}}{j\Delta_p}\right)}}{(1+y)\left(y\frac{n_{I_1}\Delta_p}{t_{ts}}\lambda_{H_2^s} + \frac{j\Delta_p}{t_{ts}}\lambda_{H_1^s}\right)} dy\right),$$

$$= \sum_{n_{I_1}=0}^{i} \frac{W\left(1 - e^{-\left(\frac{\lambda_{H_2^p} I_{it} t_{ts}}{j\Delta_p}\right)}\right)\left(e^{-\left(\frac{\lambda_{H_1^p} I_{it} t_{ts}}{(n_{I_1}+1)\Delta_p}\right)} - e^{-\left(\frac{\lambda_{H_1^p} I_{it} t_{ts}}{n_{I_1}\Delta_p}\right)}\right)}{\lambda_{H_2^s} log_e(2)\left(P^p\lambda_{H_1^s} - \frac{n_{I_1}\Delta_p}{t_{ts}}\lambda_{G^s}\right)} \tag{5.20}$$

$$\times \frac{j\Delta_p}{t_{ts}}\lambda_{H_1^s}\lambda_{G^s}\left(-e^{\left(\frac{\lambda_{H_2^s}\sigma^2 t_{ts}}{j\Delta_p}\right)} E_i\left(-\frac{\lambda_{H_2^s}\sigma^2 t_{ts}}{j\Delta_p}\right)\right.$$

$$\times \left[\frac{1}{\frac{j\Delta_p\lambda_{G^s}}{P^p\lambda_{H_2^s} t_{ts}} - 1} - \frac{1}{\frac{j\Delta_p\lambda_{H_1^s}}{n_{I_1}\Delta_p\lambda_{H_2^s}} - 1}\right]$$

$$\left. + \frac{-e^{\left(\frac{\lambda_{G^s}\sigma^2}{P^p}\right)} E_i\left(-\frac{\lambda_{G^s}\sigma^2}{P^p}\right)}{1 - \frac{j\Delta_p\lambda_{G^s}}{P^p\lambda_{H_2^s} t_{ts}}} - \frac{-e^{\left(\frac{\lambda_{H_1^s}\sigma^2 t_{ts}}{n_{I_1}\Delta_p}\right)} E_i\left(-\frac{\lambda_{H_1^s}\sigma^2 t_{ts}}{n_{I_1}\Delta_p}\right)}{1 - \frac{j\Delta_p\lambda_{H_1^s}}{n_{I_1}\Delta_p\lambda_{H_2^s}}}\right).$$

Case 3: for $\bar{C}$

$$\bar{C} = \sum_{n_{I_2}=0}^{j} \frac{W\left(e^{-\left(\frac{\lambda_{H_2^p} I_{it} t_{ts}}{(n_{I_2}+1)\Delta_p}\right)} - e^{-\left(\frac{\lambda_{H_2^p} I_{it} t_{ts}}{n_{I_2}\Delta_p}\right)}\right)\left(1 - e^{-\left(\frac{\lambda_{H_1^p} I_{it} t_{ts}}{i\Delta_p}\right)}\right)}{log_e(2)\left(P^p\lambda_{H_1^s} - \frac{i\Delta_p}{t_{ts}}\lambda_{G^s}\right)}$$
$$\times \lambda_{H_1^s}\lambda_{G^s}\left(\int_0^\infty \frac{P^p \frac{n_{I_2}\Delta_p}{t_{ts}} e^{-\left(\frac{\lambda_{H_2^s} y\sigma^2 t_{ts}}{n_{I_2}\Delta_p}\right)}}{(1+y)\left(yP^p\lambda_{H_2^s} + \frac{n_{I_2}\Delta_p}{t_{ts}}\lambda_{G^s}\right)} dy\right.$$
$$\left. - \int_0^\infty \frac{\frac{i\Delta_p}{t_{ts}}\frac{n_{I_2}\Delta_p}{t_{ts}} e^{-\left(\frac{\lambda_{H_2^s} y\sigma^2 t_{ts}}{n_{I_2}\Delta_p}\right)}}{(1+y)\left(y\frac{i\Delta_p}{t_{ts}}\lambda_{H_2^s} + \frac{n_{I_2}\Delta_p}{t_{ts}}\lambda_{H_1^s}\right)} dy\right),$$
$$= \sum_{n_{I_2}=0}^{j} \frac{W\left(e^{-\left(\frac{\lambda_{H_2^p} I_{it} t_{ts}}{(n_{I_2}+1)\Delta_p}\right)} - e^{-\left(\frac{\lambda_{H_2^p} I_{it} t_{ts}}{n_{I_2}\Delta_p}\right)}\right)\left(1 - e^{-\left(\frac{\lambda_{H_1^p} I_{it} t_{ts}}{i\Delta_p}\right)}\right)}{\lambda_{H_2^s} log_e(2)\left(P^p\lambda_{H_1^s} - \frac{i\Delta_p}{t_{ts}}\lambda_{G^s}\right)} \tag{5.21}$$
$$\times \frac{n_{I_2}\Delta_p}{t_{ts}}\lambda_{H_1^s}\lambda_{G^s}\left(-e^{\left(\frac{\lambda_{H_2^s}\sigma^2 t_{ts}}{n_{I_2}\Delta_p}\right)} E_i\left(-\frac{\lambda_{H_2^s}\sigma^2 t_{ts}}{n_{I_2}\Delta_p}\right)\right.$$
$$\times \left[\frac{1}{\frac{n_{I_2}\Delta_p\lambda_{G^s}}{P^p\lambda_{H_2^s} t_{ts}} - 1} - \frac{1}{\frac{n_{I_2}\Delta_p\lambda_{H_1^s}}{i\Delta_p\lambda_{H_2^s}} - 1}\right]$$
$$\left. + \frac{-e^{\left(\frac{\lambda_{G^s}\sigma^2}{P^p}\right)} E_i\left(-\frac{\lambda_{G^s}\sigma^2}{P^p}\right)}{1 - \frac{n_{I_2}\Delta_p\lambda_{G^s}}{P^p\lambda_{H_2^s} t_{ts}}} - \frac{-e^{\left(\frac{\lambda_{H_1^s}\sigma^2 t_{ts}}{i\Delta_p}\right)} E_i\left(-\frac{\lambda_{H_1^s}\sigma^2 t_{ts}}{i\Delta_p}\right)}{1 - \frac{n_{I_2}\Delta_p\lambda_{H_1^s}}{i\Delta_p\lambda_{H_2^s}}}\right).$$

Case 4: for $\bar{D}$

$$
\begin{aligned}
\bar{D} = \sum_{n_{I_1}=0}^{i} \sum_{n_{I_2}=0}^{j} & \frac{W\left(e^{-\left(\frac{\lambda_{H_2^p} I_{it} t_{ts}}{(n_{I_2}+1)\Delta_p}\right)} - e^{-\left(\frac{\lambda_{H_2^p} I_{it} t_{ts}}{n_{I_2}\Delta_p}\right)}\right)\lambda_{H_1^s}\lambda_{G^s}}{log_e(2)\left(P^p\lambda_{H_1^s} - \frac{n_{I_1}\Delta_p}{t_{ts}}\lambda_{G^s}\right)} \\
& \times \left(e^{-\left(\frac{\lambda_{H_1^p} I_{it} t_{ts}}{(n_{I_1}+1)\Delta_p}\right)} - e^{-\left(\frac{\lambda_{H_1^p} I_{it} t_{ts}}{n_{I_1}\Delta_p}\right)}\right) \\
& \times \left(\int_0^\infty \frac{P^p \frac{n_{I_2}\Delta_p}{t_{ts}} e^{-\left(\frac{\lambda_{H_2^s} y\sigma^2 t_{ts}}{n_{I_2}\Delta_p}\right)}}{(1+y)\left(yP^p\lambda_{H_2^s} + \frac{n_{I_2}\Delta_p}{t_{ts}}\lambda_{G^s}\right)} dy\right. \\
& \left. - \int_0^\infty \frac{\frac{n_{I_1}\Delta_p}{t_{ts}}\frac{n_{I_2}\Delta_p}{t_{ts}} e^{-\left(\frac{\lambda_{H_2^s} y\sigma^2 t_{ts}}{n_{I_2}\Delta_p}\right)}}{(1+y)\left(y\frac{n_{I_1}\Delta_p}{t_{ts}}\lambda_{H_2^s} + \frac{n_{I_2}\Delta_p}{t_{ts}}\lambda_{H_1^s}\right)} dy\right), \\
= \sum_{n_{I_1}=0}^{i} \sum_{n_{I_2}=0}^{j} & \frac{W\frac{n_{I_2}\Delta_p}{t_{ts}}\left(e^{-\left(\frac{\lambda_{H_2^p} I_{it} t_{ts}}{(n_{I_2}+1)\Delta_p}\right)} - e^{-\left(\frac{\lambda_{H_2^p} I_{it} t_{ts}}{n_{I_2}\Delta_p}\right)}\right)}{\lambda_{H_2^s} log_e(2)\left(P^p\lambda_{H_1^s} - \frac{n_{I_1}\Delta_p}{t_{ts}}\lambda_{G^s}\right)} \\
& \times \left(e^{-\left(\frac{\lambda_{H_1^p} I_{it} t_{ts}}{(n_{I_1}+1)\Delta_p}\right)} - e^{-\left(\frac{\lambda_{H_1^p} I_{it} t_{ts}}{n_{I_1}\Delta_p}\right)}\right)\lambda_{H_1^s}\lambda_{G^s} \\
& \times \left(-e^{\left(\frac{\lambda_{H_2^s}\sigma^2 t_{ts}}{n_{I_2}\Delta_p}\right)} E_i\left(-\frac{\lambda_{H_2^s}\sigma^2 t_{ts}}{n_{I_2}\Delta_p}\right)\right. \\
& \times \left[\frac{1}{\frac{n_{I_2}\Delta_p\lambda_{G^s}}{P^p\lambda_{H_2^s} t_{ts}} - 1} - \frac{1}{\frac{n_{I_2}\Delta_p\lambda_{H_1^s}}{n_{I_1}\Delta_p\lambda_{H_2^s}} - 1}\right] \\
& \left. + \frac{-e^{\left(\frac{\lambda_{G^s}\sigma^2}{P^p}\right)} E_i\left(-\frac{\lambda_{G^s}\sigma^2}{P^p}\right)}{1 - \frac{n_{I_2}\Delta_p\lambda_{G^s}}{P^p\lambda_{H_2^s} t_{ts}}} - \frac{-e^{\left(\frac{\lambda_{H_1^s}\sigma^2 t_{ts}}{n_{I_1}\Delta_p}\right)} E_i\left(-\frac{\lambda_{H_1^s}\sigma^2 t_{ts}}{n_{I_1}\Delta_p}\right)}{1 - \frac{n_{I_2}\Delta_p\lambda_{H_1^s}}{n_{I_1}\Delta_p\lambda_{H_2^s}}}\right).
\end{aligned}
\tag{5.22}
$$

Plugging Equations (5.19), (5.20), (5.21), and (5.22) back to Equation (5.18), closed-form expression for SU_2 mean capacity at system state (i,j) is given by the below Equation (5.23):

$$C_2|_{i,j} = \bar{A} + \bar{B} + \bar{C} + \bar{D}. \tag{5.23}$$

Using Equation (5.23) above, the overall SU_2 mean capacity is expressed as follows using Markovian analysis:

Case 1: With both SUs harvesting energy from SBS:

$$C_2 = \sum_{i=0}^{\frac{B_{max}}{\Delta_p}} \sum_{j=0}^{\frac{B_{max}}{\Delta_p}} C_2|_{i,j} \times \Pi(k,l). \tag{5.24}$$

Case 2: With both SUs harvesting energy from the SBS and MBS:

$$C_2 = \sum_{i=0}^{\frac{B_{max}}{\Delta_p}} \sum_{j=0}^{\frac{B_{max}}{\Delta_p}} C_2|_{i,j} \times \bar{\Pi}(k,l). \tag{5.25}$$

5.4 Simulation Results and Discussion

In this section, we generate simulation results to confirm the derived mean capacity expressions for each SU, as well as to quantify each SU mean capacity performance. Similarly to Chapter 4, the results generated in this chapter adopted the initial simulation parameter settings presented in Chapter 3 Table 3.2.

Fig. 5.1 and Fig. 5.2 show the results for SU_1 and SU_2 mean capacity versus battery level for different values of primary transmit power P^p. It is observed from the graphs that as primary transmit power is increased, there is a decrease in mean capacity for both (SU_1 and SU_2) as expected. The observed decrease is due to an increase in interference as a consequence of an increase in primary transmit power. Fig. 5.3 and Fig. 5.4 show similar results for mean capacity but for different values of interference threshold I_{it}. An increase in I_{it} relaxes the transmit power constraint imposed on SUs. Thus, its increase results in SUs being able to increase their transmit power, which consequently will results in an increase in mean capacity as observed from the simulation graphs.

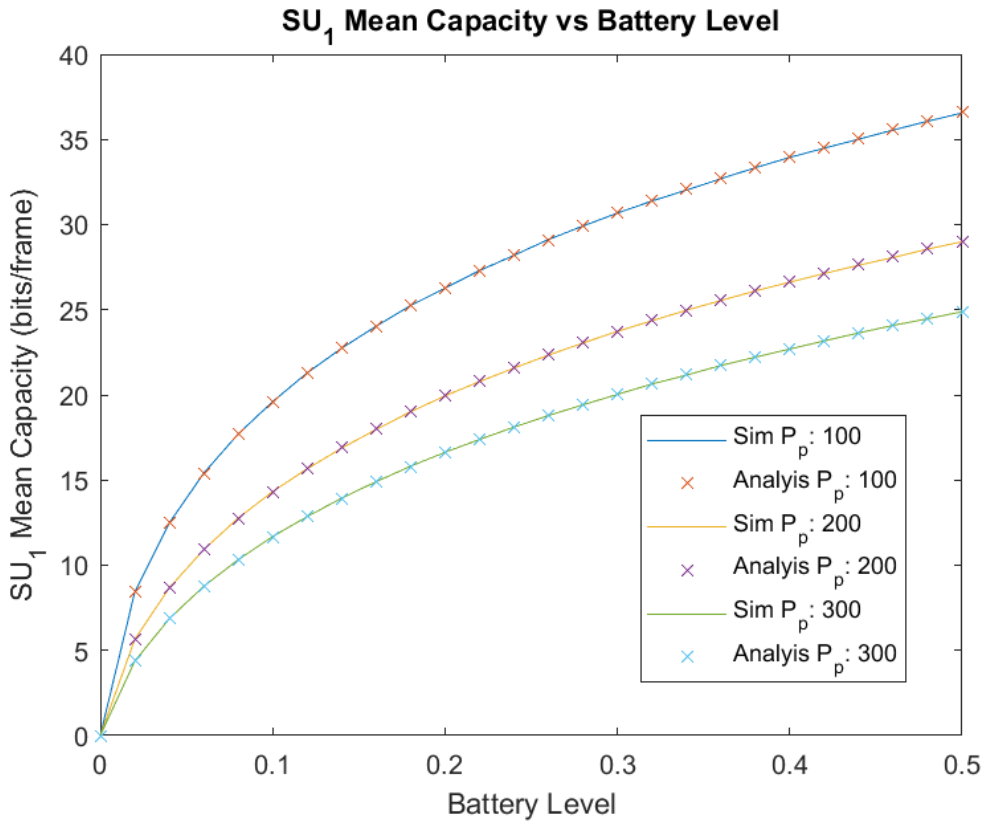


Figure 5.1: Mean Capacity vs Battery Level for Different Values of Primary Transmit Power P_p (Watts)

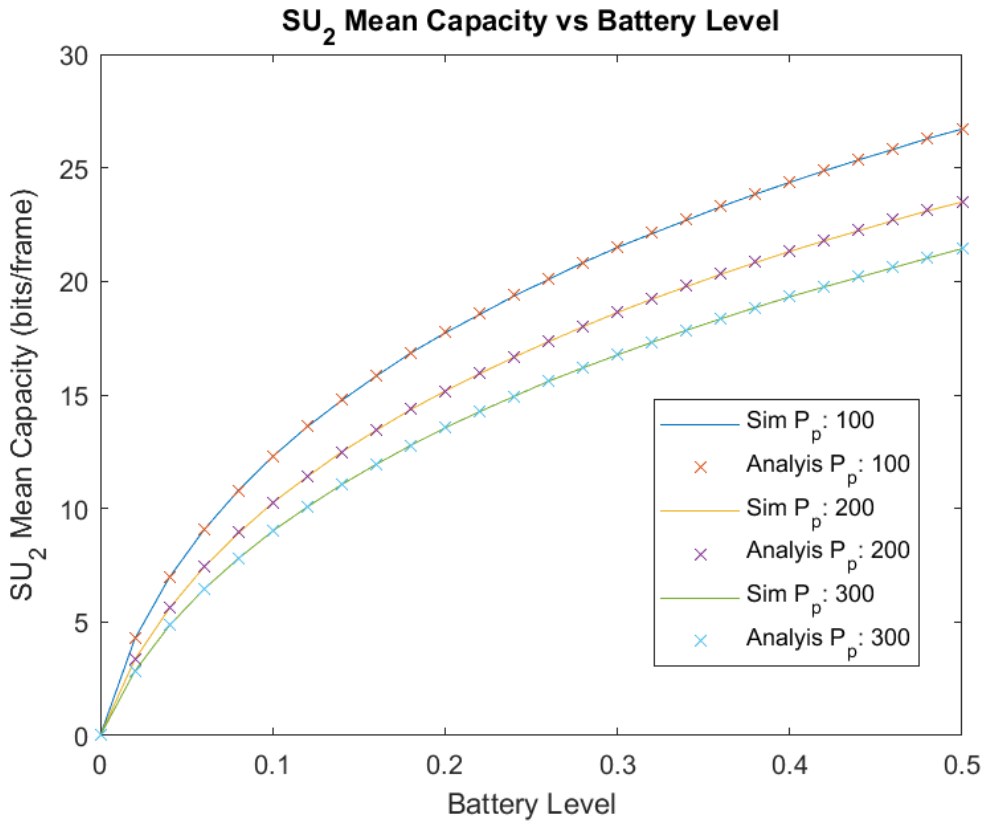


Figure 5.2: Mean Capacity vs Battery Level for Different Values of Primary Transmit Power P_p (Watts)

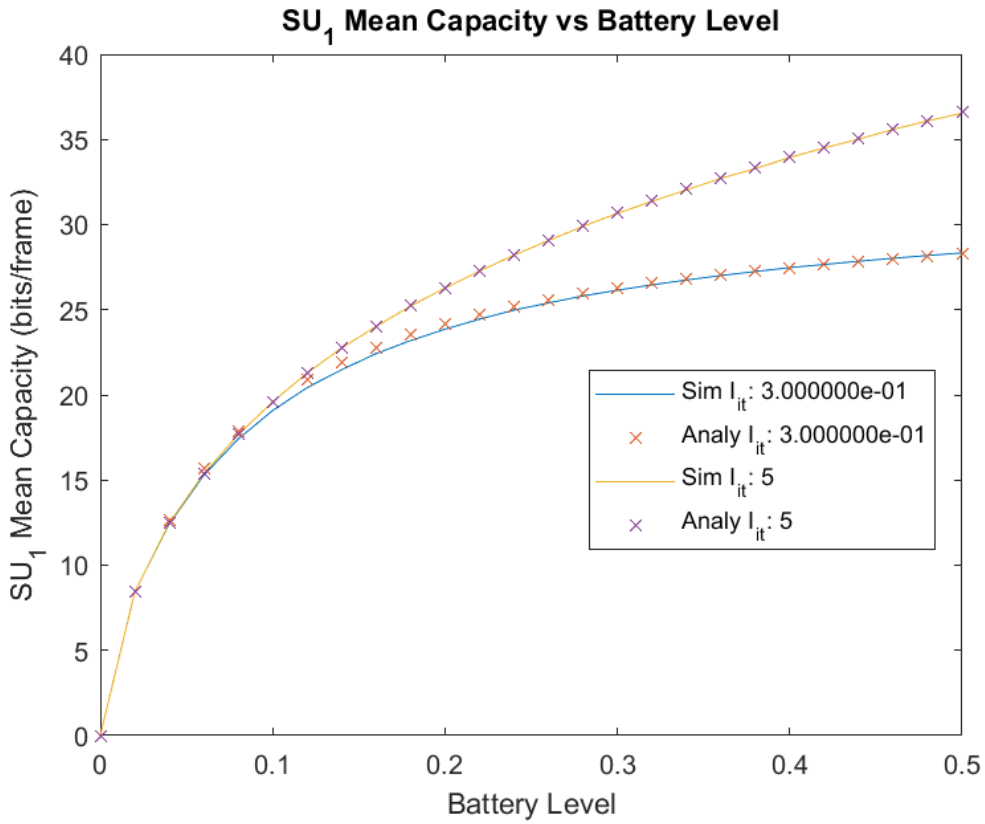


Figure 5.3: Mean Capacity vs Battery Level for Different Values of Interference Threshold I_{it}

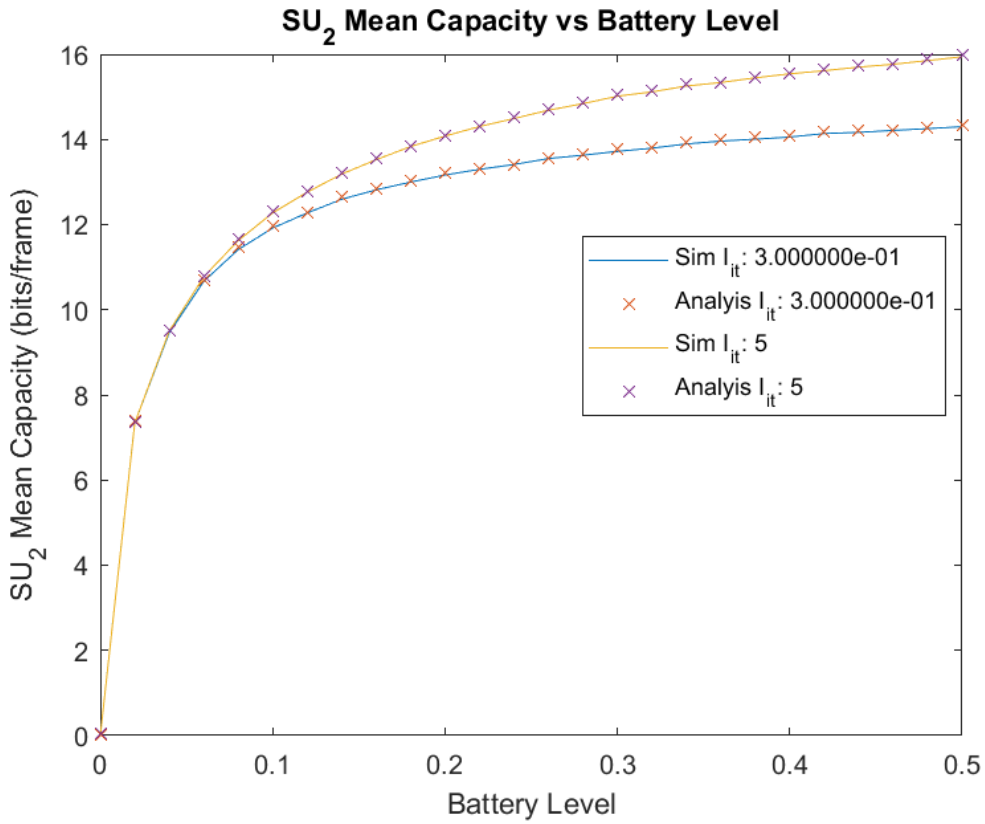


Figure 5.4: Mean Capacity vs Battery Level for Different Values of Interference Threshold I_{it}

5.5 Summary

Similar to Chapter 4, this chapter builds upon the results presented in Chapter 3 to accurately derive mean capacity analytical expressions for each SU in the proposed system model. Matlab simulation results for the derived mean capacity closed-form expressions showed a match between the simulation and analytical results, thus confirming analytical results validity.

Chapter 6

Conclusion

6.1 Introduction

This Chapter gives a summary of the work done in this research dissertation and outlines potential future research directions that can built on this work.

6.2 Summary and Conclusions

Chapter 1 presented the problem statement, research question and the methodology that has been used to answer the research questions for this dissertation. Chapter 2 covered literature review where background concepts were presented as well as relevant research work to this study. Most works covered systems with CR and NOMA with no EH component, others covered simple network models with on EH without any CR and NOMA concepts. The works that covered performance analysis of system models with both CR-NOMA and EH did the analysis on the downlink, they further did not cater for the residual energy that can occur from one transmission frame to the next. The system model presented in this dissertation had both CR-NOMA and EH components, the analyses were carried out on the uplink. This dissertation analysis caters for stochastic nature of energy harvesting as well as the residual energy from one transmission frame to the next, this is not done in any of the works done in literature.

Chapter 3 presented the considered system model for this research study. The considered system model Markovian model is derived in this Chapter, where closed-form expressions for SU_1 and SU_2 state transition probabilities were derived. Using state transition probabilities results, probabilities of each SU being in a particular state at any point in time were derived. Chapter 4 used the results of Markovian analysis in Chapter 3 to accurately derive closed-form expressions for each SU out-

age probability. In Chapter 5, mean capacity closed-form analytical expressions for each SU were derived on the basis of the Markovian analysis provided in chapter 3.

Simulation results validated the accuracy of the analytical expressions derived. The impact on system outage performance and mean capacity for varying certain network parameters is observed and analysed. Overall, the analysis show that higher primary transmit power resulted in higher outage probabilities for both users while mean user capacity decreased as expected. These results are due to an increase in interference on the SUs carrier signal at the SBS receiver. It is further observed that as the battery level or energy harvesting conversion efficiency factor are increased, each SU outage performance improved. The results for mean capacity increased as the battery level values increased. It was further observed that an increase in I_{it} results in higher attained mean capacity for each SU, this results are observed because higher values of I_{it} allow users to transmit with higher transmit power to improve their channel capacity. Results from simulation validated the derived analytical expressions as there is a match between simulation and analysis graphs for all the derived analytical expressions. Though the generated results for outage probability and mean capacity are based on the assumption that SUs are harvesting from only the SBS, similar approach can be followed to generate the same results while the SUs are harvesting from multiple sources such as SBS and MBS.

6.3 Future Work

This research work can be improved by considering the below potential future works:

- Physical Layer security analysis for the considered system model.
- Introducing an eavesdropper in the system model and propose viable secure communication model.
- Introducing Mobile-Edge server at the SBS then analyse performance and security implications.

References

[1] A. Harb, "Energy harvesting: State-of-the-art," *Renewable energy*, vol. 36, no. 10, pp. 2641–2654, 2011.

[2] B. Wang and K. R. Liu, "Advances in cognitive radio networks: A survey," *IEEE Journal of selected topics in signal processing*, vol. 5, no. 1, pp. 5–23, 2010.

[3] B. Makki, K. Chitti, A. Behravan, and M.-S. Alouini, "A survey of noma: Current status and open research challenges," *IEEE Open Journal of the Communications Society*, vol. 1, pp. 179–189, 2020.

[4] I. Budhiraja, S. Tyagi, S. Tanwar, N. Kumar, and M. Guizani, "Cr-noma based interference mitigation scheme for 5g femtocells users," pp. 1–6, 2018.

[5] L. Bariah, S. Muhaidat, and A. Al-Dweik, "Error performance of noma-based cognitive radio networks with partial relay selection and interference power constraints," *IEEE Transactions on Communications*, vol. 68, no. 2, pp. 765–777, 2020.

[6] D. T. Do, T. Anh Le, T. N. Nguyen, X. Li, and K. M. Rabie, "Joint impacts of imperfect csi and imperfect sic in cognitive radio-assisted noma-v2x communications," *IEEE Access*, vol. 8, pp. 128629–128645, 2020.

[7] D. T. Do, A. T. Le, and B. M. Lee, "On performance analysis of underlay cognitive radio-aware hybrid oma/noma networks with imperfect csi," *Electronics*, vol. 8, no. 7, 2019.

[8] D. T. Do, A. T. Le, and C.-B. Le, "Improving spectrum efficiency in d2d-assisted cognitive radio networks: Application of noma and performance analysis," pp. 1–5, 2019.

[9] S. Arzykulov, G. Nauryzbayev, T. A. Tsiftsis, and M. Abdallah, "Outage performance of underlay cr-noma networks," pp. 1–6, 2018.

[10] V. Aswathi and V. B. A., "Performance analysis of noma-based underlay cognitive radio networks with partial relay selection," *IEEE Transactions on Vehicular Technology*, vol. 70, no. 5, pp. 4615–4630, 2021.

[11] A. Kumar and K. Kumar, "A game theory based hybrid noma for efficient resource optimization in cognitive radio networks," *IEEE Transactions on Network Science and Engineering*, pp. 1–1, 2021.

[12] L. Xu, H. Xing, Y. Deng, A. Nallanathan, and C. Zhuansun, "Fairness-aware throughput maximization for underlaying cognitive noma networks," *IEEE Systems Journal*, vol. 15, no. 2, pp. 1881–1892, 2021.

[13] Y. Cheng, C. Liang, Q. Chen, and R. Yu, "Energy-efficient d2d-assisted computation offloading in noma-enabled cognitive networks," *IEEE Transactions on Vehicular Technology*, vol. 70, no. 12, pp. 13441–13446, 2021.

[14] A. H. Bastami, "Noma-based spectrum leasing in cognitive radio network: Power optimization and performance analysis," *IEEE Transactions on Communications*, vol. 69, no. 7, pp. 4821–4831, 2021.

[15] T. Zhang, W. Chen, and F. Yang, "Balancing delay and energy efficiency in energy harvesting cognitive radio networks: A stochastic stackelberg game approach," *IEEE Transactions on Cognitive Communications and Networking*, vol. 3, no. 2, pp. 201–216, 2017.

[16] A. E. Shafie, M. E. Ashour, T. M. S. Khattab, and A. M. Mohamed, "On spectrum sharing between energy harvesting cognitive radio users and primary users," *2015 International Conference on Computing, Networking and Communications (ICNC)*, pp. 214–220, 2014.

[17] D. T. Hoang, D. Niyato, P. Wang, and D. I. Kim, "Opportunistic channel access and rf energy harvesting in cognitive radio networks," *IEEE Journal on Selected Areas in Communications*, vol. 32, no. 11, pp. 2039–2052, 2014.

[18] L. Ge, G. Chen, Y. Zhang, J. Tang, J. Wang, and J. A. Chambers, "Performance analysis for multihop cognitive radio networks with energy harvesting by using stochastic geometry," *IEEE Internet of Things Journal*, vol. 7, no. 2, pp. 1154–1163, 2020.

[19] S. Samain, J. Doncel, A. Busic, and J.-M. Fourneau, "Multiclass energy packet networks with finite capacity energy queues," *Performance Evaluation*, vol. 152, p. 102228, 2021.

[20] I. Ahmed, K. T. Phan, and T. Le-Ngoc, "Optimal stochastic power control for energy harvesting systems with delay constraints," *IEEE Journal on Selected Areas in Communications*, vol. 34, no. 12, pp. 3512–3527, 2016.

[21] K. Patil, K. De Turck, and D. Fiems, "A two-queue model for optimising the value of information in energy-harvesting sensor networks," *Performance Evaluation*, vol. 119, pp. 27–42, 2018.

[22] Z. Shi, X. Xie, H. Lu, H. Yang, J. Cai, and Z. Ding, "Deep reinforcement learning-based multidimensional resource management for energy harvesting cognitive noma communications," *IEEE Transactions on Communications*, vol. 70, no. 5, pp. 3110–3125, 2022.

[23] D. Wang and S. Men, "Secure energy efficiency for noma based cognitive radio networks with nonlinear energy harvesting," *IEEE Access*, vol. 6, pp. 62707–62716, 2018.

[24] W. Zhao, R. She, and H. Bao, "Security energy efficiency maximization for two-way relay assisted cognitive radio noma network with self-interference harvesting," *IEEE Access*, vol. 7, pp. 74401–74411, 2019.

[25] M. W. Baidas and M. R. Amini, "Network sum-rate maximization via joint relay selection and power allocation in energy-harvesting noma multicast cognitive radio networks," pp. 1–6, 2021.

[26] S. Üstünbaş and Aygölü, "Ber performance of cognitive noma with energy harvesting," pp. 1–4, 2020.

[27] A. Bhowmick, S. D. Roy, and S. Kundu, "Throughput maximization of a uav assisted cr network with noma-based communication and energy-harvesting," *IEEE Transactions on Vehicular Technology*, vol. 71, no. 1, pp. 362–374, 2022.

[28] P. Kumar and A. Bhowmick, "Outage analysis of noma based non-linear energy harvesting cognitive d2d network," pp. 1–5, 2022.

[29] T.-H. Vu, T.-V. Nguyen, and S. Kim, "Wireless powered cognitive noma-based iot relay networks: Performance analysis and deep learning evaluation," *IEEE Internet of Things Journal*, vol. 9, no. 5, pp. 3913–3929, 2022.

[30] G. Kalaimagal and M. S. Vasanti, "Performance analysis of cooperative underlay crn in noma aided energy harvesting for multiple secondary users," *Journal of Physics: Conference Series*, vol. 1964, p. 062024, jul 2021.

[31] S. Poornima and A. V. Babu, "Performance analysis of energy harvesting cognitive relay networks with primary interference," *Telecommunication Systems*, pp. 445–459, jul 2018.

[32] B. Wang and K. R. Liu, "Advances in cognitive radio networks: A survey," *IEEE Journal of Selected Topics in Signal Processing*, vol. 5, no. 1, pp. 5–23, 2011.

[33] Y. Saleem and M. H. Rehmani, "Primary radio user activity models for cognitive radio networks: A survey," *Journal of Network and Computer Applications*, vol. 43, pp. 1–16, 2014.

[34] T. Weiss and F. Jondral, "Spectrum pooling: an innovative strategy for the enhancement of spectrum efficiency," *IEEE Communications Magazine*, vol. 42, no. 3, pp. S8–14, 2004.

[35] N. Devroye, M. Vu, and V. Tarokh, "Cognitive radio networks," *IEEE Signal Processing Magazine*, vol. 25, no. 6, pp. 12–23, 2008.

[36] X. Hong, Z. Chen, C.-X. Wang, S. A. Vorobyov, and J. S. Thompson, "Cognitive radio networks," *IEEE Vehicular Technology Magazine*, vol. 4, no. 4, pp. 76–84, 2009.

[37] I. F. Akyildiz, W.-y. Lee, M. C. Vuran, and S. Mohanty, "A survey on spectrum management in cognitive radio networks," *IEEE Communications Magazine*, vol. 46, no. 4, pp. 40–48, 2008.

[38] A. Benjebbour, K. Saito, A. Li, Y. Kishiyama, and T. Nakamura, "Non-orthogonal multiple access (noma): Concept, performance evaluation and experimental trials," in *2013 IEEE International Conference on Communication Systems (ICCS)*, pp. 770–774, IEEE, 2013.

[39] B. Makki, K. Chitti, A. Behravan, and M.-S. Alouini, "A survey of noma: Current status and open research challenges," *IEEE Open Journal of the Communications Society*, vol. 1, pp. 179–189, 2020.

[40] A. Benjebbour, K. Saito, A. Li, Y. Kishiyama, and T. Nakamura, "Non-orthogonal multiple access (noma): Concept, performance evaluation and experimental trials," in *2015 International conference on wireless networks and mobile communications (WINCOM)*, pp. 1–6, IEEE, 2015.

[41] O. Maraqa, A. S. Rajasekaran, S. Al-Ahmadi, H. Yanikomeroglu, and S. M. Sait, "A survey of rate-optimal power domain noma with enabling technologies of future wireless networks," *IEEE Communications Surveys Tutorials*, vol. 22, no. 4, pp. 2192–2235, 2020.

[42] Y. Liu, L.-L. Yang, P. Xiao, H. Haas, and L. Hanzo, "Spatial modulated multi-carrier sparse code-division multiple access," *IEEE Transactions on Wireless Communications*, vol. 19, no. 1, pp. 610–623, 2020.

[43] J. Zeng, X. Fan, Y. Zhong, M. Peng, T. Lv, and T. Jiang, "Downlink power allocation optimization in pattern division multiple access," *IEEE Access*, vol. 9, pp. 14649–14659, 2021.

[44] Y. Cao, H. Sun, J. Soriaga, and T. Ji, "Resource spread multiple access - a novel transmission scheme for 5g uplink," pp. 1–5, 2017.

[45] Z. Yuan, G. Yu, W. Li, Y. Yuan, X. Wang, and J. Xu, "Multi-user shared access for internet of things," pp. 1–5, 2016.

[46] Q. Xiong, C. Qian, B. Yu, and C. Sun, "Advanced noma scheme for 5g cellular network: Interleave-grid multiple access," *2017 IEEE Globecom Workshops (GC Wkshps)*, pp. 1–5, 2017.

[47] X. Li, H.-H. Chen, Y. Qian, B. Rong, and M. R. Soleymani, "Welch bound analysis on generic code division multiple access codes with interference free windows," *IEEE Transactions on Wireless Communications*, vol. 8, no. 4, pp. 1603–1607, 2009.

[48] B. Y. Kong and I.-C. Park, "A 120-mw 0.16-ms-latency connectivity-scalable multiuser detector for interleave division multiple access," vol. 67, no. 3, pp. 470–474, 2019.

[49] N. A. Khan Beigi and A. Haghighat, "On kurtosis of spreading sequences for noma," pp. 1–5, 2020.

[50] Y. Yuan, Z. Yuan, and L. Tian, "5g non-orthogonal multiple access study in 3gpp," *IEEE Communications Magazine*, vol. 58, no. 7, pp. 90–96, 2020.

[51] K. Yang, N. Yang, N. Ye, M. Jia, Z. Gao, and R. Fan, "Non-orthogonal multiple access: Achieving sustainable future radio access," *IEEE Communications Magazine*, vol. 57, no. 2, pp. 116–121, 2019.

[52] Y. Yuan, Z. Yuan, and L. Tian, "5g non-orthogonal multiple access study in 3gpp," *IEEE Communications Magazine*, vol. 58, no. 7, pp. 90–96, 2020.

[53] A. Zafar, M. Shaqfeh, M.-S. Alouini, and H. Alnuweiri, "On multiple users scheduling using superposition coding over rayleigh fading channels," *IEEE Communications Letters*, vol. 17, no. 4, pp. 733–736, 2013.

[54] S. M. R. Islam, N. Avazov, O. A. Dobre, and K.-s. Kwak, "Power-domain non-orthogonal multiple access (noma) in 5g systems: Potentials and challenges," *IEEE Communications Surveys Tutorials*, vol. 19, no. 2, pp. 721–742, 2017.

[55] V. Ozduran, "Advanced successive interference cancellation for nonorthogonal multiple access," *IEEE Wireless Communications Letters*, vol. 7, no. 6, pp. 980–983, 2018.

[56] M.-L. Ku, W. Li, Y. Chen, and K. J. Ray Liu, "Advances in energy harvesting communications: Past, present, and future challenges," *IEEE Communications Surveys Tutorials*, vol. 18, no. 2, pp. 1384–1412, 2016.

[57] J. W. Kimball, B. T. Kuhn, and R. S. Balog, "A system design approach for unattended solar energy harvesting supply," *IEEE Transactions on Power Electronics*, vol. 24, no. 4, pp. 952–962, 2009.

[58] J. P. Carmo, L. M. Goncalves, and J. H. Correia, "Thermoelectric microconverter for energy harvesting systems," *IEEE Transactions on Industrial Electronics*, vol. 57, no. 3, pp. 861–867, 2010.

[59] A. Khaligh, P. Zeng, and C. Zheng, "Kinetic energy harvesting using piezoelectric and electromagnetic technologies—state of the art," *IEEE Transactions on Industrial Electronics*, vol. 57, no. 3, pp. 850–860, 2010.

[60] M. Z. Chaari, M. Lahiani, and H. Ghariani, "Energy harvesting from electromagnetic radiation emissions by compact fluorescent lamp," in *2020 International Conference on Green Energy Conversion Systems (GECS)*, pp. 1–6, IEEE, 2020.

[61] S. Sudevalayam and P. Kulkarni, "Energy harvesting sensor nodes: Survey and implications," *IEEE Communications Surveys Tutorials*, vol. 13, no. 3, pp. 443–461, 2011.

[62] D. Gunduz, K. Stamatiou, N. Michelusi, and M. Zorzi, "Designing intelligent energy harvesting communication systems," *IEEE Communications Magazine*, vol. 52, no. 1, pp. 210–216, 2014.

[63] H. T. H. Giang, P. D. Thanh, and I. Koo, "Dynamic power allocation scheme for noma uplink in cognitive radio networks using deep q learning," *IEEE Access*, vol. 9, pp. 20249–20261, 2021.

[64] N. Airee, S. Saha, M. Adrat, M. Schrammen, and P. Jax, "Heuristic power allocation in noma-based overlay cognitive radio networks," in *2021 IEEE 93rd Vehicular Technology Conference (VTC2021-Spring)*, pp. 1–6, IEEE, 2021.

[65] H. Bany Salameh, R. Tashtoush, H. Al-Obiedollah, A. Alajlouni, and Y. Jararweh, "Power allocation technique with soft performance guarantees in hybrid ofdma–noma cognitive radio systems: Modeling and simulation," *Simulation Modelling Practice and Theory*, vol. 112, p. 102370, 2021.

[66] W. Liang, S. X. Ng, J. Shi, L. Li, and D. Wang, "Energy efficient transmission in underlay cr-noma networks enabled by reinforcement learning," *China Communications*, vol. 17, no. 12, pp. 66–79, 2020.

[67] Y. Xu, R. Q. Hu, and G. Li, "Robust energy-efficient maximization for cognitive noma networks under channel uncertainties," *IEEE Internet of Things Journal*, vol. 7, no. 9, pp. 8318–8330, 2020.

[68] A. Briones-Reyes, L. A. Vásquez-Toledo, A. Prieto-Guerrero, and R. Aguilar-Gonzalez, "Mathematical evaluation of spectrum sharing in cognitive radio networks for 5g systems using markov processes," *Computer Networks*, vol. 182, p. 107521, 2020.

[69] I. Abu Mahady, E. Bedeer, S. Ikki, and H. Yanikomeroglu, "Sum-rate maximization of noma systems under imperfect successive interference cancellation," *IEEE Communications Letters*, vol. 23, no. 3, pp. 474–477, 2019.

[70] M. Chamisa, F. Takawira, and J. M. Moualeu, "Underlay spectrum-sharing non-orthogonal multiple access network with imperfect successive interference cancellation," *IET Communications*, vol. 14, no. 19, pp. 3363–3372, 2020.

[71] V. Aswathi and A. V. Babu, "Performance analysis of noma-based underlay cognitive radio networks with partial¡? brk?¿ relay selection," *IEEE Transactions on Vehicular Technology*, vol. 70, no. 5, pp. 4615–4630, 2021.

[72] G. Im and J. H. Lee, "Outage probability for cooperative noma systems with imperfect sic in cognitive radio networks," *IEEE Communications Letters*, vol. 23, no. 4, pp. 692–695, 2019.

[73] H. A. Suraweera, P. J. Smith, and M. Shafi, "Capacity limits and performance analysis of cognitive radio with imperfect channel knowledge," *IEEE Transactions on Vehicular Technology*, vol. 59, no. 4, p. 1811–1822, 2010.

[74] Y. Liu, S. A. Mousavifar, Y. Deng, C. Leung, and M. Elkashlan, "Wireless energy harvesting in a cognitive relay network," *IEEE Transactions on Wireless Communications*, vol. 15, no. 4, pp. 2498–2508, 2015.

[75] X. Zhou, R. Zhang, and C. K. Ho, "Wireless information and power transfer: Architecture design and rate-energy tradeoff," *IEEE Transactions on communications*, vol. 61, no. 11, pp. 4754–4767, 2013.